Julius-Maximilians-Universität Würzburg

Fakultät für Biologie

Enhanced Replication of Vaccinia Virus GLV-1h68 in Cancer Stem-like Cells of Human Breast Cancer Cell Preparations

Dissertation

zur Erlangung des naturwissenschaftlichen Doktorgrades der

Julius-Maximilians-Universität Würzburg

vorgelegt von

Huiqiang Wang

aus China

Würzburg, 2011

Eingereicht am: _____

Mitglieder der Promotionskommission:

Vorsitzender: _____

Prof. Dr. T. Dandekar

Erstgutachter : _____

Prof. Dr. A. A. Szalay

Zweitgutachter: _____

Prof. Dr. G. Krohne

Tag des Promotionskolloquiums: _____

Doktorurkunde ausgehändigt am: _____

Contents

Summary

There is more and more evidence for the cancer stem cell hypothesis which believes that cancers are driven by a cellular subcomponent that has stem cell properties which is self-renewal, tumorigenicity and multilineage differentiation capacity. Cancer stem cells have been connected to the initiation of tumors and are even found to be responsible for relapses after apparently curative therapies have been undertaken. This hypothesis changes our conceptual approach of oncogenesis and shall have implications in breast cancer prevention, detection and treatment, especially in metastatic breast cancer for which no curative treatment exists. Given the specific stem cell features, novel therapeutic pathways can be targeted.

Since the value of vaccinia virus as a vaccination virus against smallpox was discovered by E. Jenner at 18th century, it plays an important role in human medicine and molecular biology. After smallpox was successfully eradicated, vaccinia virus is mainly used as a viral vector in molecular biology and increasingly in cancer therapy. The outstanding capability to specifically target and destroy cancer cells makes it a perfect agent for oncolytic virotherapy. Furthermore, the virus can easily be modified by inserting genes which encode therapeutic or diagnostic proteins to be expressed when a tumor is infected.

The emphasis in this study was the establishment of methods for the enrichment of human breast cancer stem-like cells from cancer cell lines and characterization of those cancer stem-like cells *in vitro* and *in vivo*. Furthermore, by using the Genelux Corporation vaccinia virus strain GLV-1h68, the isolated cancer stem-like cells can be targeted not only *in vitro* but also *in vivo* more efficiently.

Side-population (SP) cells within cancers and cell lines are rare cell populations known to be enriched cancer stem-like cells. In this study, we used Hoechst 33342 staining and flow cytometry to identify SP cells from the human breast cancer cell lines MCF-7 and GI-101A as models for cancer stem-like cells. Considering the cytotoxicity of Hoechst dye and the restriction of instrument, we did not carry out further studies by this method.

Utilizing *in vitro* and *in vivo* experimental systems, we showed that human breast cancer cell line GI-101A with aldehyde dehydrogenase activity (ALDH) have stem-like properties. Higher ALDH activity identifies the tumorigenic cell fraction which is

capable of self-renewal and of generating tumors that could recapitulate the heterogeneity of the parental tumor. Furthermore, the cells with higher ALDH activity display significant resistance to chemotherapy and ionizing radiation, which proves their stem-like properties again. The cells which have higher ALDH activity also are more invasive compared to cells which have lower ALDH activity, which connects the cancer stem-like cells with cancer metastases. By analyzing the popular human breast cancer stem cells surface markers CD44, CD49f and CD24, it was discovered that the cells with higher ALDH activity have stronger CD44 and CD49f expression than in those cells with lower ALDH activity, which further confirms their stem-like properties. Finally, the cells with higher ALDH activity and lower ALDH activity were infected *in vitro* and used in virotherapy in a mouse xenograft model was performed. The results indicated that the vaccinia virus GLV-1h68 can replicate in cells with higher ALDH activity more efficiently than cells with lower ALDH activity. GLV-1h68 also can selectively target and eradicate the xenograft tumors which were derived from cells with higher ALDH activity.

The epithelial-mesenchymal transition (EMT) is a key developmental program that is often activated during cancer invasion and metastases. EMT was induced in immortalized human mammary epithelial cells (HMLEs) and in GI-101A cells, which results in the acquisition of mesenchymal traits and in the expression of stem cell markers. Furthermore, the EMT-induced GI-101A cells showed resistance to chemotherapy and invasion capacity. $CD44^+/CD24^-$ cells were enriched during the EMT induction. Following flow cytometry sorting by using CD44, CD24 and ESA surface marker, the sorted cells were tested in a mouse model regarding tumorigenicity. Unexpectedly, we found that $CD44^+/CD24^+/ESA^+$ cells could initiate tumors more efficiently rather than $CD44^+/CD24^-/ESA^+$ and other fractions in EMT-induced GI-101A cells. We also infected the $CD44^+/CD24^+/ESA^+$ and $CD44^+/CD24^-/ESA^+$ cells *in vitro* and performed virotherapy in a mouse xenograft model. The results indicated that the vaccinia virus GLV-1h68 is able to replicate in $CD44^+/CD24^+/ESA^+$ cells more efficiently than in $CD44^+/CD24^-/ESA^+$ cells. GLV-1h68 was also capable to selectively target and eradicate the xenograft tumors which derived from $CD44^+/CD24^+/ESA^+$ cells. Moreover, $CD44^-$ cells have much lower

tumorigenicity in the mouse model and $CD44^-$ cells derived-tumors are not responsive to vaccinia virotherapy.

In summary, we have successfully established an *in vitro* and *in vivo* system for the identification, characterization and isolation of cancer stem-like cells from the human breast cancer cell line GI-101A by using the ALDEFLUOR assay. The vaccinia virus GLV-1h68 was able to efficiently target and eradicate the higher ALDH activity cells and tumors derived from those cells. Although contrary to the current assumption, $CD44^+/CD24^+/ESA^+$ cells in the EMT-induced GI-101A cell line showed stem-like properties and GLV-1h68 was able to efficiently target and eradicate the $CD44^+/CD24^+/ESA^+$ cells and tumors which derived from those cells.

Finally, improved understanding of cancer stem cells may have tremendous relevance for how cancer should be treated. It is menacing that cancer stem cells are resistant to almost all anti-tumor approaches which have already been established for the treatment of metastatic diseases such as ionizing radiation, hormonal therapy, chemotherapy, and small molecular inhibitors. Therefore, it is promising that our results suggest that these cancer stem cells may be susceptible to treatment with oncolytic vaccinia virus.

Zusammenfassung

Immer mehr experimentelle Hinweise stützen die Krebsstammzell-Hypothese, wonach Krebs durch eine zelluläre Teilkomponente angetrieben wird, die Stammzell-Eigenschaften hat, das heißt die Fähigkeit sich selbst zu erneuern, Tumorigenität und die Fähigkeit sich in verschiedene Richtungen zu differenzieren. Krebsstammzellen wurden mit der Enstehung von Tumorerkrankungen in Verbindung gebracht, und werden sogar für Rückfälle verantwortlich gemacht, nachdem scheinbar erfogreiche Behandlungen durchgeführt wurden. Diese Hypothese verändert unser Verständnis der Onkogenese und wird Auswirkungen auf die Brustkrebs-Prävention, -Erkennung und -Behandlung haben, vor allem in metastasierendem Brustkrebs, für den es keine kurative Behandlung gibt. Angesichts der besonderen Merkmale von Stammzellen können neue therapeutische Wege angestrebt werden.

Seit sein Nutzen als Impfvirus gegen die Pocken von E. Jenner im 18. Jahrhundert entdeckt wurde, spielt das Vaccinia-Virus in der Humanmedizin und Molekularbiologie eine wichtige Rolle. Nachdem die Pocken erfolgreich ausgerottet wurden, wird das Vaccinia-Virus hauptsächlich als viraler Vektor in der Molekularbiologie und in zunehmendem Maße in der Krebstherapie verwendet. Die außerordentliche Fähigkeit, Krebszellen gezielt zu zerstören, macht es zu einem perfekten Wirkstoff für die onkolytische Virotherapie. Des Weiteren kann das Virus durch das Inserieren von Genen modifiziert werden, die für therapeutische oder diagnostische Proteine kodieren und im infizierten Tumor exprimiert werden.

Der Schwerpunkt dieser Arbeit war die Etablierung von Methoden für die Anreicherung menschlicher Stammzell-ähnlicher Brustkrebszellen von Krebszelllinien und die Charakterisierung dieser Krebsstammzell-ähnlichen Zellen *in vitro* und *in vivo*. Darüber hinaus können mit Hilfe des Vaccinia-Virus-Stammes GLV-1h68 von Genelux Corporation die isolierten Krebsstammzell-ähnlichen Zellen nicht nur *in vitro*, sondern auch *in vivo* effizienter eliminiert werden.

Side-Population- (SP-) Zellen in Krebserkrankungen und Zelllinien sind seltene Zellpopulationen die dafür bekannt sind, reich an Krebsstammzell-ähnlichen Zellen zu sein. In dieser Studie verwendeten wir eine Hoechst 33342-Färbung und Durchflusszytometrie, um SP-Zellen aus der menschlichen Brustkrebs-Zelllinie MCF-7 zu identifizieren, als Modell für Krebsstammzell-ähnliche Zellen. In Anbetracht der

Zytotoxizität des Hoechst-Farbstoffes und der Beschränkung des Instruments, wurde diese Methode nicht weiter verfolgt.

Mit Hilfe von Experimenten *in vitro* und *in vivo* wurde gezeigt, dass die menschliche Brustkrebs-Zelllinie GI-101A mit Aldehyd-Dehydrogenase-Aktivität (ALDH) Stammzell-ähnliche Eigenschaften hat. Höhere ALDH-Aktivität identifiziert die tumorigene Zellfraktion, die zur Selbsterneuerung und zur Erzeugung von Tumoren fähig ist, was die Heterogenität des ursprünglichen Tumors deutlich macht. Darüber hinaus weisen Zellen mit hoher ALDH-Aktivität eine beachtliche Fähigkeit zur Resistenz gegen Chemotherapie und ionisierende Strahlung auf, was wiederum ihre Stammzell-ähnlichen Eigenschaften beweist. Ferner sind Zellen mit hoher ALDH-Aktivität im Vergleich zu Zellen mit niedriger ALDH-Aktivität stärker invasiv, was die Krebsstammzell-ähnlichen Zellen mit Krebsmetastasierung in Verbindung bringt. Bei der Analyse der gängigen Oberflächenmarker CD44, CD24 und CD49f in menschlichen Brustkrebs-Stammzellen beobachteten wir, dass Zellen mit hoher ALDH-Aktivität CD44 und CD49f stärker exprimieren als Zellen mit niedriger ALDH-Aktivität, was wiederum deren Stammzell-ähnliche Eigenschaften aufzeigt. Schließlich wurden die Zellen mit hoher und niedriger ALDH-Aktivität *in vitro* infiziert und Virotherapie im Maus-Xenograft-Modell durchgeführt. Die Ergebnisse zeigten, dass das Vaccinia-Virus GLV-1h68 in Zellen mit höherer ALDH-Aktivität effizienter replizieren kann als in Zellen mit niedrigerer ALDH-Aktivität. GLV-1h68 kann auch selektiv Xenograft-Tumore finden und zerstören, welche von Zellen mit hoher ALDH-Aktivität abstammten.

Der epithelial-mesenchymale Übergang (EMT) ist ein essentieller Entwicklungs-Schritt, der häufig während der Invasion und Metastasierung in Krebserkrankungen aktiviert wird. Wir induzierten EMT in immortalisierten humanen Brust-Epithelzellen (HMLEs) und GI-101A-Zellen, was im Erwerb von mesenchymalen Eigenschaften und der Expression von Stammzell-Markern resultiert. Außerdem zeigten die EMT-induzierten GI-101A-Zellen Chemoresistenz und Fähigkeit zur Invasion. $CD44^+CD24^-$-Zellen waren während der EMT-Induktion angereichert. Es wurden durchflusszytometrische Sortierung mit Hilfe von CD44-, CD24- und ESA-Oberflächenmarkern durchgeführt, und die sortierten Zellen wurden danach auf Tumorigenität in einem Mausmodell getestet. Unerwarteterweise fanden wir, dass $CD44^+CD24^-ESA^+$-Zellen effizienter Tumore initiieren konnten als $CD44^+CD24^-$ ESA^+-Zellen und andere Fraktionen in EMT-induzierten GI-101A-Zellen. Wir haben

auch die infizierten $CD44^+CD24^+ESA^{+-}$ und $CD44^+CD24^-ESA^+$-Zellen *in vitro* infiziert und Virotherapie im Maus-Xenograft-Modell durchgeführt. Die Ergebnisse zeigten, dass das Vaccinia-Virus GLV-1h68 in $CD44^+CD24^+ESA^+$-Zellen effizienter replizieren kann als $CD44^+CD24^-ESA^+$-Zellen. GLV-1h68 konnte selektiv Xenograft-Tumore finden und eliminieren, die von $CD44^+CD24^+ESA^+$-Zellen abstammten. Darüber hinaus haben $CD44^-$-Zellen eine sehr niedrige Tumorigenität im Mausmodell und Tumore, die von $CD44^-$-Zellen abstammen, sprechen nicht auf Vaccinia-Virotherapie an.

Zusammenfassend haben wir erfolgreich ein System zur Identifizierung, Charakterisierung und Isolierung von Krebsstammzell-ähnlichen Zellen aus der menschlichen Brustkrebs-Zelllinie GI-101A *in vitro* und *in vivo* mit Hilfe des ALDEFLUOR-Assays etabliert. Das Vaccinia-Virus GLV-1h68 konnte zielgenau Zellen mit erhöhter ALDH-Aktivität oder daraus etablierte Tumore finden und zerstören.

Obwohl, im Gegensatz zur gängigen Annahme, $CD44^+CD24^+ESA^+$-Zellen in der EMT-induzierten GI-101A-Zelllinie Stammzell-ähnliche Eigenschaften zeigten, konnte GLV-1h68 zielgenau $CD44^+CD24^+ESA^+$-Zellen oder daraus etablierte Tumore finden und zerstören.

Schließlich kann ein verbessertes Verständnis der Krebsstammzellen eine enorme Bedeutung dafür haben, wie Krebs behandelt werden sollte. Es ist verhängnisvoll, dass Krebsstammzellen gegen fast alle Anti-Tumor-Ansätze, die bereits für die Behandlung von Metastasen etabliert wurden, resistent sind, wie ionisierende Strahlung, Hormontherapie, Chemotherapie und kleine molekulare Inhibitoren. Gerade deshalb ist es vielversprechend, dass unsere Ergebnisse darauf hin deuten, dass diese Krebsstammzellen auf Behandlung mit dem onkolytischen Vaccinia-Virus ansprechen.

1 Introduction

1.1 Cancer Stem Cells

1.1.1 History and concept

Cancer stem cells (CSCs) are cancer cells found within tumors or hematological cancers that possess characteristics associated with normal stem cells, specifically the ability to give rise to all cell types found in a particular cancer sample. CSCs are therefore tumorigenic (tumor-forming), perhaps in contrast to other non-tumorigenic cancer cells. CSCs may generate tumors through the stem cell processes of self-renewal and differentiation into multiple cell types. Such cells are proposed to persist in tumors as a distinct population and cause relapse and metastasis by giving rise to new tumors (Fig. 1.1).

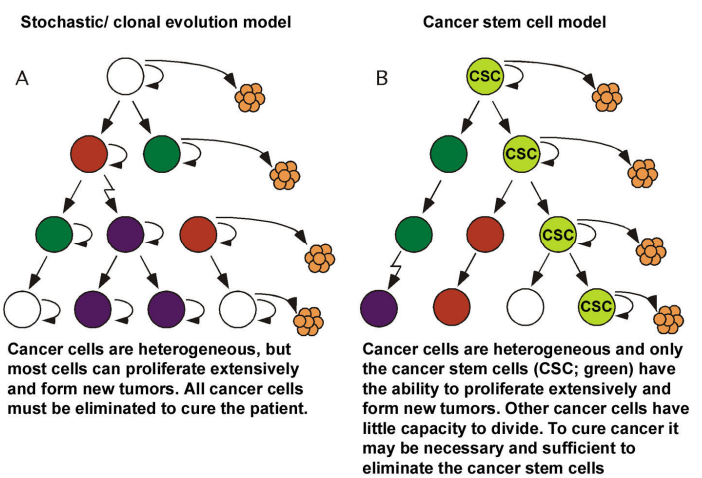

Fig. 1.1 Two general models of heterogeneity in solid cancer cells. (A) Cancer cells of many different phenotypes have the potential to proliferate extensively, but any one cell would have a low probability of exhibiting this potential in an assay of clonogenicity or tumorigenicity. (B) Most cancer cells have only limited proliferative potential, but a subset of cancer cells consistently proliferate extensively in clonogenic assays and can form new tumors on transplantation. The model shown in (B) predicts that a distinct subset of cells is enriched for the ability to form new tumors, whereas most cells are depleted of this ability. Existing therapeutic approaches have been based largely on the model shown in (A), but the failure of these therapies to cure most solid cancers suggests that the model shown in (B) may be more accurate (Reya, Morrison et al. 2001).

The existence of CSCs is a subject of debate within medical research, because many studies have not been successful in discovering the similarities and differences between normal tissue stem cells and cancer stem cells (Gupta, Chaffer et al. 2009). The first conclusive evidence for CSCs was published in 1997 in *Nature Medicine* (Bonnet and Dick 1997). Bonnet and Dick isolated a subpopulation of leukemic cells that express a specific surface marker CD34, but lack the CD38 marker. The authors established that the $CD34^{+}/CD38^{-}$ subpopulation is capable of initiating tumors in NOD/SCID mice that is histologically similar to the donor. The existence of leukemic stem cells prompted further research into other types of cancer. CSCs have recently been identified in several solid tumors, including cancers of the brain (Singh, Clarke et al. 2003), breast (Al-Hajj, Wicha et al. 2003), colon (O'Brien, Pollett et al. 2007), ovary (Zhang, Balch et al. 2008), pancreas (Li, Heidt et al. 2007), prostate (Maitland and Collins 2008; Lang, Frame et al. 2009), melanoma (Schatton, Murphy et al. 2008; Boiko, Razorenova et al. 2010) and multiple myeloma (Matsui, Huff et al. 2004; Matsui, Wang et al. 2008).

The origin of cancer stem cells is still an area of ongoing research. Several camps have formed within the scientific community regarding the issue (Bersenev 2009), and it is possible that several answers are correct, depending on the tumor type and the phenotype the tumor presents. One important distinction that will often be raised is that the cell of origin for a tumor cannot be demonstrated using the cancer stem cell as a model. This is because cancer stem cells are isolated from end-stage tumors. Therefore, describing a cancer stem cell as a cell of origin is often an inaccurate claim, even though a cancer stem cell is capable of initiating new tumor formation.

With that caveat mentioned, various theories define the origin of cancer stem cells. In brief, they may be: mutants in developing stem or progenitor cells, mutants in adult stem cells or adult progenitor cells, or mutant cells that acquire stem like attributes. These theories often do focus on a tumor's cell of origin and as such must be approached with skepticism. Some researchers favor the theory that the cancer stem cell is caused by a mutation in stem cell niche populations during development. The logical progression claims that these developing stem populations are mutated and then expand such that the mutation is shared by many of the descendants of the

mutated stem cell. These daughter stem cells are then much closer to becoming tumors, and since there are many of them there is more chance of a mutation that can cause cancer (Wang, Yang et al. 2009). Another theory associates adult stem cells with the formation of tumors. This is most often associated with tissues with a high rate of cell turnover (such as the skin or gut). In these tissues, it has long been expected that stem cells are responsible for tumor formation. This is a consequence of the frequent cell divisions of these stem cells compared to most adult stem cells in conjunction with the extremely long lifespan of adult stem cells. This combination creates the ideal set of circumstances for mutations to accumulate; accumulation of mutations is the primary factor that drives cancer initiation. In spite of the logical backing of the theory, only recently has evidence appeared that this association represents an actual phenomenon. It is important to bear in mind that, due to the heterogeneous nature of evidence, it is possible that any individual cancer could come from an alternative origin. A third possibility often raised is the potential de-differentiation of mutated cells such that these cells acquire stem cell like characteristics. This is often used as a potential alternative to any specific cell of origin, as it suggests that any cell might become a cancer stem cell. Another related concept is the concept of tumor hierarchy. This concept claims that a tumor is a heterogeneous population of mutant cells, all of which share some mutations but will vary in specific phenotype. In this model, the tumor is made up of several types of stem cells, one optimal to the specific environment and several less successful lines. These secondary lines can become more successful in some environments, allowing the tumor to adapt to its environment, including the methods by which tumors can be treated. If this situation is accurate, it has severe repercussions on the realism of a cancer stem cell-specific treatment regime (Clarke, Dick et al. 2006). Within a tumor hierarchy model, it would be extremely difficult to pinpoint the cancer stem cell's origin.

Not only is finding the source of cancer cells necessary for successful treatments, but if current treatments of cancer do not properly destroy enough CSCs, the tumor will reappear (Fig.1.2). Including the possibility that the treatment of for instance, chemotherapy, will leave only chemotherapy-resistant CSCs, then the ensuing tumor

will most likely also be resistant to chemotherapy. If the cancer tumor is detected early enough, enough of the tumor can be killed off and marginalized with traditional

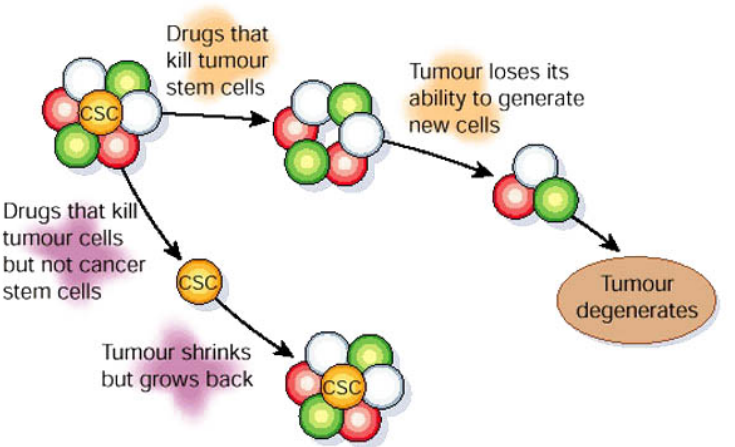

Fig. 1.2 Conventional therapies may shrink tumors by killing mainly cells with limited proliferative potential. If the putative cancer stem cells are less sensitive to these therapies, then they will remain viable after therapy and re-establish the tumor. By contrast, if therapies can be targeted against cancer stem cells, then they might more effectively kill the cancer stem cells, rendering the tumors unable to maintain themselves or grow. Thus, even if cancer stem cell-directed therapies do not shrink tumors initially, they may eventually lead to cures (Reya, Morrison et al. 2001).

treatment. But as the tumor size increases, it becomes more and more difficult to remove the tumor without conferring resistance and leaving enough behind for the tumor to reappear. The existence of CSCs has several implications in terms of future cancer treatment and therapies. These include disease identification, selective drug targets, prevention of metastasis, and development of new intervention strategies. Normal somatic stem cells are naturally resistant to chemotherapeutic agents. They have various pumps (such as MDR) that pump out drugs, DNA repair proteins and they also have a slow rate of cell turnover (chemotherapeutic agents naturally target rapidly replicating cells). CSCs that have mutated from normal stem cells may also express proteins that would increase their resistance towards chemotherapeutic agents. These surviving CSCs then repopulate the tumor, causing relapse. By selectively targeting CSCs, it would be possible to treat patients with aggressive, non-resectable tumors, as well as preventing the tumor from metastasizing. The

hypothesis suggests that upon CSC elimination, cancer would regress due to differentiation and/or cell death. What fraction of tumor cells are CSCs and therefore need to be eliminated is not clear yet (Dirks 2010). A number of studies have investigated the possibility of identifying specific markers that may distinguish CSCs from the bulk of the tumor as well as from normal stem cells. Proteomic and genomic signatures of tumors are also being investigated. In 2009, scientists identified one compound, salinomycin, which selectively reduces the proportion of breast CSCs in mice by more than 100-fold relative to paclitaxel, a commonly used chemotherapeutic agent (Gupta, Onder et al. 2009).

The design of new drugs for the treatment of CSCs will likely require an understanding of the cellular mechanisms that regulate cell proliferation. The first advances in this area were made with hematopoietic stem cells (HSCs) and their transformed counterparts in leukemia, the disease for which the origin of CSCs is best understood. It is now becoming increasingly clear that stem cells of many organs share the same cellular pathways as leukemia-derived HSCs. Additionally, a normal stem cell may be transformed into a cancer stem cell through dysregulation of the proliferation and differentiation pathways controlling it or by inducing oncoprotein activity.

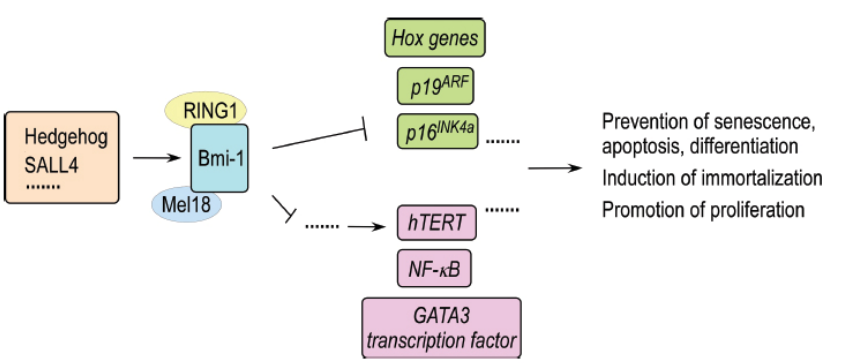

Fig. 1.3 Bmi-1 plays important roles in the regulation of stem cells via the activation of multiple pathways. Bmi-1, which could be up-regulated by SALL4 and Hedgehog (Hh) signal, regulates stem cell self-renewal through repression of Hox genes and INK4a locus genes, $p16^{INK4a}$ and $p19^{ARF}$, and activation of telomerase, transcriptional factor GATA3, and NF-kB pathway. These genes and signaling are likely to play a role in stem cell fate decisions including the prevention of senescence, apoptosis and differentiation, as well as the induction of immortalization and promotion of proliferation (Jiang, Li et al. 2009).

The Polycomb group transcriptional repressor Bmi-1 was discovered as a common oncogene activated in lymphoma (Haupt, Bath et al. 1993) and later shown to specifically regulate HSCs (Park, Qian et al. 2003). The role of Bmi-1 (Fig. 1.3) has also been illustrated in neural stem cells (Molofsky, Pardal et al. 2003). The pathway appears to be active in CSCs of pediatric brain tumors (Hemmati, Nakano et al. 2003).

The Notch pathway (Fig. 1.4) has been known to developmental biologists for decades. Its role in control of stem cell proliferation has now been demonstrated for several cell types including hematopoietic, neural and mammary stem cells (Dontu, Jackson et al. 2004). Components of the Notch pathway have been proposed to act

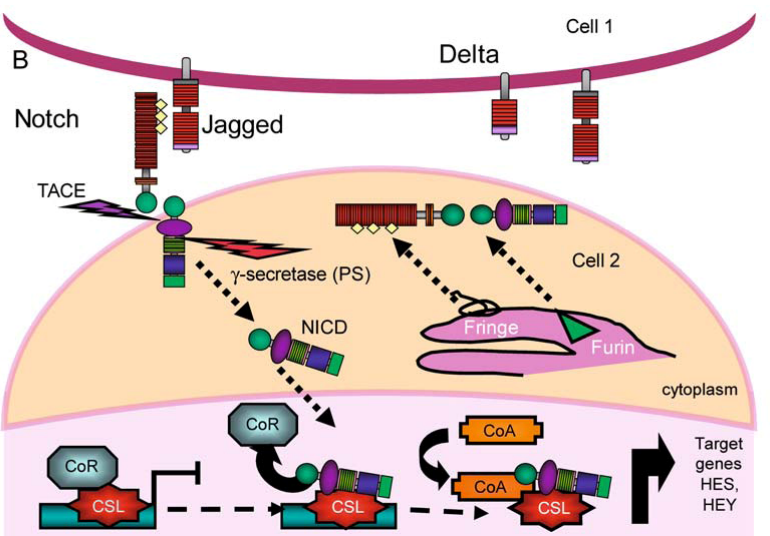

Fig. 1.4 Notch signaling pathway. Notch receptors are synthesized as single precursor proteins that are cleaved during transport to the cell surface, where they are expressed as heterodimers. Following the binding of the ligand, placed in the surface of a neighboring cell, NOTCH is activated by two consecutive proteolytic cleavages that release its intracellular domain (NICD). The first proteolytic cleavage is mediated by the metalloprotease TACE, which cleaves the receptor on the extracellular side, near the transmembrane domain. The second cleavage occurs within the transmembrane domain and is mediated by a gamma-secretase activity whose key component is presenilin. This final cleavage liberates the NICD, which subsequently translocates to the nucleus where it binds to the transcription factor CBF1. This interaction converts CBF1 from a transcriptional repressor into a transcriptional activator by displacing nuclear co-repressor proteins (CoR) and through the recruitment of nuclear co-activator proteins (CoA) (Bolos, Blanco et al. 2009).

as oncogenes in mammary (Dievart, Beaulieu et al. 1999) and other tumors. These developmental pathways are also strongly implicated as stem cell regulators (Beachy, Karhadkar et al. 2004).

Both Sonic hedgehog (SHH) (Fig. 1.5) and Wnt pathways (Fig.1.6) are commonly hyperactivated in tumors and are required to sustain tumor growth. However, the Gli transcription factors that are regulated by SHH take their name from gliomas, where they are commonly expressed at high levels. A degree of crosstalk exists between

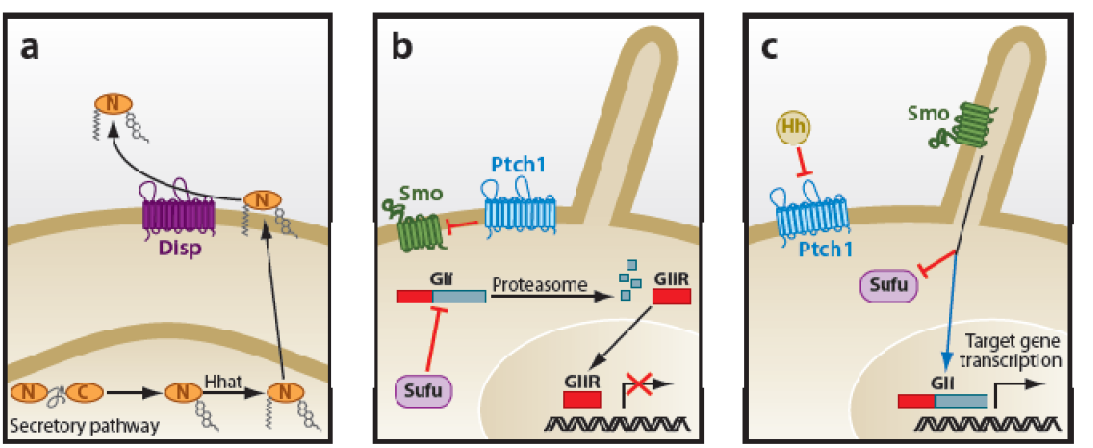

Fig. 1.5 Hh signaling in mammals. (a) Hh protein production. Autocatalytic cleavage of the Hh precursor protein yields a cholesterol-modified signaling peptide (HhN) that is further palmitoylated by Hh acyltransferase (Hhat). Lipophilic HhN released from the plasma membrane by Dispatched (Disp) is distributed to other cells. (b, c) Hh pathway response. The suppressive action of Patched 1 (Ptch1) on Smoothened (Smo) (b) is inhibited by binding of Hh to Ptch1, a 12-transmembrane protein with structural similarities to the resistance nodulation division (RND) family of small-molecule transporters (c). Smo controls activity of Ci/Gli transcription by regulating nuclear localization and proteolytic processing into repressor molecules. Suppressor of fused homolog (Sufu) appears to be the primary pathway suppressor in mammals, although its regulation by Smo has not been demonstrated. Abbreviations: GliR, glioma-associated oncogene family zinc finger, repressor domain; Hh, Hedgehog signaling molecule (Dodge and Lum 2010).

the two pathways and their activation commonly goes hand-in-hand (Zhou and Hung 2005). This is a trend rather than a rule. For instance, in colon cancer hedgehog signaling appears to antagonize Wnt (Akiyoshi, Nakamura et al. 2006). Sonic hedgehog blockers are available, such as cyclopamine. There is also a new water

soluble cyclopamine that may be more effective in cancer treatment. There is also DMAPT, a water soluble derivative of parthenolide (induces oxidative stress, inhibits NF-κB signaling (She and Chen 2009)) for AML, and possibly myeloma and prostate cancer. A clinical trial of DMAPT was to start in England in late 2007 or 2008. Furthermore, GRN163L was recently started in trials to target myeloma stem cells. If it is possible to eliminate the cancer stem cell, then a potential cure may be achieved if there are no more CSCs to repopulate a cancer. Finally, the enzyme telomerase may qualify as a study subject in CSC physiology (Bollmann 2008).

1.1.2 Tools and methods to study cancer stem cells

The success of our efforts in translating cancer stem cell research into clinical

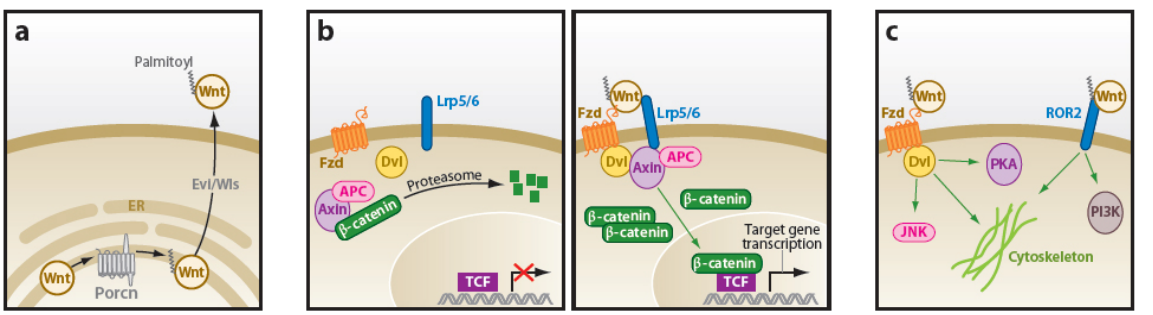

Fig. 1.6 Wnt-dependent pathway responses. (a) Production of Wnt proteins. Production of active Wnt molecules is dependent on the extracellular acyltransferase porcupine (Porcn) that adds a palmitoyl adduct to Wnts in the endoplasmic reticulum (ER). Acylated Wnt is then chaperoned by a seven-transmembrane protein—Evenness interrupted/Wntless (Evi/Wls)—to the extracellular milieu. (b) Activation of the Wnt/β-catenin pathway. A Wnt protein, Lrp5/6, and a Fzd receptor complex (right) recruit the APC/Axin complex, β-catenin, and a Disheveled (Dvl) scaffolding protein to the membrane, thus abrogating destruction of β-catenin (left). Accumulated β-catenin activates members of the TCF/LEF transcription factor family. (c) Examples of β-catenin-independent (noncanonical) Wnt pathway responses include the Wnt/JNK, Wnt/PKA, and Wnt/ROR2 pathways. Other pathway responses include Wnt-mediated control of cytoskeletal rearrangement. Like the Wnt/β-catenin pathway, many of these pathways utilize Dvl as an intracellular signaling molecule. Abbreviations: APC, adenomatous polyposis coli; JNK, c-Jun NH2-terminal kinase; LEF, lymphocyte enhancement factor; PI3K, phosphoinositide 3-kinase; PKA, protein kinase A; ROR2, receptor tyrosine kinase-like orphan receptor 2; TCF, T-cell factor (Dodge and Lum 2010).

practice depends on how thorough and rigorous we are at characterizing these cells. It also relies on how practical and reliable the markers and assays are designed to study CSCs. Currently, the techniques for the characterization of cancer stem cells include: Side Population (SP) technique, expression of cell surface markers, ALDEFLUOR assay, *in situ* detection and anchorage-independent cell culture (Charafe-Jauffret, Ginestier et al. 2009).

The SP technique has been used for many years to isolate both normal and tumor stem cells from different organs and species (Hirschmann-Jax, Foster et al. 2004; Montanaro, Liadaki et al. 2004; Setoguchi, Taga et al. 2004; Ho, Ng et al. 2007; Minn, Gupta et al. 2007). It is based on the abilities of stem cells to exclude vital dyes. Normal and cancer stem cells express transmembrane transporters, such as the ATP-binding cassette protein, ABC transporter ABCG2/BCRP1 (breast cancer resistance protein 1). These molecules exclude dyes such as Hoechst 33342 or Rhodamin 123 from the cells, a property not found in differentiated cells that remain positive for the dye. The SP technique for CSCs has also been successfully used in different species and tissues. However, functional studies using Hoechst staining are limited by the toxicity of this agent. Consequently, if Hoechst-positive cells do not grow *in vivo* or *in vitro*, the reason could be a direct toxic effect of the dye, shedding doubts on the reliability of the experiments. Furthermore, evidence from mouse models indicates that the mammary repopulating units with functional stem cell activity are not contained within the SP (Montanaro, Liadaki et al. 2004; Pearce and Bonnet 2007). This is mainly why the SP technique is no longer the preferred approach for stem cell studies.

Expression of cell surface markers has been widely used to isolate stem cells, but the choice of marker can greatly vary depending on tissues or species. For breast cancer stem cells study, the following markers have been used: $CD44^{+}/CD24^{-/low}/lin^{-}$ (Al-Hajj, Wicha et al. 2003; Ginestier, Hur et al. 2007), CD49f/ITGA6/α6-integrin (Stingl, Eirew et al. 2006; Cariati, Naderi et al. 2008), CD133/PROM/prominin (Wright, Calcagno et al. 2008; Meyer, Fleming et al. 2010), CD29/β1-integrin and CD61/β3-integrin (Shackleton, Vaillant et al. 2006; Asselin-Labat, Sutherland et al. 2007; Vaillant, Asselin-Labat et al. 2008). Flow cytometry methods using cell surface markers have been successfully applied to mice and human samples to isolate stem

cell populations. Markers available for cell sorting of stem cell populations of the mouse mammary gland are numerous, the functional assays well validated and the cellular hierarchy partly established. In contrast, in the human mammary gland, the markers are scarce, the assays difficult to standardize, and the actual hierarchy remains to be defined. Furthermore and curiously, the markers used in mice to sort specific stem cell populations are rarely valid in human. This observation emphasizes the need for other, more "universal" assays.

The ALDEFLUOR assay may fit the universality required for a stem cell marker to be reliable across species and tissues. It is based on the enzymatic activity of Aldehyde Dehydrogenase 1 (ALDH1) which is a detoxifying enzyme responsible for the oxidation of retinol to retinoic acid. ALDH1 may have a role in early differentiation of stem cells (Duester 2000; Sophos and Vasiliou 2003). High ALDH1 activity is associated with several types of murine and human stem hematopoietic and neural stem and progenitor cells (Armstrong, Stojkovic et al. 2004; Hess, Meyerrose et al. 2004; Matsui, Huff et al. 2004; Hess, Wirthlin et al. 2006). As few as 10 ALDEFLUOR-positive cells isolated from the rat hematopoietic system are capable of long term repopulation of bone marrow upon transplantation in sub-lethally irradiated animals (Armstrong, Stojkovic et al. 2004). ALDH1 activity also identified CSCs in multiple myeloma and leukemia patients with high capability of engraftment into NOD/SCID mice (Matsui, Huff et al. 2004; Pearce, Taussig et al. 2005). A recent study showed that ALDEFLUOR-positive cells isolated from the mouse brain were capable of self-renewal and able to generate neurospheres and neuroepithelial stem-like cells. These cells were capable of differentiation into multiple cell lineages *in vitro*, generating neurons and glia in culture. Furthermore, ALDEFLUOR-positive cells had a higher capacity to engraft *in vivo*, upon transplantation in brain, compared to ALDEFLUOR-negative cells (Corti, Locatelli et al. 2006). This method has been recently used with success to isolate stem and progenitor cells from mammary tissues. ALDEFLUOR-positive cells isolated from both normal and tumoral human breast had phenotypic and functional characteristics of mammary stem cells. Furthermore, the ALDEFLUOR-positive population isolated from human breast tumors contained the CSC population as demonstrated by the ability of these cells, but not of ALDEFLUOR-negative cells to generate tumors in NOD/SCID mice. Serial

passages of ALDEFLUOR-positive cells generated tumors recapitulating the phenotypical diversity of the initial tumor (Ginestier, Hur et al. 2007). However, the ALDEFLUOR assay does have some limitations for the isolation of the most tumorigenic population, notably in tumors of different origin. For example, both ALDEFLUOR (bright) and ALDEFLUOR (low) from the lung carcinoma cell line H 522 were able to initiate tumors after inoculation into NOD/SCID mice. Moreover, tumors generated from ALDEFLUOR (low) cells grew faster and bigger than the tumors from ALDEFLUOR (bright) and this remained true among passages. These results suggest that the ALDEFLUOR-positive population in lung carcinoma is not stem cell-enriched compared to the ALDEFLUOR-negative population (Ucar, Cogle et al. 2009). Furthermore, the stem cell population identified using the ALDEFLUOR assay is probably heterogeneous, and needs to be dissected using additional markers. In breast cancer cell lines, the ALDEFLUOR-population has been divided by the use of $CD44^+$, $CD24^-$ and CD133. ALDEFLUOR-positive $CD44^+/CD24^-$ and ALDEFLUOR-positive $CD44^+/CD133^+$ populations displayed the greatest tumorigenic and metastatic potential. This is the first time that CSCs obtained with a given marker are further divided using additional markers into distinct metastatic or not metastatic subpopulations (Croker, Goodale et al. 2009). In human hematopoietic stem cells, the $ALDEFLUOR^{high}lin^-$ population has also been separated in CD133-positive and negative subsets, with the former showing enhanced repopulating capacity in recipients of serial, secondary transplants (Hess, Wirthlin et al. 2006).

In situ detection of stem cells has the potential to transfer stem cell quantification to routine clinical practice for patient treatment and prognosis evaluation. It also allows the determination of the CSCs' location within the tumor either primary or metastatic sites, and the detection of stem cells in pre-invasive stages as well as their modifications during pre-malignant to malignant progression. So far, ALDH1A1 (Ginestier, Hur et al. 2007) and $CD44^+/CD24^{-/low}$ (Mylona, Giannopoulou et al. 2008) were successfully detected in paraffin-embedded human breast tumors which were associated with lymph node metastasis and poor prognosis. However, the use of ALDH1A1 to detect stem cells is not free of controversy. In transgenic mice, ALDH1A1 deficiency did not affect hematopoiesis and hematopoietic stem cell (HSC) function, or ALDEFLUOR staining (Levi, Yilmaz et al. 2009); it is possible that other

isoforms of ALDH, notably cytoplasmic isoforms such as ALDH1A3 were responsible both for the maintenance of HSC function and the remaining ALDEFLUOR staining. Even if the $CD44^{+}/CD24^{-/low}$ phenotype is a valuable marker for the isolation of breast CSCs it cannot be used in clinical settings. As pointed out by Gabriela Dontu in a recent commentary, the use of these markers raises several important questions (Dontu 2008).

Anchorage-independent cell culture in non-adherent conditions was initially adapted to normal breast tissue obtained from reduction mammoplasty. Human mammary stem and progenitor cells were able to survive in suspension and produce spherical colonies (mammosphere) composed of both stem and progenitor cells. These non-adherent mammosphere were enriched in early progenitor/stem cells and able to differentiate along the three mammary epithelial lineages and to clonally generate complex functional structures in reconstituted 3D culture systems as well as to reconstitute human normal mammary gland in mice (Dontu, Abdallah et al. 2003). This system is now widely used to study underlying mechanisms of growth under anchorage-independent conditions, and by extension, to discover pathways implicated in stem/progenitor cells survival. The mammosphere assay, based on the unique property of stem/progenitor cells to survive and grow in serum-free suspension, was also successfully used to establish long term-cultures enriched in stem/progenitor cells from invasive tumor samples. The mammosphere formed in these conditions were called tumorspheres. They showed an increase in SP fraction and in $CD44^{+}/CD24^{-/low}$ cells, over-expressed neoangiogenic and cytoprotective factors, expressed the putative stem cell marker OCT4, and displayed high tumorigenic potential in NOD/SCID mice (Ponti, Costa et al. 2005). Thus, the development of *in vitro* suspension culture systems not only provides an important new tool for the study of mammary cell biology, but also has important implications for understanding key molecular pathways in both normal and neoplastic stem cells. Thus, the development of *in vitro* suspension culture systems not only provide an important new tool for the study of mammary cell biology, but also has important implications for understanding key molecular pathways in both normal and neoplastic stem cells.

1.1.3 Cancer stem cells and metastases

Recent reports have suggested an interesting conjunction between studies of CSC and one of the primary cellular mechanisms believed to be involved in the metastatic process, namely the so-called Epithelial-Mesenchymal Transition (EMT) (Ben-Porath, Thomson et al. 2008; Mani, Guo et al. 2008; Morel, Lievre et al. 2008; Weinberg 2008). Epithelial cells, which form stable cell-cell interactions through adherent junctions, can be reprogrammed to adopt a mesenchymal phenotype by transcription factors, such as SNAIL and TWIST that suppress E-cadherin (Guarino, Rubino et al. 2007; Tse and Kalluri 2007; Gavert and Ben-Ze'ev 2008; Thompson and Williams 2008; Turley, Veiseh et al. 2008). This is characterized by the loosening of cell-cell contact and increased extracellular matrix interaction via integrins and focal adhesion kinase (FAK). Cells undergoing EMT typically show a less well-differentiated morphology, express vimentin rather than cytokeratin, and become more motile. The presence of tumor cells with these features appears to correlate with poor prognosis because of the development of metastases and drug resistance (Berx, Raspe et al. 2007; Tse and Kalluri 2007; Gavert and Ben-Ze'ev 2008; Yang, Wu et al. 2008). Another link between CSCs and metastasis is the overexpression of stem cell-associated genes in metastatic tumors. For instance, the polycomb group genes EZH2 and BMI1, which function as transcriptional repressors, play a crucial role in stem cell maintenance (Valk-Lingbeek, Bruggeman et al. 2004) and are over-expressed in several metastatic cancers (Varambally, Dhanasekaran et al. 2002; Kleer, Cao et al. 2003; Kim, Yoon et al. 2004; Berezovska, Glinskii et al. 2006). EZH2 levels increase with tumor progression and both a BMI1-related (Glinsky, Berezovska et al. 2005) and an EZH2-based (Yu, Rhodes et al. 2007) “stem cell gene signature” can predict poor survival and metastasis in cancer patients. Researchers from the groups of Chang and Weinberg showed that an embryonic stem cell gene expression module is present in several tumor types, and is predictive for metastasis and poor survival (Ben-Porath, Thomson et al. 2008; Wong, Liu et al. 2008). Stem cell-like subpopulations isolated from lung tumor cell lines display higher in vitro invasiveness than non stem cell-like cells (Ho, Ng et al. 2007). Hermann et al. identified CSCs in human pancreatic tumors and showed that a proportion of CSCs at the invasive front

express CXCR4 (Hermann, Huber et al. 2007). Whereas all pancreatic CSCs formed tumors in nude mice, only the CXCR4-positive subpopulation metastasized. Migrating cancer stem cells have been described also for colon cancer (Brabletz, Hlubek et al. 2005), where nuclear staining of β-catenin (normally found in colon epithelium stem cells) can be detected in tumor cells at the invasive front (Brabletz, Jung et al. 2001). However, the stem cell potential of these cells was not directly investigated in that study. What has been shown is that WNT signaling mediates migration and invasion of human mesenchymal stem cells (Neth, Ciccarella et al. 2006). Another example of stem cell-like features playing a role in metastasis is provided by the morphogen NODAL, which maintains pluripotency in human embryonic stem cells (Hendrix, Seftor et al. 2007). NODAL is over-expressed also in aggressive melanomas, in which it may be involved in maintaining a dedifferentiated phenotype, while it is required for the formation of tumors in nude mice (Topczewska, Postovit et al. 2006).

1.1.4 Breast cancer stem cells

Breast cancer is the most frequent malignancy among women in Western countries, with an incidence in the U.S. of 111 cases per 100,000 woman-years (wy) and a mortality rate of 24 deaths per 100,000 wy (Howe, Wingo et al. 2001). Although the mortality of breast cancer has been decreasing (Peto, Boreham et al. 2000; Howe, Wingo et al. 2001), which was believed to be the result of widespread mammography screening and the implementation of adjuvant therapy with tamoxifen and polychemotherapy (EBCT 1998; EBCT 1998), breast cancer still is the most fatal disease for women in Western countries (Howe, Wingo et al. 2001). In 2003, Clarke and colleagues demonstrated that a highly tumorigenic subpopulation of breast cancer stem cells expressing $CD44^+/CD24^-$ surface marker in clinical specimen had the capacity to form tumors with as few as one hundred cells whereas tens of thousands of the bulk cells did not (Al-Hajj, Wicha et al. 2003). Recently, accumulating evidence indicates that breast cancer is originated from breast cancer stem cells, a rare population within breast tumor (Al-Hajj, Wicha et al. 2003; Al-Hajj, Becker et al. 2004). The current cancer drugs, which are developed extensively based on their activity to inhibit bulk replicating cancer cells, may not be able to eliminate the cancer stem cells effectively, as has been demonstrated in a variety of

tumors (Costello, Mallet et al. 2000; Reya, Morrison et al. 2001; Graham, Jorgensen et al. 2002; Guzman and Jordan 2004; Jones, Matsui et al. 2004; Angstreich, Matsui et al. 2005; Donnenberg and Donnenberg 2005). It is conceivable that improved breast cancer treatment requires eradication of cancer stem cells (Reya, Morrison et al. 2001; Al-Hajj, Becker et al. 2004; Jones, Matsui et al. 2004; Behbod and Rosen 2005; Dean, Fojo et al. 2005).

1.2 Vaccinia Virus

Vaccinia virus (VACV or VV) is a large, complex, enveloped virus belonging to the poxvirus family (Ryan and Ray 2004). It has a linear, double-stranded DNA genome approximately 190 kbp in length, and which encodes for approximately 250 genes. The dimensions of the virion are roughly 360 × 270 × 250 nm, with a mass of approximately 5-10 fg (Johnson, Gupta et al. 2006). Vaccinia virus is well-known for its role as a vaccine that eradicated the smallpox disease, making it the first human disease to be successfully eradicated by science. This endeavour was carried out by the World Health Organization under the Smallpox Eradication Program. Post eradication of smallpox, scientists study vaccinia virus to use as a tool for delivering genes into biological tissues (gene therapy and genetic engineering).

1.2.1 Taxonomy

The vaccinia virus belongs to the family of poxviruses, which are complex DNA viruses that replicate in the cytoplasm of vertebrate or invertebrate cells. Poxviridae are divided into two subfamilies, the chordopoxviridae and the entomopoxviridae. This distinction is based on their host range, which are insects for the entomopoxviridae and vertebrates for the chordopoxviridae. The subfamily of the chordopoxviridae consists of eight genera: orthopoxviruses, parapoxviruses, avipoxviruses, capripoxviruses, leporipoxviruses, suipoxviruses, molluscipoxviruses and yatapoxviruses. The orthopoxviruses have been studied most intensively. Both the human pathogen variola virus and the vaccinia virus belong to the orthopoxviruses whereas vaccinia virus is most studied virus of the genus.

1.2.2 History

The originof the idea of vaccination and the original vaccine for smallpox, the cowpox virus, was reported in 1796 by Edward Jenner. (Henderson and Moss 1988). The Latin term used for Cowpox was variolae vaccinae, essentially a direct translation of "cow-related pox". That term lent its name to the whole idea of vaccination. When it was realized that the virus used in smallpox vaccination was not, or was no longer, the same as the Cowpox virus, the name 'vaccinia' stayed with the vaccine-related virus. Vaccine potency and efficacy prior to the invention of refrigerated methods of transportation was unreliable. The vaccine would be rendered impotent by heat and sunlight, and the method of drying samples on quills and shipping them to countries in need often resulted in an inactive vaccine. Another method employed was the "arm to arm" method. This involved vaccinating an individual then transferring it to another as soon as the infectious pustule forms, then to another, etc. This method was used as a form of living transportation of the vaccine, and usually employed orphans as carriers. However, this method was problematic due to the possibility of spreading other blood diseases, such as hepatitis and syphilis. Forty-one Italian children contracted syphilis after being vaccinated by the arm to arm method in 1861(Tucker and Jonathan 2001). In 1913, E. Steinhardt, C. Israeli, and R. A. Lambert grew vaccinia virus in fragments of guinea pig corneal tissue culture (Steinhardt, Israeli et al. 1913). In 1939 Downie showed that the smallpox vaccines being used in the 20th century and cowpox virus were not the same, but some sorts of cousins (Mccarthy and Mcentegart 1989; Smith and L 2004).

1.2.3 Morphology

Poxviruses are large DNA viruses. They contain a double-strand DNA molecule between 130 and 300 kb (Knipe, Howley et al. 2007) that encodes for around 200 genes. The DNA is associated with a number of virus-encoded proteins like RNA polymerase, transcription factors and enzymes for RNA capping, methylation and polyadenlation, which are packaged within the core to enable early viral protein synthesis (Shen and Nemunaitis 2005). In molecular biology it is very useful as a vector because up to 25 kb can be integrated in its genome (Smith and Moss 1983).

The basic infectious form of the poxvirus is the mature virion. The virions have a barrel shape with dimensions of ~360×270×250 nm (Fig. 1.7). The thickness (5-6 nm) and density of the outer layer is comparable to one lipid membrane bilayer. The internal structure of the virion consists of a dumbbell-shaped core and aggregates of heterogeneous material which are called lateral bodies between the concavities and the outer membrane. The core wall consists of two layers. The inner layer is continuous except for a few channels and has a diameter resembling a lipid membrane. The outer layer has a palisade structure that is made of T-shaped spikes that are anchored in the lower membrane. The main components are protein (90%), lipid (5%) and DNA (3.2%). The lipid components of vaccinia virus are predominantly cholesterol and phospholipids (Stern and Dales 1974; Sodeik, Doms et al. 1993).

1.2.4 Vaccinia virus replication cycle

The infection of a cell begins with the binding of a vaccinia virus particle to the cell. It is not known exactly how the virus binds the cell membrane, but the virus is thought to be taken in by membrane fusion. After the fusion of the viral and cellular membranes, the viral core that contains the necessary proteins for early replication is released into the cytoplasm and transported further into the cell along microtubules to the cytoplasmic side of the endoplasmatic reticulum (ER). Unlike other DNA viruses,

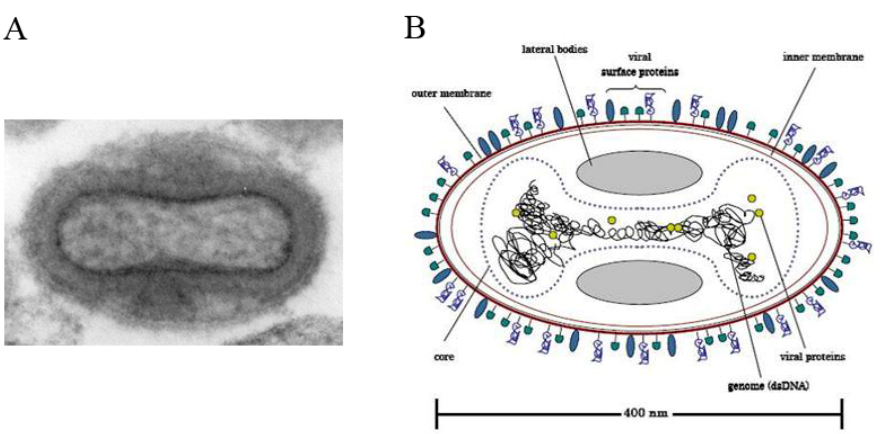

Fig. 1.7 Morphology of vaccinia virus. (A) Transmission electron micrograph of poxvirus virions. (B) Schematic structure of the vaccinia virus.

vaccinia virus remains in the host cytoplasm for the duration of the infectious cycle. After entry into the cytoplasm, the core partially uncoats to synthesize early viral mRNA which resembles host cell mRNAs. This happens in a period of 20 minutes after infection of the virus particle. The cellular translational apparatus is recruited for translation of these mRNAs that encode for proteins involved in viral DNA synthesis. Other early proteins serve to modify the host cell to the advantage of the virus and destroy the viral nuclear membrane to free the genome (Sieczkarski and Whittaker 2005). Replication of the viral DNA starts one to two hours after infection (Knipe, Howley et al. 2007). After the DNA replication has started in so-called mini-nuclei, which are surrounded by rough ER membranes, immediate genes and late genes are transcribed (Tolonen, Doglio et al. 2001). Immediate genes serve mainly for the transcription of late genes, which are involved in packaging of the new viral particles and for essential proteins that start the early gene transcription in an infected cell. After synthesis of all the necessary proteins, assembly of mature virus particles begins (Harrison, Alberts et al. 2004). Assembly involves condensation of viral DNA, packing in the nuclear membrane and proteolytic cleavage of some capsid proteins (Smith and Moss 1983). Intracellular mature virions (IMVs) will either be released by lysis of the cell or move away from DNA sites by binding to microtubules of the host cell and get a second double membrane from a trans-Golgi or early endosomal

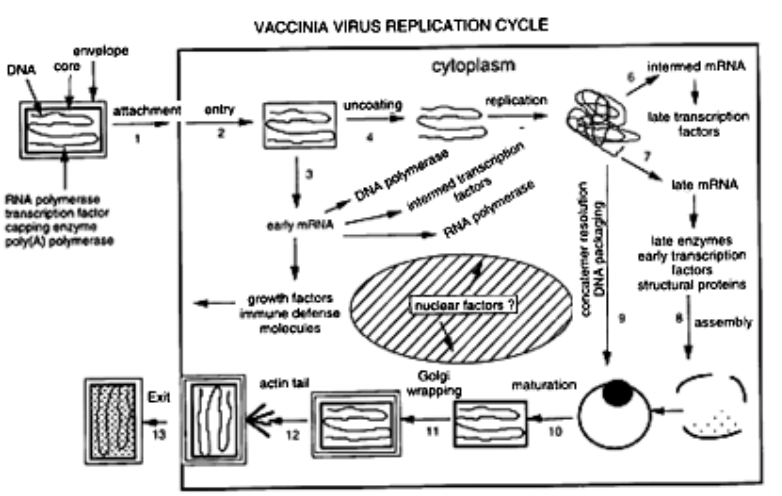

Fig. 1.8 Replication cycle of Vaccinia Virus.

compartment to become intracellular enveloped virions (IEVs) (Harrison, Alberts et al. 2004). The IEV particles use microtubules and kinesins to move towards the cell membranes and fuse with the membranes to form cell-associated enveloped virus (CEVs). CEVs can use actin from the cytoplasm to be transported to neighboring cells or dissociated from the cell membrane to become extracellular enveloped viruses (EEVs). Most of the EEVs are still bound to the cell membrane even at late stages of infection (Blasco and Moss 1992).

The replication and assembly of new virus particles is regulated by a time-dependent control of the gene expression. Proteins, which are used for DNA replication, nucleotide biosynthesis and destruction of the nuclear membrane to free the DNA, are synthesized early in the infection cycle. Proteins, which are used for the morphogenesis and assembly of the new viruses, are intermediate and late gene products (Rosel and Moss 1985).

Gene expression is mainly regulated at the initiation step of the transcription. Transcription factors for intermediate genes are synthesized as early proteins and transcription factors for late genes are products of intermediate genes. Transcription factors for early genes are made as late proteins of the previous cycle and packaged into new virions so they are brought into the cell by the infecting viruses and can start early gene transcription immediately. Around 50% of all genes belong to the early genes (Oda and Joklik 1967). These genes are synthesized in the viral nucleus. The intermediate and late transcription happens in the cytoplasm and uses also proteins of the host cell for initiation and termination of the transcription instead of only viral proteins in the early transcription (Broyles 2003).

1.2.5 Oncolytic virotherapy and cancer stem cells

The past decade has seen an explosion of research into the field of gene therapy and therapeutic or so-called “oncolytic,” viruses (Liu and Kirn 2008). Such viruses fall into broad categories of (1) wild-type animal viruses that do not typically infect human cells but are cytotoxic to human cancer cells, (2) attenuated mutants of human viruses in which critical genes for virus replication that are dispensable in cancer cells have been deleted or mutated, and (3) viruses that have been attenuated by serial passage in culture, such as most live virus vaccines. These agents hold much

promise as they have been shown to be efficacious against malignant tissues, yet minimally toxic to their normal cell and tissue counterparts. Oncolytic viruses are effective against a wide variety of human cancers in preclinical models and encouraging results from clinical trials are beginning to accumulate. Novel methods of delivery, including cell-based schemes, appear to increase their ability to reach distant metastatic sites of disease, counteracting a major criticism that they will be useful only for localized disease (Power and Bell 2007). Oncolytic viruses may also be engineered to deliver therapeutic transgenes, thereby increasing their anti-tumor effects.

The question of whether oncolytic viruses are well suited to eliminate cancer stem cells has begun to be addressed. Oncolytic viruses seem like ideal candidates to target CSCs because they are cytotoxic and are not subject to the typical mechanisms of drug resistance such as drug efflux pumps and defective apoptotic signaling (Coukos, Makrigiannakis et al. 2000). In addition, viruses may be engineered to express therapeutic transgenes that specifically target properties that CSCs rely upon for self-renewal and cell division. Indeed, initial studies suggest that oncolytic viruses may be effective against and may be directed toward CSCs (Mahller, Williams et al. 2009). According to the fundamental difference of its life cycles, oncolytic viruses were divided to two subgroups: DNA viruses which replicate in the nucleus and RNA viruses which replicate in the cytoplasm. So far, in the category of DNA viruses, Herpes simplex virus (Todo, Martuza et al. 2001; Otsuki, Patel et al. 2008; Mahller, Williams et al. 2009; Wakimoto, Kesari et al. 2009), adenovirus (Eriksson, Guse et al. 2007; Jiang, Gomez-Manzano et al. 2007; Skog, Edlund et al. 2007), myxoma virus (Redding, Zhou et al. 2009) were used for CSCs therapy study; in the category of RNA viruses, reovirus (Marcato, Dean et al. 2009), vesicular stomatitis virus (Cripe, Wang et al. 2009) were used for CSCs therapy study. Those studies mainly focus on the three cancer types of glioblastoma, breast cancer and neuroblastoma. For many different cancer types there is now considerable evidence supporting the stem cell theory of cancer, which suggests that a relatively small subpopulation of cells (CSCs) within a tumor are actually tumorigenic and responsible for generating the bulk of non-tumorigenic cancer cells. Although not yet proven, the identification, isolation, and characterization of such

cells is likely to be paramount to discover effective new cancer therapies that prevent relapse and improve long-term overall survival. With the recent resurgence of interest in the use of oncolytic viruses as cancer therapeutics, their effects on CICs may ultimately determine whether they play a significant role in improving survival rates. Because they are not subject to the same mechanisms mediating resistance to cytotoxic chemotherapy and irradiation, there is ample reason to postulate that oncolytic viruses will be effective eradicating CSCs. Although this topic is only beginning to be addressed as the identification of CSCs in various cancers are revealed, the data so far present a mixed picture. Some CSCs appear susceptible to virus infection and some do not, depending on the virus mutation and mechanism of attenuation (Cripe, Wang et al. 2009). Although there do not appear to be universal themes yet emerging, of this we are certain: with the myriad different virus types and genetic mutations under investigation as oncolytic agents and the rapidly expanding list of CSCs being discovered, the interaction of oncolytic viruses with CSCs will be a fruitful area of investigation for years to come.

1.2.6 Vaccinia virus strain used in this study

The recombinant virus GLV-1h68 (Fig. 1.9A) is a genetically stable oncolytic vaccinia virus that has been constructed by Genelux Corporation (San Diego, CA). It was shown that it is capable to locate, enter, colonize and destroy cancer cells without harming healthy cells (Zhang, Yu et al. 2007). GLV-1h68 was derived from the vaccinia virus Lister strain (*LIVP wt*), a European vaccine strain. Three expression cassettes were inserted into the *F14.5L*, *J2R* and *A56R* loci of the viral genome. These three expression cassettes are the *Renilla* luciferase *Aequorea* green fluorescent protein fusion gene (*RUC-GFP*), the β-galactosidase gene (*lacZ*) and the β-glucuronidase gene (*gusA*). The *RUC-GFP* fusion protein gene located in the *F14.5L* locus is under control of an early/late promoter whereas the marker gene the β-galactosidase in the *J2R* locus is under control of the $P_{7.5}$ promoter. Another marker gene coding for β-glucuronidase was inserted into *A56R* locus and is under control of the P_{11k} promoter. The recombinant virus GLV-1h190 (Fig. 1.9B) is derived from GLV-1h68 and the difference is Katushka, a far red fluorescent protein fusion gene

(*FUKW*) which is under control of P_{SL} promoter was inserted into *A56R* locus rather than β-glucuronidase gene (*gusA*).

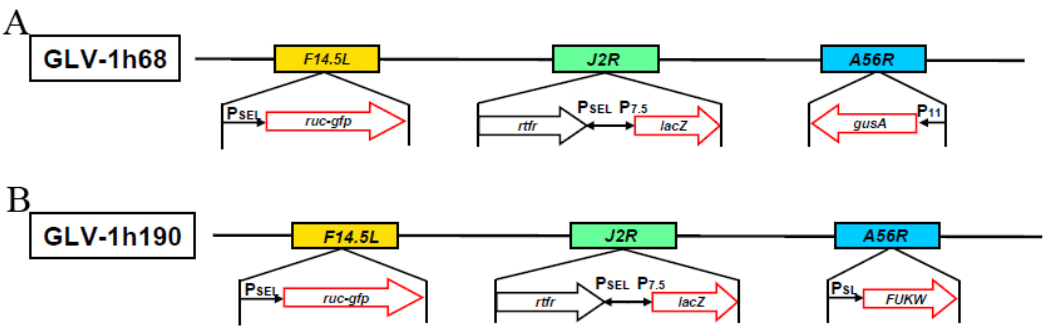

Fig. 1.9 Constructs and marker genes of (A) GLV-1h68 and (B) GLV-1h190.

1.3 Cancer

1.3.1 Concept and epidemiology

Cancer (medical term: malignant neoplasm) is a class of diseases in which a cell, or a group of cells display uncontrolled growth (division beyond the normal limits), invasion (intrusion on and destruction of adjacent tissues), and sometimes metastasis (spread to other locations in the body via lymph or blood). These three malignant properties of cancers differentiate them from benign tumors, which are self-limited, and do not invade or metastasize. Most cancers form a tumor but some, like leukemia, do not. The branch of medicine concerned with the study, diagnosis, treatment, and prevention of cancer is oncology. Cancer can affect people at all ages with the risk for most types increasing with age (Cancer-Research-UK 2007). It caused about 13% of all human deaths in 2007 (WHO 2006) (7.6 million) (Dunham 2007). Cancers are primarily an environmental disease with 90-95% of cases due to lifestyle and environmental factors and 5-10% due to genetics (Anand, Kunnumakkara et al. 2008). Common environmental factors leading to cancer death include: tobacco (25-30%), diet and obesity (30-35%), infections (15-20%), radiation, stress, lack of physical activity, environmental pollutants (Anand, Kunnumakkara et al. 2008). These environmental factors cause abnormalities in the genetic material of cells (Kinzler and Vogelstein 2002). Genetic abnormalities found in cancer typically

affect two general classes of genes. Cancer-promoting oncogenes are typically activated in cancer cells, giving those cells new properties, such as hyperactive growth and division, protection against programmed cell death, loss of respect for normal tissue boundaries, and the ability to become established in diverse tissue environments. Tumor suppressor genes are then inactivated in cancer cells, resulting in the loss of normal functions in those cells, such as accurate DNA replication, control over the cell cycle, orientation and adhesion within tissues, and interaction with protective cells of the immune system. Definitive diagnosis requires the histological examination of a biopsy specimen, although the initial indication of malignancy can be symptomatic or radiographic imaging abnormalities. Most cancers can be treated and some forced into remission, depending on the specific type, location, and stage. Once diagnosed, cancer is usually treated with a combination of surgery, chemotherapy and radiotherapy. As research develops, treatments are becoming more specific for different varieties of cancer. There has been significant progress in the development of targeted therapy drugs that act specifically on detectable molecular abnormalities in certain tumors, and which minimize damage to normal cells. The prognosis of cancer patients is mostly influenced by the type of cancer, as well as the stage, or extent of the disease. In addition, histological grading and the presence of specific molecular markers can also be useful in establishing prognosis, as well as in determining individual treatments.

As of 2004, worldwide cancer caused 13% of all deaths (7.4 million). The leading causes were: lung cancer (1.3 million deaths/year), stomach cancer (803,000 deaths), colorectal cancer (639,000 deaths), liver cancer (610,000 deaths), and breast cancer (519,000 deaths) (WHO 2009). More than 30% of cancer are preventable via avoiding risk factors including: tobacco, overweight or obesity, low fruit and vegetable intake, physical inactivity, alcohol, sexually transmitted infections, and air pollution (WHO 2006). In the United States, cancer is responsible for 25% of all deaths with 30% of these from lung cancer. The most commonly occurring cancer in men is prostate cancer (about 25% of new cases) and in women is breast cancer (also about 25%). Cancer can occur in children and adolescents, but it is uncommon (about 150 cases per million in the U.S.), with leukemia the most common (Jemal,

Siegel et al. 2008). In the first year of life the incidence is about 230 cases per million in the U.S., with the most common being neuroblastoma (Gurney, Smith et al. 1999). In the developed world, one in three people will develop cancer during their lifetimes. If all cancer patients survived and cancer occurred randomly, the lifetime odds of developing a second primary cancer would be one in nine (Rheingold, Neugut et al. 2003). However, cancer survivors have an increased risk of developing a second primary cancer, and the odds are about two in nine (Rheingold, Neugut et al. 2003). About half of these second primaries can be attributed to the normal one-in-nine risk associated with random chance (Rheingold, Neugut et al. 2003). The increased risk is believed to be primarily due to the same risk factors that produced the first cancer (such as the person's genetic profile, alcohol and tobacco use, obesity, and environmental exposures), and partly due to the treatment for the first cancer, which typically includes mutagenic chemotherapeutic drugs or radiation (Rheingold, Neugut et al. 2003). Cancer survivors may also be more likely to comply with recommended screening, and thus may be more likely than average to detect cancers (Rheingold, Neugut et al. 2003).

1.3.2 Classification

Cancers are classified by the type of cell that resembles the tumor and, therefore, the tissue presumed to be the origin of the tumor. These are the histology and the location, respectively. Examples of general categories include:

Carcinoma: Malignant tumors derived from epithelial cells. This group represents the most common cancers, including the common forms of breast, prostate, lung and colon cancer.

Sarcoma: Malignant tumors derived from connective tissue, or mesenchymal cells.

Lymphoma and leukemia: Malignancies derived from hematopoietic (blood-forming) cells.

Germ cell tumor: Tumors derived from totipotent cells. In adults most often found in the testicle and ovary; in fetuses, babies, and young children most often found on the body midline, particularly at the tip of the tailbone; in horses most often found at the poll (base of the skull).

Blastic tumor or blastoma: A tumor (usually malignant) which resembles an immature or embryonic tissue. Many of these tumors are most common in children. Malignant tumors (cancers) are usually named using -carcinoma, -sarcoma or –

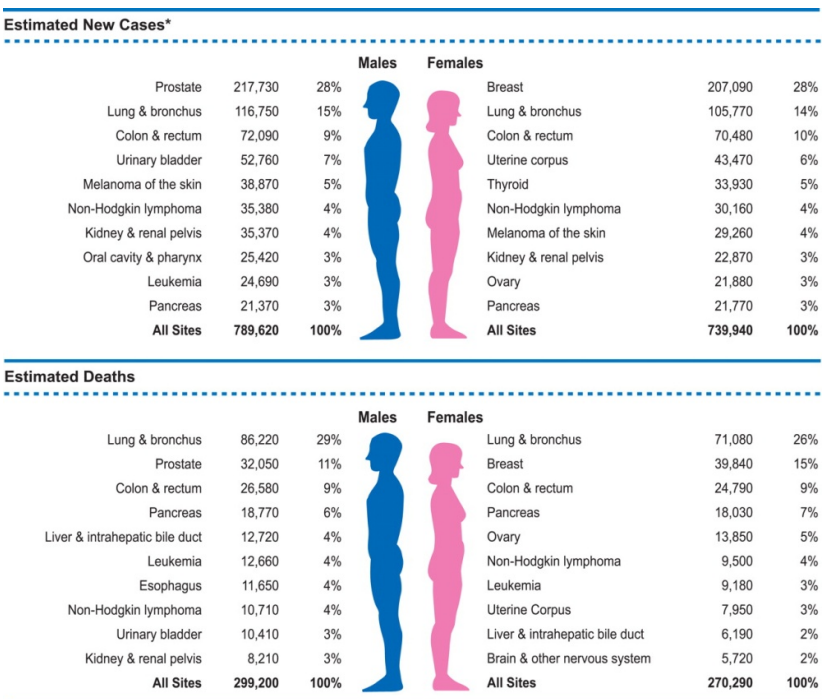

Estimated New Cases*

	Males			Females		
Prostate	217,730	28%		Breast	207,090	28%
Lung & bronchus	116,750	15%		Lung & bronchus	105,770	14%
Colon & rectum	72,090	9%		Colon & rectum	70,480	10%
Urinary bladder	52,760	7%		Uterine corpus	43,470	6%
Melanoma of the skin	38,870	5%		Thyroid	33,930	5%
Non-Hodgkin lymphoma	35,380	4%		Non-Hodgkin lymphoma	30,160	4%
Kidney & renal pelvis	35,370	4%		Melanoma of the skin	29,260	4%
Oral cavity & pharynx	25,420	3%		Kidney & renal pelvis	22,870	3%
Leukemia	24,690	3%		Ovary	21,880	3%
Pancreas	21,370	3%		Pancreas	21,770	3%
All Sites	**789,620**	**100%**		**All Sites**	**739,940**	**100%**

Estimated Deaths

	Males			Females		
Lung & bronchus	86,220	29%		Lung & bronchus	71,080	26%
Prostate	32,050	11%		Breast	39,840	15%
Colon & rectum	26,580	9%		Colon & rectum	24,790	9%
Pancreas	18,770	6%		Pancreas	18,030	7%
Liver & intrahepatic bile duct	12,720	4%		Ovary	13,850	5%
Leukemia	12,660	4%		Non-Hodgkin lymphoma	9,500	4%
Esophagus	11,650	4%		Leukemia	9,180	3%
Non-Hodgkin lymphoma	10,710	4%		Uterine Corpus	7,950	3%
Urinary bladder	10,410	3%		Liver & intrahepatic bile duct	6,190	2%
Kidney & renal pelvis	8,210	3%		Brain & other nervous system	5,720	2%
All Sites	**299,200**	**100%**		**All Sites**	**270,290**	**100%**

Fig. 1.10 Ten Leading Cancer Types for the Estimated New Cancer Cases and Deaths by Sex, 2010 (Jemal, Siegel et al. 2010).

as a suffix, with the Latin or Greek word for the organ of origin as the root. For instance, a cancer of the liver is called hepatocarcinoma; a cancer of the fat cells is called liposarcoma. For common cancers, the English organ name is used. For instance, the most common type of breast cancer is called ductal carcinoma of the breast or mammary ductal carcinoma. Here, the adjective ductal refers to the appearance of the cancer under the microscope, resembling normal breast ducts.

Benign tumors which are not cancers are named using -oma as a suffix with the organ name as the root. For instance, a benign tumor of the smooth muscle of the uterus is called leiomyoma (the common name of this frequent tumor is fibroid). Unfortunately, some cancers also use the -oma suffix, examples being melanoma and seminoma (Weinberg 2007).

1.4 Aims of this Study

The biological and therapeutic importance of cancer stem cells has become increasingly clear over the past several years (Jordan, Guzman et al. 2006). The success or failure of cancer treatment approaches may be influenced greatly by the presence and treatment sensitivity of these cells. Cancer cures may therefore require effective targeting and destruction of the cancer stem cell population. For therapeutics to be effective against such cells, they must be effective against quiescent, apoptosis-resistant, and drug transporter–overexpressing cells. Further complicating this challenge, normal stem cells share many of these same features, to the extent that selectively targeting the cancer stem cell while leaving the normal stem cells unharmed is a difficult proposition.

Many investigators now believe that many tumor cell relapses following cytoreductive treatments may be due to the inherent resistance and subsequent outgrowth of cancer stem cell clones (Dean, Fojo et al. 2005). These cells may be more resistant to many standard chemotherapeutics because of their relatively quiescent state; as a result, cell cycle–dependent chemotherapies would be relatively ineffective. In addition, these cells typically overexpress cell membrane drug transporters of the ATP-binding cassette class. Therefore, cancer stem cells are frequently resistant to the chemotherapeutics that are transported by these molecules. Finally, survival pathways that are activated in these cells (e.g., the hedgehog-patched pathway) can make them resistant to apoptosis induction.

Oncolytic viruses may represent an effective therapeutic approach to target cancer stem cells (Parato, Senger et al. 2005; Liu, Galanis et al. 2007). These agents are inherently or genetically targeted to replicate in and selectively kill cancer cells.

It has recently been demonstrated that oncolytic virotherapy using vaccinia virus may provide a powerful new tool in cancer therapy. It is specifically targeting cancer cells and can potentially be used in combination with conventional cancer therapies. It was shown that a recombinant vaccinia virus could not only reveal the exact location of solid tumors and metastasis in mice but also successfully eradicate human breast tumor in mice xenografts (Yu, Shabahang et al. 2004; Zhang, Yu et al. 2007). Recently, this recombinant vaccinia virus almost finished phase I clinical trials in human cancer patients.

To prove the efficacy of vaccinia virotherapy against cancer stem cells, we designed and performed this study. “Cancer stem cells” is still a novel concept in both cancer biology and therapy. The first step of the study is to establish a method which could identify, isolate and characterize cancer stem cells from samples. Then vaccinia virus will be used to treat those cancer stem cells *in vitro* and *in vivo*. Furthermore, the mechanism of “oncolysis” should be elucidated. In addition, cancer stem cells could be used for vaccinia virus strains screening, which came from the idea of chemical drug screening by using cancer stem cells.

2 Materials

2.1 Chemicals and Enzymes

Materials	Manufacturer
2-Mercaptoethanol	Fisher Scientific
3-(4,5-Dimethylthiazol-2-yl)-2,5-diphenyltetrazolium bromide	Sigma
Accutase	Innovative Cell Technologies
Acetic Acid	VWR
Antibiotic-Antimycotic Solution	Cellgro
β-Estradiol	Sigma
cis-Diammine(1,1-cyclobutanedicarboxylato) platinum(II)	Sigma
cis-diamminedichloroplatinum(II)	Sigma
Citric Acid	Sigma
Clearslip Mounting Media	IMEB Inc.
Crystal Violet	Sigma
Deoxycholic Acid	Fisher Biotech
Dimethyl sulfoxide	Sigma
DMEM medium 1x	Cellgro
DMEM/F-12 medium 1x	Cellgro
Dulbecco's Phosphate Buffered Saline (DPBS) 1x	Cellgro
EDTA	Fisher Scientific
Epidermal Growth Factor	Stemgent
Fetal bovine serum	Omega Scientific
Fibroblast Growth Factor-basic	Stemgent
Fluorouracil	Sigma
Formaldehyde	EMD
Formalin 1:10 Dilution, Buffered	Fisher Diagnostics
Glucose	Cellgro
Glycerol	Fisher Scientific

HBSS 1x	Cellgro
HEPES	Gibco
Hoechst 33342	Sigma
Hydrochloric Acid Solution 2N	VWR
Hydrogen Peroxide Solution	Sigma
Hydroxymethylaminomethanehydrochloride (Tris-HCl)	Fisher Scientific
Matrigel	BD
Methanol, Absolute	Sigma
Mitomycin C	Sigma
Paraformaldehyde	Sigma
Propidium iodide	Sigma
Proteinase Inhibitor Cocktail Tablets	Roche
RPMI Medium 1640 1x	Cellgro
Salinomycin	Sigma
Sodium Acetate	Fisher Scientific
Sodium Azide	Fisher Scientific
Sodium dodecyl sulfate	Fisher Scientific
Sodium Pyruvate	Cellgro
TGF-β1	Stemgent
Trichloroacetic Acid	VWR
Tris (Base)	Fisher Scientific
Tris-Borate-EDTA (TBE) Buffer	Sigma
Triton-X 100	Sigma
Tween-20	Biorad
Xylene Substitute	Sigma

2.2 Cell Lines and Cell Culture Media

GI-101A:	human breast carcinoma (adherent)
MCF-7:	human breast adenocarcinoma (adherent)
MDA-MB-231:	human breast adenocarcinoma (adherent)

Hs 578T:	human breast carcinoma (adherent)
SUM149PT:	human breast carcinoma (adherent)
A549:	human lung carcinoma (adherent)
CV-1:	green monkey kidney fibroblasts (adherent)

Cell culture media:

GI-101A:	500ml RPMI-1640
	20% FBS
	5.6ml 45%Glucose
	1% HEPES
	1% Sodium Pyruvate
	1% Antibiotics-Antimycotics
	5ng/ml β-Estradiol
	5ng/ml Progesterone
MCF-7:	500ml RPMI-1640
	20% FBS
	5.6ml 45%Glucose
	1% HEPES
	1% Sodium Pyruvate
	1% Antibiotics-Antimycotics
	5ng/ml β-Estradiol
	5ng/ml Progesterone
MDA-MB-231:	500ml DMEM
	10% FBS
Hs 578T:	500ml RPMI-1640
	20% FBS
	5.6ml 45%Glucose
	1% HEPES
	1% Sodium Pyruvate

	1% Antibiotics-Antimycotics
	5ng/ml β-Estradiol
	5ng/ml Progesterone
SUM149PT:	500ml Ham's F-12
	5% FBS
	2.5ml 1mg/ml Insulin
	500µl 1mg/ml Hydrocortisone
	1% HEPES
A549:	500ml RPMI-1640
	10% FBS
CV-1:	500ml DMEM
	10% FBS

2.3 Kits

Kit	Manufacturer
ImmPACT™ DAB Diluent and Chromogen	Vector
Vectastain ABC Kit Rabbit IgG	Vector
MammoCult® Human Medium Kit	STEMCELL TECHNOLOGIES
ALDEFLUOR® Kit	STEMCELL TECHNOLOGIES
Cultrex® 96 Well BME Cell Invasion Assay	Trevigen

2.4 Antibodies

Antibody	Source	Manufacturer
anti-human CD44	Mouse	BD
anti-human CD24	Mouse	BD
anti-human EpCAM	Mouse	BD
anti-human CD49f	Mouse	BD
anti-vaccinia A27L	rabbit	Genescript (custommade)

anti-human ALDH1A1	rabbit	Geneway

2.5 Laboratory Animals

For in *vivo* experiments, female athymic nude FoxN1 mice were used. The FoxN1 mouse model is characterized by an autosomal recessive mutation in the *nu* locus on chromosome 11. This leads to a completely hairless phenotype in the mice. Additionally, these animals feature a dysfunctional and rudimental thymus which manifests in a T-cell deficiency. By contrast, B-cell function is normal in athymic nude FoxN1 mice. Due to the defects in the immune system of the mouse, athymic nude FoxN1 mice are suited as adequate laboratory animals in oncology, immunology and additional fields of biomedical research. Another advantage of the used mouse model is that xenotransplants will not be rejected by the mouse.
All animals were purchased from Harlan. Mice were cared for and maintained in accordance with animal welfare regulations under the approved protocol by the Institutional Animal Care and Use Committee of Explora Biolabs (San Diego Science Center) and of the University of California, San Diego.

2.6 Laboratory Equipments and Other Materials

Equipment	Manufacturer
Balance PL1501-S	Mettler Toledo
Bio Doc-It™ System	UVP
Biosafety Cabinet	The Baker Company Inc.
Cell Culture Cluster 24-well Costar 3526	Corning Inc.
Cell Culture Cluster 6-well Costar 3516	Corning Inc.
Cell Culture Cluster 96-well Costar 3595	Corning Inc.
Cell Culture Flask 75cm^2	Corning Inc.
Cell Lab Quanta SC	Beckman
Cell Scraper	Corning Inc.

Cell Spreader	VWR International
Centrifuge Sorvall RC 6 Plus	Thermo
Centrifuge Centra CL2	Thermo
Centrifuge Micro CL 21	Thermo
Combitips Plus 25ml	Eppendorf
Cryotubes 2ml	Nalgene
Digital Caliper	VWR
Digital Dry Bath Incubator	Boekel Scientific
Dish 10cm	Fisher Scientific
Embedding Mold TISSUE-TEK®	IMEB Inc.
Falcon 15ml Tubes	BD
Falcon 50ml Tubes	BD
FACS Aria III	BD
Fluorescence Microscope IX71	Olympus
Heater	VWR International
Hotplate Stirrer 375	VWR Scientific Products
Incubator HERA Cell 150	Thermo Electron Corporation
Incubator Shaker C25	New Brunswick Scientific
Insulin SyringeU-100 29G1/2	BD
MagNA Lyser	Roche
MagNA Lyser Green Beads	Roche
Microfuge Tubes 2.0ml	Avant
Microfuge Tubes Easy Open Cap 1.5ml	Saarstedt
Microplate Reader SpectraMax MS	Molecular Devices
Microscope Cover Glass	Fisher Scientific
Microslides Premium Superfrost®	VWR International
Microwave Carousel	Sharp
Multipipette	Eppendorf
Parafilm Laboratory Film	Pechiney Plastic Packaging
pH Meter Accumet AR15	Fisher Scientific
Pipet Aid	Drummond
Pipet Tips 200-1000µl, 100µl, 10µl	VWR International

Pipettes 1000µl, 100µl, 10µl	Rainin
Pipettes 25ml, 10ml, 5ml	Corning Inc.
Rocking Platform	VWR International
RS 2000 X-ray Biological Irradiator	Rad Source Technologies
Sectioning Machine Leica RM 2125	IMEB Inc.
Slide Staining Set TISSUE-TEK®II	IMEB Inc.
Slide Warmer	Barnstaed Labline
Sonifier 450	Branson
Sterile Disposable Scalpel	Sklar Instruments
Syringe 1ml	BD
Syringe 5ml	BD
Syringe Driven Filter Unit Millex®-VV PVDF 0.1µm	Millipore
Thermocycler Mastercycler Personal	Eppendorf
Tissue Culture Dish 60mm	BD
Tissue Embedding Center	Reichert – Jung
Tissue Grinder	Kimble
Tissue Processing/Embedding Cassettes with Lid	Simport
Vortex VX100	Labnet
Water Bath	Boekel Scientific
Water Bath Isotemp	Fisher Scientific

3 Methods

3.1 Flow Cytometry and Fluorescence-Activated Cell Sorting (FACS)

3.1.1 Side population identification using Hoechst 33342

Prepare mouse bone marrow cells and human cancer cells

Sacrifice the mouse according to accepted institutional protocol, lay the body on its back, and spray the abdomen with 70% ethanol to sterilize. Make a horizontal (leg-to-leg) incision with the rugged scissors through the skin of the abdomen a little lower than the level of the hips. From the incision, pull the skin up and down simultaneously-the skin should come off over the legs. Grab the knees with the forceps and pull out of the skin until the legs are exposed completely. Remove the tibias by cutting through the knees with delicate scissors. Take as much muscle off the bone as possible. Use the tendons where they connect at the ankle to remove all the muscle in one motion and take the foot off at the same time. Get the bone as clean as possible. Place the tibias in a 10-cm petri dish containing ~5 ml HBSS+ (HBSS supplemented with 2% FBS and 10 mM HEPES), kept on ice. Clean the muscle off the femur, using the tendons at the knee while the bone is still attached to the mouse. Cut the femurs off the mouse at the hips. This is where the majority of marrow is, so try to get most of the femur. If muscle is still attached to the femur, try to cut as much off as possible before putting it into the petri dish with the other bones. Having 4 bones in the petri dish (from one mouse), take a 10-ml syringe with a 27-G needle and fill with HBSS+. With forceps, hold a bone vertically over a fresh petri dish, insert the needle into the end of the bone, and expel liquid through the bone to push marrow onto the plate. If the opening is too small for the needle, trim the end of the bone slightly. In both femurs, move the needle around a little to ensure expulsion of as much of the marrow as possible. Also, flip the bone upside down and expel medium through the other end as well. If 10 ml is not sufficient to clean all 4 bones, put a little more medium into syringe to finish. Replace the 27-G needle with an 18-G needle. Aspirate the bone marrow up and down in the petri dish four or five times to break the chunks of marrow into single cells. Avoid getting air in the syringe,

as air bubbles kill cells. Finally, expel the marrow into a 50-ml tube. If desired, filter through a 70-µm filter or mesh at this point to make sure that no bone or other chunks remain.

For cancer cell lines, cells were detached with accutase and washed twice with DMEM+ (supplemented with 2% FBS and 10 mM HEPES).

Check the circulating water bath with a thermometer to ensure that the temperature is precisely 37°C. Prewarm DMEM+ while preparing the mouse bone marrow or cancer cells. Count the nucleated cells as carefully and accurately as possible, excluding red blood cells or dead cells. Centrifuge bone marrow or cancer cells 5 min at 500 × g, 4°C. Resuspend at 10^6 cells/ml in prewarmed DMEM+ and mix well by gently inverting the 250-ml polypropylene centrifuge tube.

Stain with Hoechst 33342

Add 1 mg/ml Hoechst 33342 to a final concentration of 5 µg/ml (a 200-fold dilution of the stock), cap the tube, and mix by gentle inversion. Incubate tubes exactly 90 min in the 37°C water bath. Make sure that the water level is sufficiently high to ensure that cell temperature is maintained at 37°C. Mix tubes several times during the incubation. After 90 min, centrifuge cells 5 min at 500 × *g*, 4°C and resuspend in ice-cold HBSS+. If the samples are not going to be further stained with antibodies, the cold HBSS+ should contain 2 µg/ml propidium iodide (PI) for dead cell discrimination. All further manipulations must be performed at 4°C to inhibit efflux

of Hoechst dye from the cells. At this point, samples may be run directly on the cytometer or further stained with antibodies to confirm the identity of the population, followed by resuspension of cells in cold HBSS+ containing 2 µg/ml PI. Magnetic enrichments may also be employed at this stage if the entire procedure is carried out at 4°C.

Set up flow cytometer

Beckman Coulter Cell Lab Quanta SC was used for Side Population analysis (Fig. 3.1). Excite Hoechst 33342 at 365 nm and collect blue fluorescence with 465 band-pass (BP) filter and red fluorescence with a 670-nm edge filter long-pass (EFLP). Use a 550-nm dichroic long-pass (DLP) to separate the emission wavelengths (Fig. 3.2).

Laser alignment and quality control

Run beads and check the pulse shape on the UV parameters, especially for blue

emission. Improve the UV parameter pulse shape until the pulse width is uniform.

Fig. 3.1 Beckman Coulter Cell Lab Quanta SC

Again run beads on the system and acquire data against time to monitor the stability of the UV path over time. Check the stability from a “cold start-up” of the system and

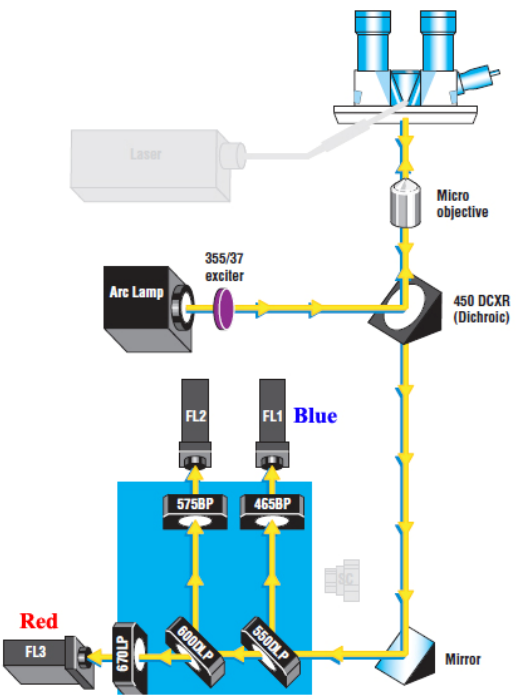

Fig. 3.2 Mercury Arc Lamp Optical Filter Configuration Output Process-Lamp 365 nm

also following restart after a 1-hr shutdown. Try to find the minimum time of laser

warm-up for beam stability. After the warm-up period, check for any laser drift in the system over time. If possible and for laser alignment, try to set the power low to seek for the best CV. Maximize the UV fluorescence and scatter signals using beads. Adjust the detector in linear mode. Adjust the flow rate to less than 300 events per sec.

Run on the flow cytometer

Place Hoechst-stained cells on the cytometer. If possible, keep cold by the use of a cooling apparatus. It is not necessary to establish live gates on forward versus side scatter parameters. First, display the histogram of Hoechst red (*x*-axis) versus blue (*y*-axis) fluorescence. With the detectors in linear mode, adjust the voltages so that the red blood cells are seen in the lower left corner and the dead cells (stained with PI and very bright) line up on a vertical line to the far right. Acquire data and analyze the data using Flowjo software from Tree Star Inc.

3.1.2 Immunofluorescence analysis and high speed sorting

Generating single cell suspension from human xenograft tumor sample

Sacrifice the mouse according to accepted institutional protocol, lay the body on its back, and spray the abdomen with 70% ethanol to sterilize. Remove the xenograft tumor from mouse and place tumor fragment in 2 to 3 ml HBSS in a 35-mm petri dish. Using a razor blade and forceps, mince the tissue as much as possible. Pipet tumor solution up and down 3 to 5 min with a 5-ml disposable pipet. Place the solution into a 50-ml conical tube. Add the triple enzyme tumor digestion solution (0.1% collagenase, type IV; 30 u/ml deoxyribonuclease, type IV; 0.01% hyaluronidase, type V) solution to the tumor cells. Incubate 30 to 60 min at 37°C. Pipet up and down a few times every 15 min. Pass the tumor solution through a 45-µm filter. Use a plunger from a 3- to 5-ml syringe and gently mash the tumor pieces to enable more tumor cells to pass through. Wash the filter with 4 to 5 ml of HBSS. Centrifuge the tumor cell suspension 10 min at 450 × *g*, 4°C. Resuspend the pellet in ~5 ml of ammonium chloride (0.8% w/v NH_4Cl with 0.1 mM EDTA). Leave for 10 min at room temperature to lyse the red blood cells. After 10 min add an equal volume of HBSS and centrifuge 10 min at 450 × *g*, 4°C. Resuspend the pellet in 10 ml HBSS. If the solution appears clumpy then pass it through another 45-µm filter. Count an

aliquot of the cells using a hemacytometer and trypan blue to determine the percentage of dead cells.

Generating single cell suspension from human xenograft cancer cell lines

Medium was removed from the 80% confluence healthy growing cells. Wash cells twice with DPBS and detach with accutase. Collect the detached cells and centrifuge 10 min at 450 × *g*, 4°C. Resuspend the pellet in DPBS. If the solution appears cell aggregates then pass it through another 45-µm filter. Count an aliquot of the cells using a hemacytometer and trypan blue to determine the percentage of dead cells.

Stain cells with antibody

Centrifuge cell suspension 10 min at 300 × *g*, 4°C, and discard supernatant. Resuspend cell pellet to 2 × 10^7 cells/ml in staining buffer, 4°C. Add 50 µl cell suspension (10^6 cells) to 12 × 75–mm round-bottom test tubes or the wells of a 96-well round-bottom microtiter plate. Add 10 µl appropriately diluted, labeled antibody to each tube or well containing cells and mix gently. Incubate 30-45 min in an ice bath.

Wash cells in preparation for flow cytometry

Wash cells by adding 2 ml staining buffer, 4°C. Centrifuge cell suspension 6 min at 300 × *g*, 4°C. Discard supernatant by aspiration or rapid inversion of the tubes. Repeat wash steps one time. Resuspend stained cell pellets in 400 µl of 4°C staining buffer. Keep cell suspension on ice until analyzed by flow cytometry.

Single-, two- and three colors flow cytometry analysis

Beckman Coulter Cell Lab Quanta SC was used for immunofluorescene analysis (Fig. 3.3). For single color, start up FACS machine and computer. Create Dot Plot and Histogram Plot with different parameters (FSC, SSC, FL1). Increase or decrease FSC gain to position the majority of the cells near the midpoint of the FSC axis as displayed on the histogram. Increase or decrease SSC gain on PMT to position cells near the midpoint of the SSC axis. Use the Polygon Region tool to define region 1 on the FSC versus SSC dot plot as that which encloses and defines live cells and excludes dead cells, debris, and red blood cells. Apply region 1 as a gate to the FSC × FL1 dot plots and the FL1 histogram display by selecting the dot plot or histogram, and then choosing Format from the Plots menu. Adjust the FL1 PMT voltage so that the majority of unstained cells show between 1and 10 fluorescence units (U) on the

FL1 histogram. Run and acquire data. Analyze the data using Flowjo software from Tree Star Inc.

For two colors, place isotype antibody stained control cells and Adjust FL1 and FL2 PMT voltages so that control cells appear in the lower-left corner of the histogram.

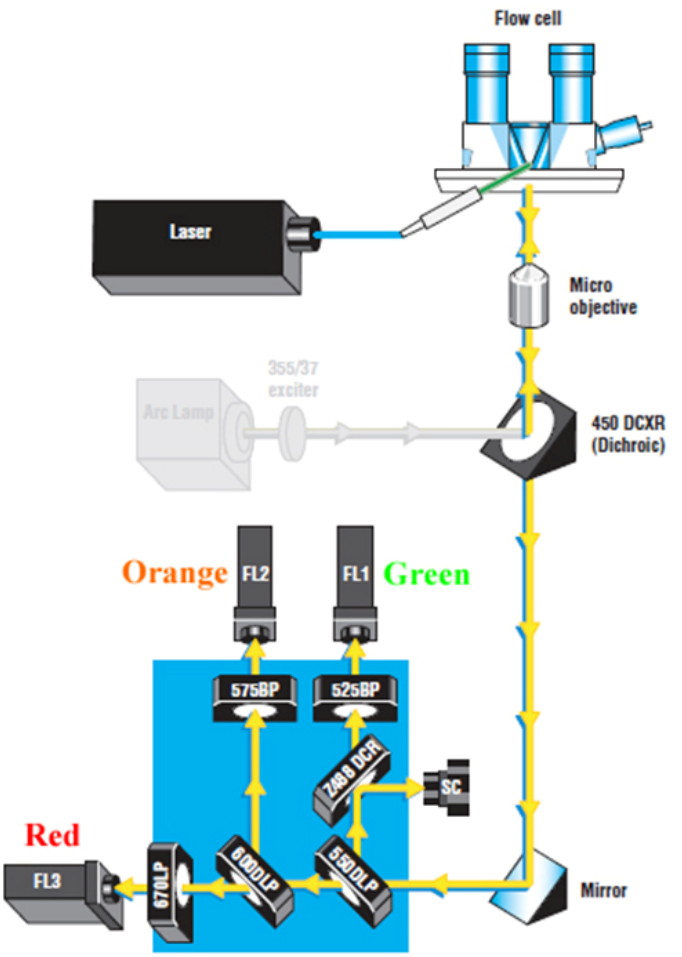

Fig. 3.3 Laser Optical Filter Configuration Output Process-Laser 488 nm

Run FITC-stained positive control cells and observe the FL1 versus FL2 dot plot. Adjust FL2-%FL1 compensation so that FL1-bright and FL1-negative cells have the same low level of FL2. Run PE-stained positive control cells and observe the FL1 versus FL2 dot plot. Adjust FL1-%FL2 compensation so that FL2-bright and FL2-negative cells have the same low level of FL1. Run a mixture of unstained cells, FITC-stained positive control cells, and PE-stained positive control cells. Make fine

adjustments to compensation if necessary. Run and acquire data. Analyze the data using Flowjo software from Tree Star Inc.

For three colors, discriminate live cells from dead cells and debris using region 1 (FSC versus SSC dot plot). Perform two-color analysis to adjust FL1 and FL2 voltages and compensation for analysis of FITC- and PE-stained cells. Set up a display as an FL2 versus FL3 dot plot. Set the FL3 PMT voltage so that control cells appear in the lower left corner of the dot plot. Run unstained, then PE-stained control cells. Adjust the FL3-%FL2 compensation so that unstained and PE-stained cells have the same (background) level of FL3. Run unstained, then red-stained control cells. Adjust the FL2-%FL3 compensation so that unstained and APC-stained cells have the same (background) level of FL2. Run a mixed sample containing isotype antibody stained control cells and FITC-, PE-, and APC-stained control cells. By observing the live displays and verifies that compensation has been set properly for each dye pair (FITC/PE, PE/APC). Alter electronic compensation if necessary. Run and acquire data. Analyze the data using Flowjo software from Tree Star Inc.

High speed sorting

BD FACS Aria III cells sorter (Fig. 3.4) was used for cell sorting. Before sorting, two- or three colors antibody stained cells were analyzed. Then specific cells populations were gated and went through high speed sorting. Sorted cells were kept in 20% FBS contained medium on ice and used for following assays.

3.1.3 Analysis of cellular DNA content by flow cytometry

Harvest cells

Prepare fixative by filling 12 × 75–mm centrifuge tubes with 4.5 ml of 70% ethanol. Keep tubes on ice. Collect cells to be stained and, in fresh centrifuge tubes, suspend 10^6 to 10^7 cells (estimate by eye) in 5 ml DPBS. Centrifuge cells 6 min at ~200 × *g*, room temperature.

Fix cells in ethanol

Discard the supernatant. Using a Pasteur pipet, resuspend cells in 0.5 ml PBS until a monodisperse cell suspension is achieved. Using a Pasteur pipette, transfer the cell suspension into the tubes containing 70% ethanol. Keep cells in fixative more than 2 hours.

Stain cells with PI

Centrifuge the ethanol-suspended cells 5 min at 200 × *g*, room temperature. Decant ethanol thoroughly. Suspend the cell pellet in 5 ml PBS, wait 60 sec, then centrifuge 5 min at 200 × *g*, room temperature. Suspend the cell pellet in 1 ml PI/Triton X-100 staining solution with RNase A. Incubate either 15 min at 37°C or 30 min at room temperature.

Measure cell fluorescence

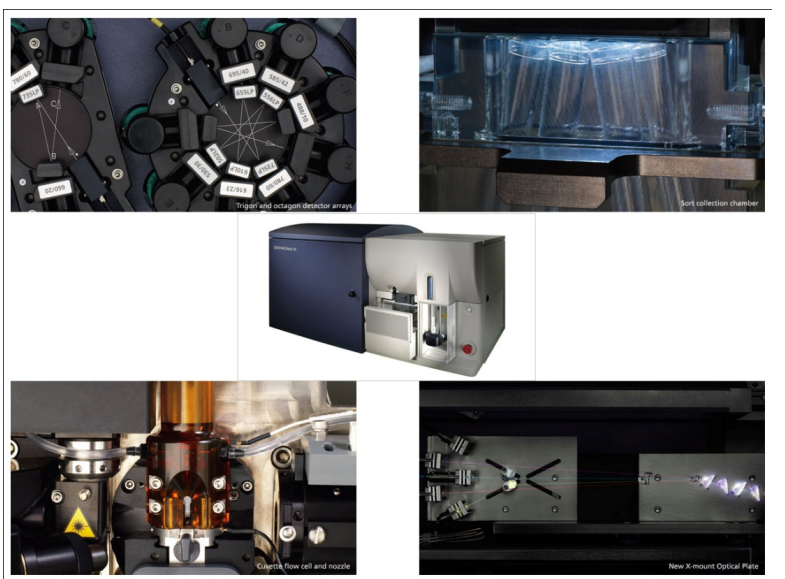

Fig. 3.4 BD FACS Aria III cells sorter

Set up and adjust a flow cytometer for excitation with blue light (488-nm light source) and detection of PI emission at red wavelengths.

Measure cell fluorescence using a pulse width–pulse area signal to discriminate between G2/M cells and cell doublets, gating out the latter. Analyze the data using Flowjo software from Tree Star Inc.

3.2 Virological Methods

3.2.1 Infection of cells with vaccinia virus

Cells are seeded in 6-well plates and infected at a stage of 95-100% confluence. The required amount of virus is calculated using the following formula:

$$\frac{Plaque\ forming\ units\ (pfu) \times dilution\ factor}{infection\ volume} = pfu/ml$$

The virus titer is defined as plaque forming units (pfu)/ml. Prior to infection, virus aliquots are thawed on ice and sonicated for 30 seconds at 4°C. This procedure prevents the formation of virus aggregates. The medium is aspirated from the cells and to 500 µl of new medium the desired amount of virus is added. After one hour of incubation at 37°C and 5% CO_2 with gentle agitation every 20 minutes, fresh culture medium is added.

3.2.2 Viral replication

For the viral replication assay, cells are grown in 6-well plates and infected with an multiplicity of infection (MOI) of 0.01. After one hour of incubation at 37°C and 5% CO_2 with gentle agitation every 20minutes, fresh culture medium is added. The cells are harvested after 24, 48 and 72 hours by scraping the cells off the culture plate with a cell scraper. Following three freeze-thaw cycles, serial dilutions of the lysates are tittered by standard plaque assay on CV-1 cells. All samples are measured in triplicates.

3.2.3 Plaque assay

The standard plaque assay is a method to determine viral titers in a suspension. CV-1 cells are grown in 24-well plates to 100% confluence. Samples are sonicated three times for 30 seconds and diluted depending on the expected virus titer. Then CV-1 cells are infected with 200 µl of dilutions. After one hour of incubation at 37°C and 5% CO_2 with gentle agitation every 20 minutes, 1 ml of carboxymethylcellulose (CMC) overlay medium is added and the cells are incubated at 37°C and 5% CO_2 until after

48 hours the cells are stained with 250 µl of crystal violet per well. Several hours after the staining plates can be washed and colorless viral plaques can be identified and counted. Every viral plaque represents one infectious virus particle. All samples are measured are triplicates and the results are averaged to obtain better accuracy. The following formula is used to determined the final pfu/ml:

$$\frac{Plaque\ forming\ units\ (pfu) \times dilution\ factor}{infection\ volume} = pfu/ml$$

Virus Plaque Overlay Medium:

CMC	15 g
weighed in 1 L bottle and autoclaved	
DMEM	1000 ml
Antibiotic-Antimycotic solution	10 ml
stir until dissolved	
FBS	50 ml

Crystal Violet Solution:

Crystal violet	1.3 g
Ethanol	50 ml
37% formaldehyde	300 ml
stir overnight	

3.3 Cells-based *in vitro* Assays

3.3.1 ALDEFLUOR assay

The ALDEFLUOR kit (StemCell technologies) was used to identify and isolate the population with a high ALDH enzymatic activity. Trypsinized and dissociated ells were suspended in ALDEFLUOR assay buffer containing ALDH substrate (BAAA, 1 µM per 1 × 10^6 cells) and incubated for 45 min at 37°C. In each experiment, a sample of cells was incubated with 50 mM of the specific ALDH inhibitor diethylaminobenzaldehyde (DEAB) as negative control. Flow cytometry analysis and

sorting was conducted as described before. ALDEFLUOR fluorescence was excited at 488 nm and fluorescence emission was detected using a standard FITC 530/30 band pass filter. The sorting gates were established using the propidium iodide-stained cells for viability and the ALDEFLUOR-stained cells treated with DEAB as negative controls.

3.3.2 Growth factors-induced Epithelia-Mesenchymal Transition (EMT) assay

One day before EMT inducing, healthy and 50%-80% confluence cells were removed medium. Wash cells with DPBS twice and trypsinize with trypsin-EDTA. Seed the dissociated single cells in culture wares with proper concentration. Change to EMT inducing medium in next day. The cells were cultured in DMEM/F-12 (1:1) medium supplemented with insulin, hydrocortisone, and 5% FBS and treated with 10 ng/ml of EGF, 10ng/ml of bFGF and 2.5 ng/ml of TGF-β1 for 12 days. The medium was refreshed every 3 days.

3.3.3 Resistance to cytotoxic agents MTT assay

Plate cells at 1×10^4 cells/well by adding 200 µl of a 5×10^4 cells/ml suspension to each well of a 96-well tissue culture plate. Include control wells with medium and without cells. Incubate overnight at 37°C, 5% CO_2. Carefully aspirate off the medium, avoiding removal of cells. If not previously incubated with toxicant, replace medium with fresh medium (200 µl) containing up to 0.1 ml of test substance. Include wells with medium without cells or test compound, medium without cells but with test compound, cells without test compound (but with test compound vehicle) as controls. Incubate at 37°C, 5% CO_2, for predetermined times (e.g., several hours, overnight, and/or for several days). After incubation with test compound, carefully aspirate off medium and replace with medium and 20 to 50 µl MTT solution for a total volume of 200 µl. Incubate for 4 to 6 hr at 37°C, 5% CO_2. Carefully remove the MTT-containing medium. Add 200 µl stop solution per well. Mix the plate until the formazan crystals are dissolved. Read plate on microtiter plate reader at 550 to 570 nm. Compare absorbance in wells containing the test substance with wells containing untreated control cells.

3.3.4 Resistance to ionizing radiation clonogenic assay

RS 2000 X-ray Biological Irradiator from Rad Source Technologies, Inc was used for cells ionzing radiation treatment (Fig. 3.5). Prepare single cell suspension as described before. Transfer the cells to 35 mm cell culture dishes. One dish for one ionizing radiation dose. Harvest cells after treatment. Count the number of cells in the resulting cell suspension using a Coulter counter, and dilute in sterile tubes so that 100 or up to 10^4 cells after severe treatment can be pipetted into the test wells. To study potentially lethal damage repair after ionizing radiation, cells are re-plated immediately or delayed after treatment. Pipette the cells in the test dishes and at least in duplicate.Place the dishes in an incubator and leave them there until cells in control dishes have formed sufficiently large clones. Remove the medium above the cells. Rinse carefully with DPBS. Remove the PBS and add 2–3 ml of a mixture of 6.0% glutaraldehyde and 0.5% crystal violet. Leave this for at least 30 min. Remove the glutaraldehyde crystal violet mixture carefully and rinse with tap water. Do not place the dishes or plates under the running tap, but fill the sink with water and

Fig. 3.5 RS 2000 X-ray Biological Irradiator

immerse the dishes or plates carefully. Leave the dishes or plates with colonies to dry in normal air at room temperature (20°C). Count the colonies and calculate the platting efficiency (PE) and survival fraction (SF) according to the following formula:

$$PE=\frac{no.of\ colonies\ formed}{no.of\ cells\ seeded} \times 100\%$$

$$SF=\frac{no.of\ colonies\ formed\ after\ treatment}{no.of\ cells\ seeded \times PE} \times 100\%$$

To generate a radiation survival curve, the surviving fraction at each radiation dose was normalized to that of the sham-irradiated control, and curves were fitted using a linear-quadratic model (surviving fraction = $e^{(-\alpha\ dose\ -\beta\ dose\ 2)}$, in which α is the number of logs of cells killed per gray from the linear portion of the survival curve and β is the number of logs of cells killed per $[gray]^2$ from the quadratic component) (Albright 1987) . Three independent experiments were performed.

3.3.5 Immunofluorescence staining and cell imaging

Olympus 1×71 Iinverted Microscope was used for cell imaging (Fig. 3.6) and MicroFire® digital CCD camera system was used for images acquisition. For adherent cells, 1 to 2 days prior to experiment trypsinize cells and seed onto 10-cm culture dishes, each containing 15 to 20 sterilized coverslips, so that on day of experiment cells are 20% to 50% confluent. On day of experiment, transfer each coverslip individually to a well of a 12-well tissue culture dish containing 1 ml culture medium. Subject cells to the desired experimental conditions (e.g., treat with various drugs, inhibitors, or temperatures prior to fixation and immunostaining). Aspirate medium and add 1 ml of 2% formaldehyde to each well. Allow cells to fix at room temperature for 10 min. Aspirate the formaldehyde fixative and wash coverslips twice, each time

Fig. 3.6 Olympus 1×71 inverted microscope

by adding 1 ml PBS, pH 7.4, letting stand 5 min, then aspirating the PBS. Add 1 ml PBS/FBS to the fixed coverslips and let stand 10 to 20 min to block nonspecific sites of antibody adsorption. In 1.5 ml microcentrifuge tubes dilute primary antibodies in 0.1% saponin/PBS/FBS. Prepare controls containing only 0.1% saponin/PBS/FBS or (if available) containing pre-immune antiserum (if rabbit polyclonal antibody is being used) or specific (primary) antibody with the antigen added in excess. Microcentrifuge antibody dilutions and control solutions 5 min at maximum speed, room temperature, to bring down aggregates in pellet. Place a 10 × 10 cm^2 piece of Parafilm in the bottom of a 150 mm petri dish. In a grid pattern that replicates the 12 wells used to incubate the coverslips, label the appropriate place on the Parafilm for each coverslip with a marker. Apply a 25 µl drop of appropriate primary antibody solution to each numbered section. Carefully remove each coverslip from the 12-well plate with watchmaker's forceps, blot the excess fluid by touching the edge to a Kimwipe, then invert the coverslip over the appropriate 25 µl drop, making sure that the side with the cells is facing down. Place the top on the petri dish and incubate 1 hr at room temperature. Carefully pick up each inverted coverslip and flip it over so that it is cell-side-up, then place in a well of a 12-well plate. Wash each coverslip three times to remove unbound antibody, each time by adding 1 ml PBS/FBS, letting stand 5 min, then aspirating the solution. Dilute fluorophore-conjugated secondary antibodies in 0.1% saponin/PBS/FBS. Mix, then microcentrifuge as described before to remove aggregates. Prepare an incubation chamber as described before. Apply 25 µl of appropriate secondary antibody solution to each numbered section and invert coverslip over drop as in previous step. Cover petri dish and protect from light with aluminum foil or place chamber in drawer. Incubate 1 hr at room temperature. Wash coverslips as described before. After removal of last PBS/FBS wash, add 1 ml PBS. Label slides and place 1 drop of mounting medium onto slide. Pick up coverslip from well, gently blot off excess PBS by touching the edge to a Kimwipe, then invert coverslip, cell-side-down, onto drop. Gently blot mounted coverslip with paper towel, and then seal edge of coverslip onto slide by painting the edge with a rim of nail polish. Let dry. View specimen on fluorescence microscope using different objective lens and record the image with digital CCD camera.

3.3.6 Live cell video animation

WeatherStation system from PrecisionControl, which installed on Olympus 1×71 Iinverted Microscope, was used for maintaining the live cells on microscope when taking time sequential image (Fig. 3.7). The cells were infected by vaccinia virus in 6-well plate as described before. Place the cells in WeatherStation chamber and adjust the temperature and CO_2 concentration which are similar to tissue culture incubator. Observe the virus replication according to cells morphology change and fluorescent protein expression. Start to capture the image at 6 hours post infection and stop at 12 hours. 20 min intervals were given. Sequential images were compiled to a video animation by Image J software.

3.3.7 Cells migration and invasion assay

The CULTREX® 96-well BME cell invasion assay kit (Trevigen) was used to quantify cell migration and invasion ability. Culture cells per manufacturer's recommendation and adherent cells should be cultured to no more than 80% confluence. Each well requires 50,000 cells, so plan accordingly. Coat membrane of top invasion chamber (leave three chambers uncoated for a migration control) with 50 µl of 0.1X to 1X BME solution, and incubate for 4 hours or overnight at 37°C in a CO_2 incubator. Harvest and count cells. Centrifuge cells at 250 × g for 10 min, remove supernatant, wash with 1× wash buffer, count and resuspend at 1 × 10^6 cells/ml in a serum free medium (0.5% FBS may be used if needed). Aspirate top chamber of cell invasion device. Add 50 µl of cells per well to top chamber (with or without inhibitors/stimulants). Using

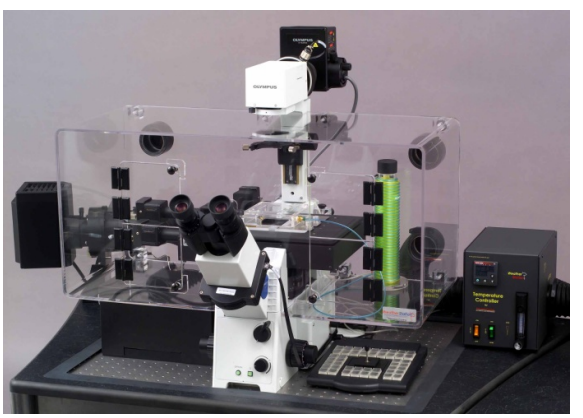

Fig. 3.7 WeatherStation Live Cell Imaging System

access port, add 150 µl of medium per well to bottom chamber (with or without chemoattractants). Incubate chamber at 37°C in CO_2 incubator for 24 hours. Assay remaining cells for standard curve and each cell type will require a separate standard curve. Carefully aspirate top chamber (do not puncture membrane), and wash each well with 100 µl of 1× Wash Buffer. Aspirate bottom chamber, and wash each well twice with 200 µl 1× Wash Buffer. Transfer top chambers to assay chamber plate (black). Add 12 µl of Calcein-AM solution to 10 ml of Cell Dissociation Solution. Add 150 µl of Cell Dissociation Solution/Calcein-AM to bottom chamber, assemble cell invasion device, and incubate at 37°C in CO_2 incubator for one hour. Remove top chamber, and read plate at 485 nm excitation, 520 nm emission. Using standard curves, convert RFU to Cell Number; determine percent invasion.

3.3.8 Mammosphere formation

Prepare single cell suspension as described before. Seed the cells in ultra-low attachment surface culture wares at a density of 8000 cells/cm^2 with serum-free medium. Add EGF/bFGF supplements every 3-4 days and passage the mammosphere about 12 days. The mammosphere were dissociated by either mechanical or enzymatic disruption. For mechanical disruption, centrifuge the mammosphere solution for 10 min at 450 × *g*, 4°C. Resuspend the pellet in 3 ml of serum-free medium and pipet up and down for 10 min with a 5 ml disposable pipet. Pass solution through a 45 µM filter, count an aliquot of the cells, and resuspend in the desired volume of serum-free medium for replating. For enzymatic disruption, centrifuge the mammosphere solution for 10 min at 450 × *g*, 4°C. Resuspend the pellet in 3 to 5 ml of 1× trypsin/EDTA and pipet up and down for 3 min with a 5-ml disposable pipet. At this point, place the tube in the incubator 10 min at 37°C. After 10 min remove the cells from the incubator and add an equal volume of serum-free medium. Pass the cells through a 0.45 µM filter. Centrifuge the cell solution 10 min at 450 × *g*, 4°C. Resuspend the cell solution and count the number of viable cells using trypan blue.

3.3.9 Soft agar colony forming assay

Prepare 0.5% base agar layer in 6-well plates. Store the pre-coated plates in 4°C and let them sit at room temperature for 30 min before using. Prepare 0.7% top agarose solution. Harvest and make single cell suspension as described before. Count cells and adjust the appropriate cell concentration. Resuspend cells in top agarose solution. Seed the cell suspension on the top of base agar layer. Incubate in 37°C for two weeks around and feed cells with medium twice a week. Stain plates with 0.5 ml of 0.005% crystal violet for more than 1 hour. Count colonies using a dissecting microscope.

3.4 *in vivo* Studies

3.4.1 Xenograft tumor implantation and monitoring

Thaw an aliquot of Matrigel and draw it up into a 0.3 ml syringe with needle. Then remove the plunger from a 0.3 ml insulin syringe with a 29 G needle, 1/2-inch. long and insert a small amount of Matrigel into the back of the syringe. Use a pipet to inject the cell suspension (aim to resuspend the cells in 10 µl of serum-free medium) into the middle of the Matrigel. Then reinsert the plunger into the syringe and push the mixture to the top of the syringe. Handle mice using sterile technique and anesthetize using inhalational anesthesia. Invert tube or vortex the cell suspension gently to mix settled cells. Be certain that the cells are free of aggregates to prevent embolic obstruction. Gently mix the cells periodically and prior to each inoculation. Use scissors to make an incision along the abdominal midline and laterally between the fourth and fifth nipples midway down to right hind leg (ventral side up). Carefully separate the skin flap from the body wall. The separated skin flap should be pinned to the surgery board thus exposing the #4 MFP (Fig. 3.8). Locate MFP under a dissection microscope. Inject the cells suspension into the intact fat pad (below the draining lymph node). Close the wound by using 4–5 surgical staples. Perform the same procedure for the other #4 mammary gland, if necessary. The primary tumor outgrowth should be monitored weekly by taking measurements of the tumor length (L) and width (W). Tumor volume was calculated as the following formula:

$$Tumor\ Volume = \frac{length \times width \times width}{2}$$

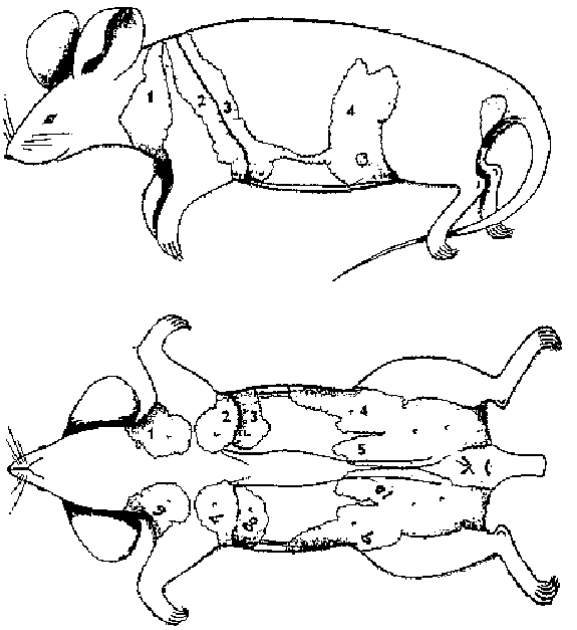

Fig. 3.8 Indication of mouse mammary gland. Like the human, the mouse mammary gland originates from the milk bud. The mouse forms five to six pairs of mammary glands that extend from the neck to the groin. At puberty, the mammary ducts extend into the mammary fat pad in an orderly manner. These wholemounts of mouse mammary glands show the structure of the growing gland at 4 through 16 weeks. These images show thoracic (#3 and #8) and abdominal (#4 and #9) glands. The thoracic glands are also conventionally numbered as #3 right and left and #4 right and left, respectively.

Also the weight of each mouse is noted to keep track of any changes of body weights after tumor implantation and injection with the virus. By holding the mice under UV light and looking at the tumors, a successful infection can be confirmed by the visible green GFP or red RFP/TunorFP650 expression mediated by the viruses and can be photographed for the records.

3.4.2 Virus preparation for mouse injection

Mice are infected with 5×10^6 pfu in 100 µl DPBS. The right amount of virus is calculated for each virus that is to be injected with the titer of each virus and mixed with DPBS to get 100 µl total volume per mouse. A small amount of virus is prepared

additionally to what is needed for the injections to be able to confirm the prepared viruses' titers by making dilution series and performing a plaque assay. 100 µl of virus containing DPBS are injected retro-orbitally with insulin syringes. The remaining virus is titrated with CV-1 cells in 24-well plates as described before.

3.4.3 Tumor and organ preparations for virus titration

After dissection of the tumors and organs (spleen, liver, heart, lungs), they are weighted and placed in MagNA Lyser Green Beads tubes (Roche) containing 500 µl DPBS with proteinase inhibitors. One tablet of proteinase inhibitor cocktail was previously dissolved in 50 ml DPBS. If the weight exceeds 0.8 g, additional tubes were used for the same tumor or organ. It has to be noted how many tubes were used so that it can be calculated into the end result. The tubes are kept on ice at all times. After all tumors and organs are dissected, they are shredded at 3000 rpm for 30 seconds with MagNA Lyser (Roche). Then they are frozen at -80°C until the day of titration. Samples are frozen and thawed three times before further use. Then they were sonicated three times for one minute to further break up the tissue and virus aggregates. Tissues that were split into more than one tube are combined. Then the samples are centrifuged for five minutes at 6000 rpm. The virus is titrated with CV-1 cells in 24-well plates as described before.

3.4.4 Histology

After dissection of the tumors they are cut into slices no thicker than 3 mm and placed in a beaker with 10% neutral buffered formalin for fixation over night at room temperature.

Dehydration

To dehydrate the tissue is subjected to the following steps on a rocking platform for one hour per step:

1. 0.9% NaCl
2. 30% EtOH in 0.9% NaCl
3. 50% EtOH in 0.9% NaCl
4. 70% EtOH in 0.9% NaCl
5. 90% EtOH in 0.9% NaCl

6. 100% EtOH
7. 100% EtOH

At this stage the tissues are stored over night until they are embedded in paraffin the next day.

Embedding

Paraffin wax is melted ahead of time. A small aliquot of wax is heated in a beaker and mixed with an equal amount of xylene substitute. Prior to embedding the tissue is processed through the following solutions on a rocking plate, each step for one hour:

1. 100% Ethanol, at room temperature
2. EtOH/Xylene 1:1, at room temperature
3. Xylene, at room temperature
4. Xylene/wax, at 58˚C
5. Wax, three times at 58˚C

Subsequent to infiltration, the tissue is placed into an embedding mold and melted paraffin is poured into the mold to form a block. The blocks are allowed to cool and are ready for sectioning.

Sectioning

A water bath set between 45 ˚C and 50 ˚C and a slide warmer set at 38 ˚C are placed next to the sectioning machine. The blade angle is set to 10 ˚ and 5 µm slice thickness. Ribbons of sections are cut and put into the water bath. To mount the tissue, a Superfrost Plus slide is positioned underneath the ribbons and single sections are lifted out of the water. The slides are allowed to dry on the slide warmer for at least two hours, then they are stored in a cool dry place.

Deparaffinization and Rehydration of Tissue Sections

Before deparaffinization the slides are placed in a 55 ˚C oven for ten minutes to melt the paraffin. Slides are placed into a slide holder and subjected to the following steps:

1. Xylene substitute, three minutes
2. Xylene substitute, three minutes
3. Xylene substitute, three minutes
4. 100% EtOH, three minutes
5. 100% EtOH, three minutes
6. 100% EtOH, three minutes

7. 95% EtOH in H_2O, three minutes
8. 80% EtOH in H_2O, three minutes
9. deionized H_2O, five minutes

Hematoxylin and Eosin (H&E) Staining

Slide holder with slides it put through following steps:

1. Hematoxylin, three minutes
2. Slides are rinsed in deionized H2O
3. Tap water to allow the stain to develop, five minutes
4. eight to twelve dips in acid ethanol (1 ml concentrated HCl in 400 ml 70% EtOH)
5. Slides are rinsed twice for two minutes each in tap water
6. Slides are rinsed in deionized H_2O for two minutes
7. excess water is blotted from slide holder
8. Eosin, 30 seconds
9. 95% EtOH, five minutes
10. 95% EtOH, five minutes
11. 95% EtOH, five minutes
12. 100% EtOH, five minutes
13. 100% EtOH, five minutes
14. 100% EtOH, five minutes
15. Xylene substitute, fifteen minutes
16. Xylene substitute, fifteen minutes
17. Xylene substitute, fifteen minutes

The slides are cover slipped using mounting medium. A drop of mounting medium is placed on the slide using a glass rod, taking care not to leave bubbles. The coverslip is angled and placed gently onto the slide. The medium will spread beneath the coverslip, covering all tissue. The slides are dried over night.

Immunohistochemical Staining of Vaccinia Virus

The sections are deparaffinized and rehydrated. After rinsed for five minutes in tap water they are incubated for 20 minutes in steamed citrate buffer in a steamer. Then they are cooled down at room temperature for another 20 minutes. The slides are rinsed for five minutes in tap water. Then the sections are incubated in 3% H_2O_2 for

five minutes and rinsed with water again for two minutes. The slides are washed in PBS for five minutes. To block the sections are treated with diluted normal blocking serum (three drops of serum stock in 10 ml PBS) (Vector) for 20 minutes. After excess serum is blotted from the sections, they are incubated with primary antibody (Genelux custom made rabbit polyclonal antibody against vaccinia A27L) diluted 1:1000 in blocking serum for 30 minutes. Slides are washed for five minutes in PBS and incubated with diluted biotinylated secondary antibody (one drop in 10 ml diluted blocking serum) (Vector). Slides are washed for five minutes in PBS and incubated for 30 minutes with Vectastain Elite ABC reagent. After that slides are washed for five minutes in PBS and ImmPACT DAB Peroxidase Substrate is added to the sections until suitable staining develops. The slides are washed in water again and the counterstained with Hematoxylin (Vector) for 30 seconds. Sections are rinsed in water until it is colorless. The sections are then dehydrated with 100% EtOH, one minute each for three changes, followed by Xylene substitute, three minutes each for three changes. Then coverslips are mounted on slides using mounting medium.

Citrate buffer:

Sodium citrate 0.1 M	4.1 ml
Citric Acid 0.1 ml	9 ml
H_2O	450 ml
pH 6	

Immunohistochemical Staining of ALDH1

The staining is performed as previously described for vaccinia virus A27L. As primary antibody the rabbit polyclonal antibody against human ALDH1 (Geneway) diluted 1:200 in blocking serum was used. The secondary antibody and all other solutions were used as described before.

4 Results

4.1 General Characteristics of Human Breast Cancer Cell Lines Used in This Study

Breast cancers are broadly categorized into two classes: those that express luminal keratins (luminal-type) and those that express stratified epithelial keratins (basal-type) (Perou, Sorlie et al. 2000; Sorlie, Perou et al. 2001; van 't Veer, Dai et al. 2002; Sorlie, Tibshirani et al. 2003). Five human breast luminal-type or basal-type cancer cell lines which include GI-101A, MCF-7, MDA-MB-231, HS578T and SUM149PT were used in the study of human breast cancer stem cells. Table 4.1 summarizes source, clinical, and pathological features of tumors from which the cancer cell lines derived according to published literature (Neve, Chin et al. 2006) and Figure 4.1 shows the cell morphology during adherent culture. GI-101A is a novel metastatic human breast cancer cell line which derived from tumor xenograft model (Hurst, Maniar et al. 1993; Morrissey and Raney 1998). During the past two decades, only few laboratories showed interest about the GI-101A cell line and the research mainly focused on its metastatic characteristics (Rathinavelu, Malave et al. 1999; Lev, Kiriakova et al. 2003; Wang, Lee et al. 2007). Due to lacking accessibility of human patient primary tumor tissue, a lot of laboratories choose human or mouse breast cancer cell lines to identify and isolate breast cancer stem cells by using different tools and methods (Christgen, Ballmaier et al. 2007; Cariati, Naderi et al. 2008; Fillmore and Kuperwasser 2008; Al-Assar, Muschel et al. 2009; Bartkowiak, Wieczorek et al. 2009; Charafe-Jauffret, Ginestier et al. 2009; Han and Crowe 2009; Magnifico, Albano et al. 2009; Meyer, Fleming et al. 2009; Wang, Kao et al. 2009; Deng, Yang et al. 2010; Du, Li et al. 2010; Gasparini, Bertolini et al. 2010; Louie, Nik et al. 2010; Rappa and Lorico 2010; Sajithlal, Rothermund et al. 2010; Singh, Cook et al. 2010; Stuelten, Mertins et al. 2010). Those cell fractions which were purified from cell lines and expressed certain markers that display the properties of self-renew, tumorigenicity, resistance to chemotherapy and ionizing radiation ability, compared to their counterparts. However, they were given the terms of cancer stem-like cells or

Tab. 4.1. Source, clinical, and pathological features of tumors used to derive breast cancer cell lines used in this study.

	Cell line	Gene cluster	ER	PR	HER2	TP53	Source	Tumor type	Age (years)	Ethnicity	Tumorigenicity	Culture media	Culture conditions
1	GI101A	Lu	+/-*	-	+	$+^{M}$	XG	IDC	57		Y	RPMI, 20% FBS	37°C, 5% CO_2
2	MCF7	Lu	+	[-]	Low	$+/-^{WT}$	PE	IDC	69	W	Y**	RPMI, 20% FBS	37°C, 5% CO_2
3	MDAMB231	BaB	-	[-]	-	$++^{M}$	PE	AC	51	W	Y	DMEM, 10% FBS	37°C, 5% CO_2
4	HS578T	BaB	-	[-]		$+^{M}$	P.Br	IDC	74	W	N	RPMI, 20% FBS	37°C, 5% CO_2
5	SUM149PT	BaB	[-]	[-]	-	[+]	P.Br	Inf Duc.Ca			Y	Ham's F12, 5% FBS-IH	37°C, 5% CO_2

AC, adenocarcinoma; BaB, Basal B; Duc.Ca, ductal carcinoma; IDC, invasive ductal carcinoma; Inf, inflammatory; Lu, luminal; P.Br, primary breast; PE, pleural effusion; W, White. ER/PR/HER2/TP53 status: ER/PR positivity, HER2 overexpression, and TP53 protein levels and mutational status (obtained from the Sanger web site; M, mutant protein; WT, wild-type protein) are indicated; XG, xenograft.
Square brackets indicate that levels are inferred from mRNA levels alone where protein data is not available.
Media conditions: FBS, fetal bovine serum; I, Insulin (5µg/ml); H, hydrocortisone (1µg/ml); DMEM, Dulbecco's modified Eagle's medium; RPMI, RPMI medium 1640; Ham's F12, F-12 nutrient mixture (Ham).
* Positive in mRNA levels and negative in protein level.
**With estrogen supplement.

tumor/cancer-initiating cells for distinguishing cancer stem cells which exist in primary tumors *in vivo*. Though controversies about it (Li 2009; Neumeister and Rimm 2009), cell line derived cancer stem-like cells are still necessary supplements for cancer stem cells research and prove the concept of cancer stem cells more or less.

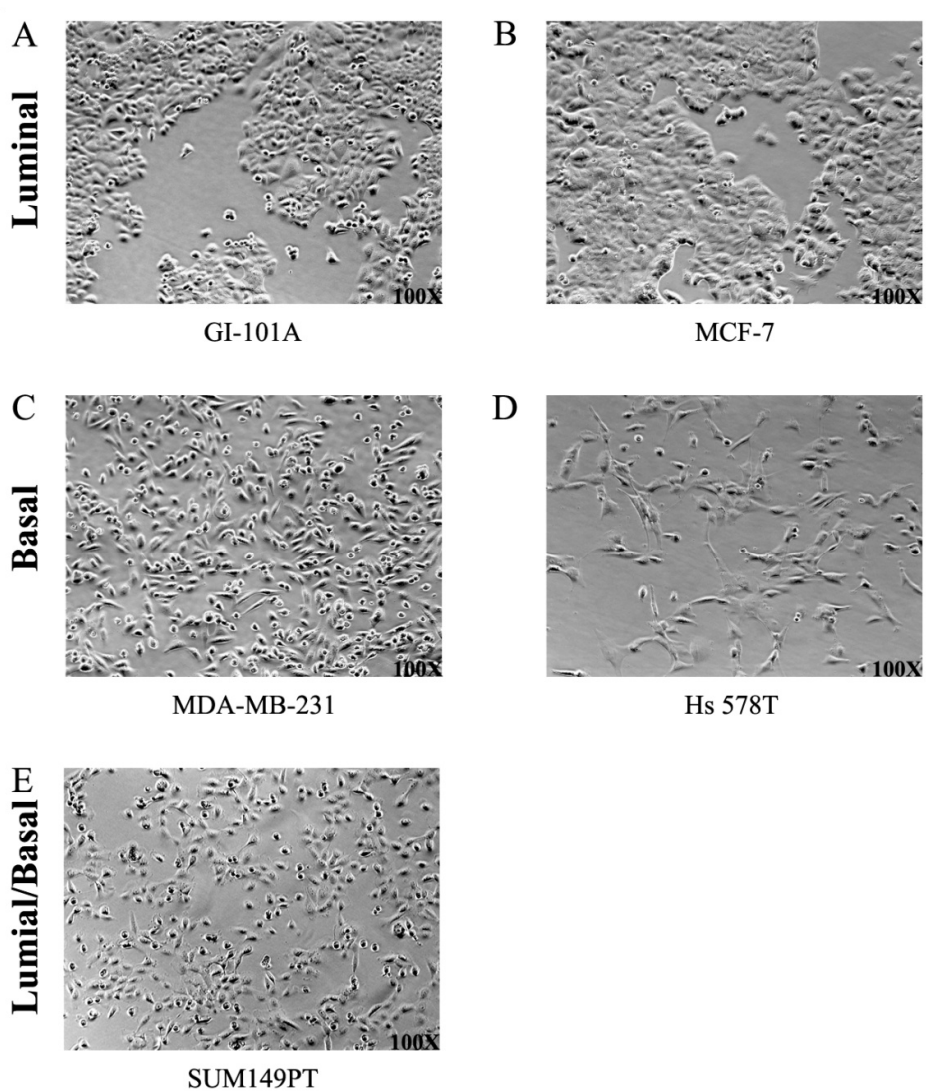

Fig. 4.1 Morphology of human breast cancer cell lines which are undergoing adherent culture. (A) GI-101A cells; (B) MCF-7 cells; (C) MDA-MB-231 cells; (D) HS578T cells; (E) SUM149PT cells.

4.2 Human Breast Cancer Cell Lines Contain Very Few Side Population Cells

Side population (SP) cells were first defined by Goodell (Goodell, Brose et al. 1996). Although the mechanism for producing the SP phenotype is unclear, it is widely believed that certain ATP-binding cassette (ABC) transporters, including ABCG2/BCRP, ABCB1/MDR1, and ABCA3, which can pump out the fluorescent dye Hoechst 33342, or the relative quiescence of the cancer stem cells that limit the intake of the dye, may cause the SP phenotype (Zhou, Schuetz et al. 2001; Hirschmann-Jax, Foster et al. 2004). Accumulating evidence suggests that side-population (SP) cells, a small population of cells from cancer cell lines, are enriched in a subset of cancer stem-like cells (Patrawala, Calhoun et al. 2005; Kruger, Kaplan et al. 2006; Christgen, Ballmaier et al. 2007; Li, Kong et al. 2007; Zhou, Wulfkuhle et al. 2007; Engelmann, Shen et al. 2008; Liu, Lu et al. 2008; Steiniger, Coppinger et al. 2008; Yin, Castagnino et al. 2008; Zhou, Zhang et al. 2008; Christgen, Geffers et al. 2009; Dey, Saxena et al. 2009; Han and Crowe 2009; Tanaka, Nakamura et al. 2009; Zhou, Zhang et al. 2009; Guo, Zhou et al. 2010; Hiraga, Ito et al. 2010; Huang, Li et al. 2010; Nakanishi, Chumsri et al. 2010). In these studies, the human breast cancer cell line MCF-7 was widely used, and SP cells were successfully identified and isolated. To prove this method, we performed the SP analysis. The bone marrow from one week old C57Bl/6 mouse was prepared following protocol and it was used to adjust and standardize the flow cytometry machine. As shown in Fig. 4.2A, mouse bone marrow was found to contain 4.52±0.2% SP cells, which was presented as a distinct ‘‘tail’’ in the flow cytometry histogram. The SP population could be blocked by known ABC transporter inhibitors, including verapamil, reserpine, and fumitremorgin C (FTC). When 50 or 100 μM verapamil was added during the Hoechst 33342 staining process, the SP percentages decreased to 3.74±0.3% and 1.76±0.1%, respectively (Fig. 4.2B-C). Then we determined SP ratio in human breast cancer cell lines GI-101A and MCF-7. The GI-101A were found to contain 2.21±0.3% SP cells (Fig. 4.2D), higher than 0.77±0.1% of MCF-7 SP cells (Fig. 4.2G). The SP cells of GI-101A and MCF-7 also can be blocked by verapamil with different doses (Fig. 4.2 E-F,

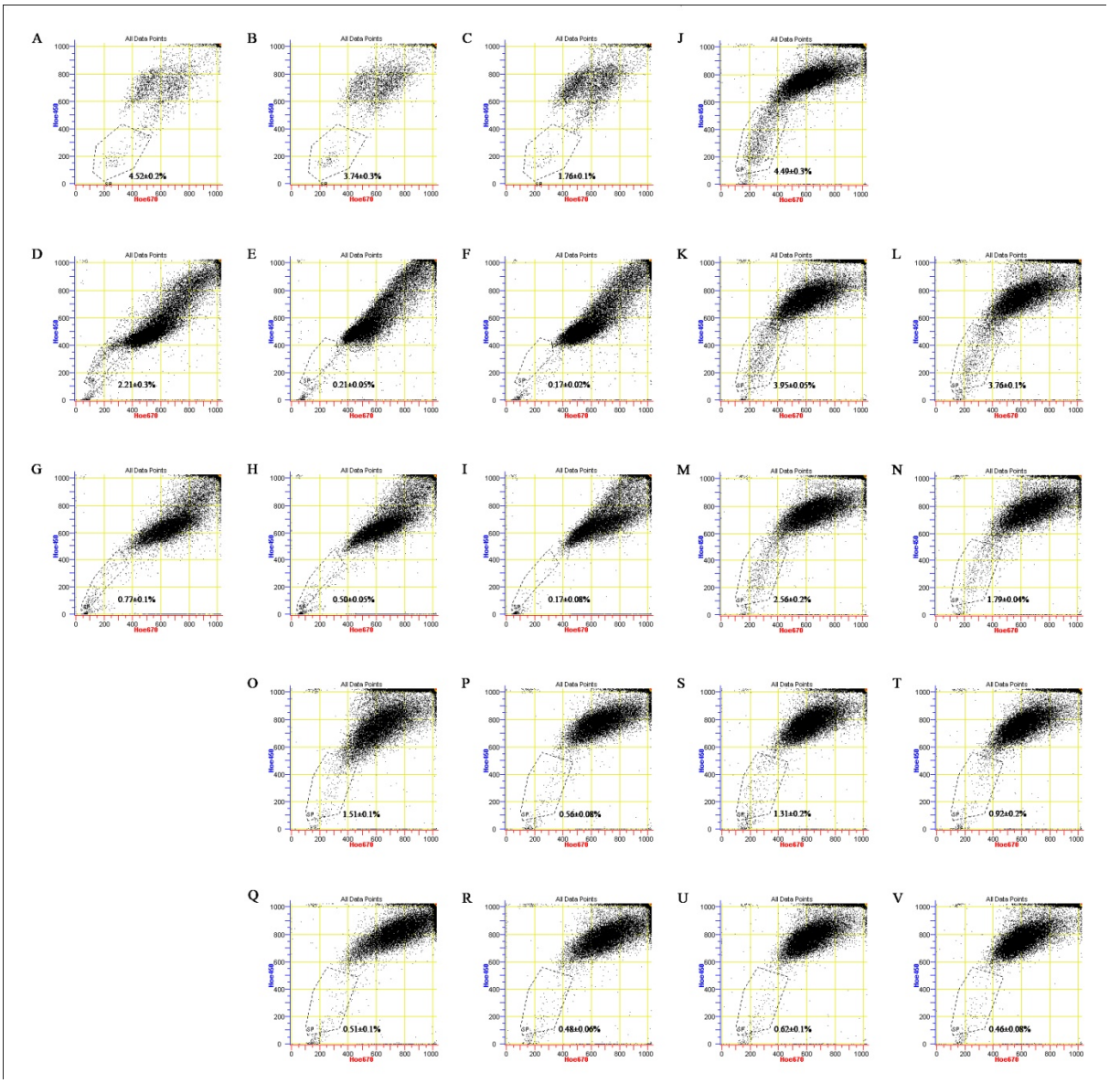

Fig. 4.2 Flow cytometry analysis of SP cells in mouse bone marrow and human cancer cell line. (A-C) Fresh prepared mouse bone marrow contained SP cells when stained with 5 µg/ml Hoechst 33342 in the absence (A) or presence of 50 µM (B) or 100 µM (C) verapamil. Exponentially growing GI-101A (D-F) and MCF-7 (G-I) cells were stained with 5 µg/ml Hoechst 33342 in the absence (D, G) or presence of 50 µM (E, H) or 100 µM (F, I) verapamil. Exponentially growing A549 (J-V) cells were stained with 5 µg/ml Hoechst 33342 in the absence (J) or presence of 25 µM (K), 50 µM (L), 100 µM (M) and 200 µM (N) verapamil or 12.5 µM (O), 25 µM (P), 50 µM (Q) and 100 µM (R) reserpine or 6.25 µM (S), 12.5 µM (T), 25 µM (U) and 50 µM (V) FTC.

H-I). Unexpectedly, the human lung cancer cell line A549 contains much more SP cells (Fig. 4.2J) and the SP cells can be blocked by verapamil (Fig. 4.2K-N), reserpine (Fig. 4.2O-R) and FTC (Fig. 4.2S-V) at different dose. Similar studies of A549 lung cancer cell line has been done by another group (Patrawala, Calhoun et al. 2005; Seo, Sung et al. 2007; Sung, Cho et al. 2008) and A549 cells were proved to be enriched in SP cells, which displayed some properties of cancer stem cells such as self-renewal, chemoresistance and *in vivo* tumorigenicity. So the SP cells from those cancer cell lines were recognized as cancer stem-like cells. Though the SP method worked well on not only bone marrow which contains hemopoietic stem cells but cancer cell lines, advanced flow cytometry facilities requirements restrict its utilization.

4.3 Enriched GI-101A ALDEFLUOR-positive Cells Have Properties of Cancer Stem Cells

4.3.1 Isolation of ALDEFLUOR-positive population from GI-101A cell line

The enzyme ALDH has been a useful marker for isolating primitive stem cell populations. It was shown previously that normal human mammary stem and progenitor cells as well as transformed tumor-initiating stem cells may be isolated by virtue of their expression of ALDH activity, as assessed by flow cytometry using the ALDEFLUOR assay (Ginestier, Hur et al. 2007). To determine whether those five breast cancer cell lines studied contain ALDEFLUOR-positive cells, we used ALDEFLUOR assay kit and performed flow cytometry analysis. Surprisingly, both GI-101A and SUM149PT contained a significant higher percentage of ALDEFLUOR-positive components comprising 6.43 ± 1.2% and 24.11 ± 5.3% of the total cell population (Fig. 4.3), respectively. We also stained adherent GI-101A cells with ALDEFLUOR dye in tissue culture ware and compared the images under two conditions of with or without ALDH inhibitor DEAB. The results proved that the DEAB can block ALDH enzyme activity and flow cytometry data are reliable (Fig. 4.4). SUM149PT derived from a patient with primary inflammatory breast cancer (IBC) (van Golen, Davies et al. 1999) and ALDEFLUOR-positive cancer stem cells were

already isolated from this cell line successfully (Charafe-Jauffret, Ginestier et al. 2009). Then we focused on the study of GI-101A.

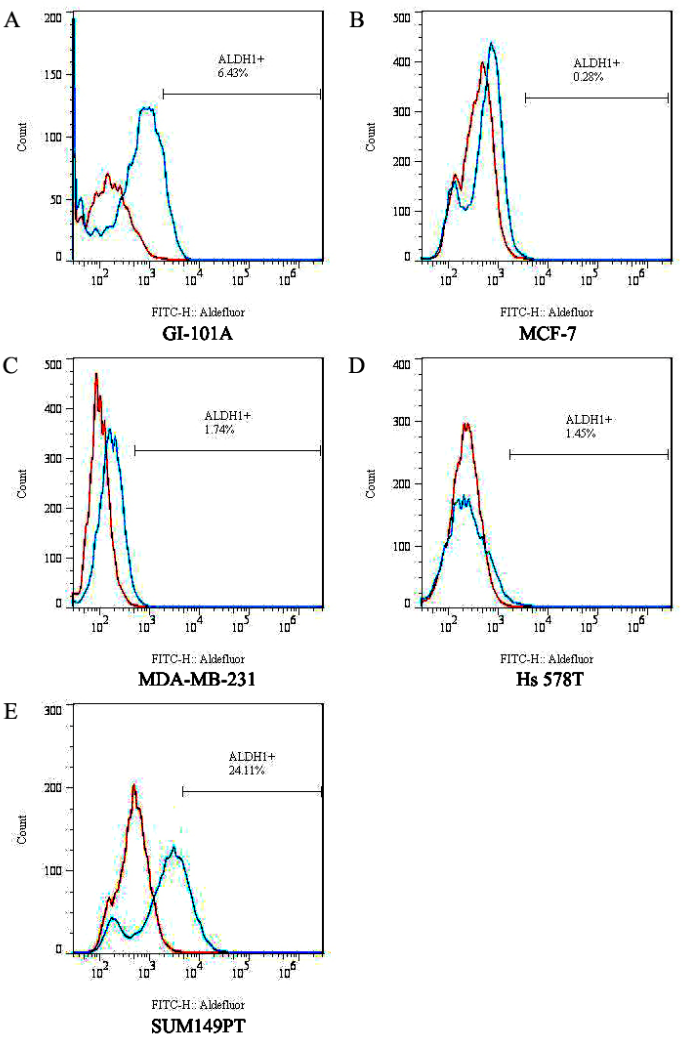

Fig. 4.3 Percentage of ALDEFLUOR-positive cells in human breast cancer cell lines. Representative flow cytometry analysis of ALDH activity in GI-101A (A), MCF-7 (B), MDA-MB-231 (C), HS578T (D) and SUM149PT (E). Red line indicates the ALDEFLUOR stained cells with the specific ALDH inhibitor diethylaminobenzaldehyde (DEAB) and blue line indicates stained cells without DEAB.

GI-101A ALDEFLUOR-positive and its counterpart, ALDEFLUOR-negative cells were isolated by using BD FACS Aria III cells sorter (Fig. 4.5A-D). The sorted cell fractions were checked concerning purity (Fig. 4.5E) and kept in growth medium for the

following experiments. Due to the instability of ALDEFLUOR dye in cells, the fluorescence intensity of the dye will decrease dramatically with time relapse. The final percentage of sorted ALDEFLURO-positive cells was 60-70% rather than almost 100%.

4.3.2 GI-101A ALDEFLUOR-positive cells have tumorigenic potential *in vitro* and *in vivo*

To test the tumorigenic potential of GI-101A ALDEFLUOR-positive cells, mammosphere formation assay and nude mice mammary fat pad xenograft assay were performed. For mammosphere formation assay, after the ALDEFLUOR-positive, ALDEFLUOR-negative cells were sorted based on the ALDH activity; single cells were plated in ultra-low attachment 96-well plates at different density of 1, 10 or

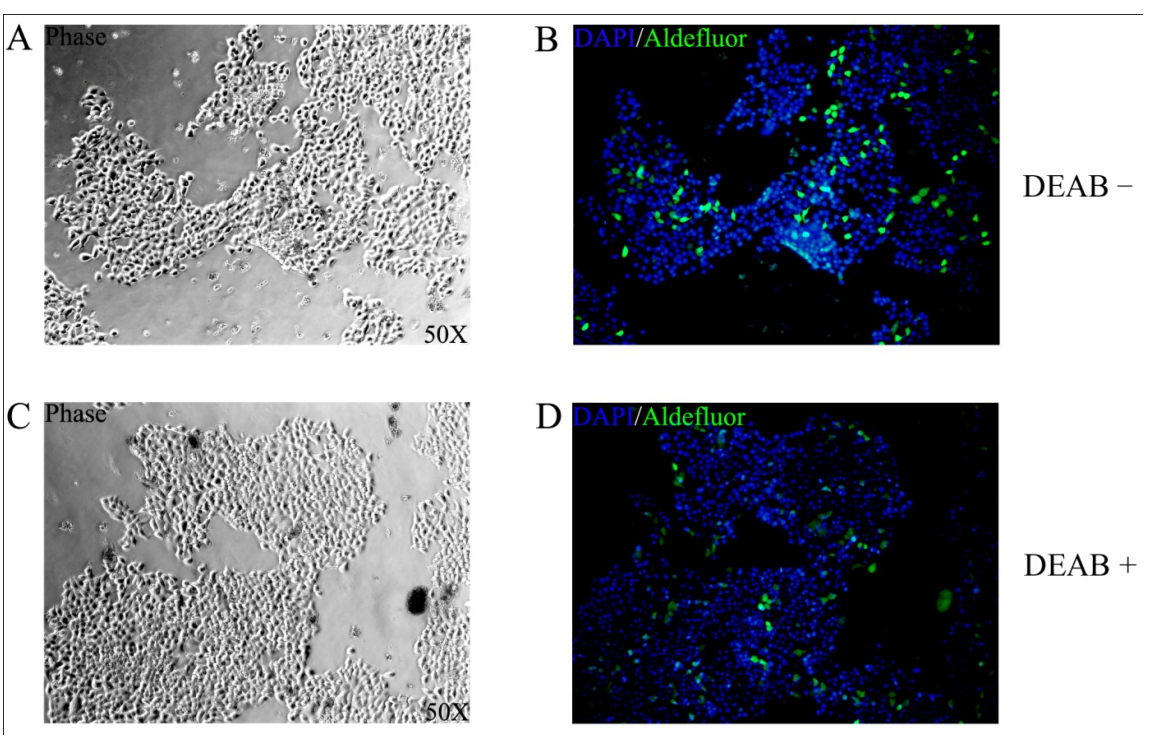

Fig. 4.4 Live cell imaging of ALDEFLUOR assay. GI-101A cells were stained by ALDEFLUOR dye without DEAB (A, B) or with DEAB (C, D).

100 viable cells/well. Serum-free medium which contained 10 ng/ml EGF and 20 ng/ml bFGF were added for culturing of mammosphere. The mammosphere formation was checked under the light microscope after 12 days culturing. We found

that mammosphere only formed at the density of 100 viable cells/well (Fig. 4.6A-C). The number of mammosphere was counted in each plate. The statistic analysis showed that GI-101A ALDEFLUOR-positive cells had significantly higher mammosphere formation efficiency than ALDEFLUOR-negative cells (Fig. 4.6 D). Six-week-old athymic *nu*/*nu* nude mice were used to assess the *in vivo* tumorigenicity properties of ALDEFLUOR-positive population, compared to ALDEFLUOR-negative population and unseparated population. Those three populations were tested by inoculation of limiting dilution of cells (50,000, 5,000 and 500 cells) into mammary fat pad of nude mice. Both tumor occurrence and tumor size were monitored after injection. The fat pads injected with 50,000 ALDEFLUOR-positive cells generated tumors starting after 5 weeks inoculation (Fig. 4.7 A). Then during the following weeks, ALDEFLUOR-positive cells always showed the highest frequency of tumor formation (Fig. 4.7 B-D). The tumor sizes generated from ALDEFLUOR-positive population were dramatically higher compared to ALDEFLUOR-negative populations (Fig. 4.7E). As shown in Fig. 4.7F and Fig. 4.7G, the size and latency of tumor formation correlated with the number of cells injected. Remarkably, 50,000 and 5,000 ALDEFLUOR- positive cells generated tumors more efficiently than ALDEFLUOR-negative cells. This is consistent with the results of the *in vitro* mammosphere formation experiment. Above all, both *in vitro* and *in vivo* experiments showed us the tumorigenic potential of GI-101A ALDEFLUOR-positive cells.

4.3.3 Both GI-101A ALDEFLUOR-positive and ALDEFLUOR-negative cells can reconstitute the parental cell line

The ability to both self-renewal and differentiate into heterogeneous cell types is the definition of a stem cell that is thought to be functionally mimicked by cancer stem cells (Bonnet and Dick 1997; Pardal, Clarke et al. 2003; Singh, Clarke et al. 2003; Ponti, Costa et al. 2005; Li, Heidt et al. 2007). To assess the ability of the various populations to differentiate and reconstitute the parental cell line, the sorted ALDEFLUOR-positive, ALDEFLUOR-negative and unseparated population were

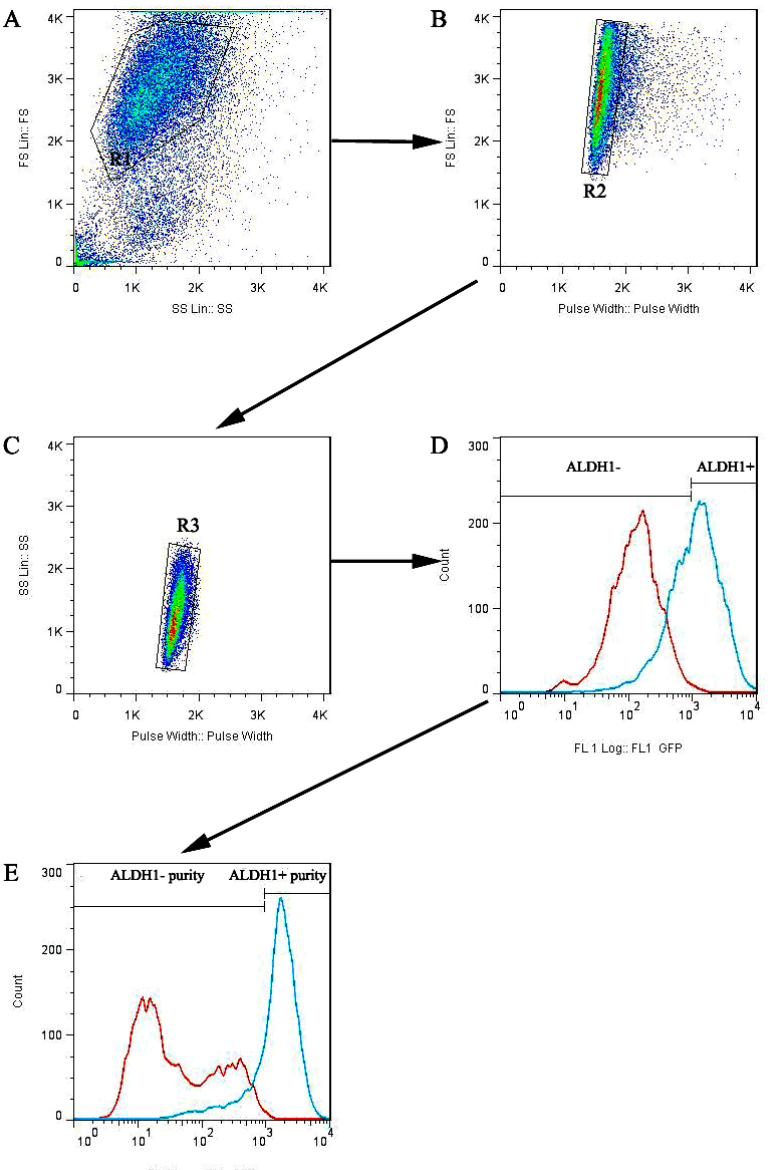

Fig. 4.5 Strategy for isolation of human breast cancer stem-like cells from the GI-101A cell line. Fluorescence-activated cell sorting (FACS) was used to isolate GI-101A ALDEFLUOR-positive and ALDEFLUOR-negative human breast cancer cells for functional assays. GI-101A cells were labeled with ALDEFLUOR dye. Cell subsets were isolated using single-color protocol on BD FACS Aria III cells sorter. (A-D): Representative scheme of a sequentially gated GI-101A cell line sort. (A) Cells were first selected for viability based on electronic gate R1. (B, C) Cells were then selected for singlet based on electronic gate R2 and R3. (D) Finally, cells were selected based on light scatter and divided into ALDH1+ (about 6% of parent population) and ALDH1- (about 80% of parent population) based on ALDH activity. (E) The sorted cell fractions were checked concerning purity based on ALDH activity. The ALDH1 fraction was about 60-70%.

plated and allowed to expand *in vitro* for 12 days. Expanded cultures were then analyzed by flow cytometry for reconstitution and differentiation (Fig. 4.8A-J). The cultures seeded with both ALDEFLUOR-positive and ALDEFLUOR-negative enriched

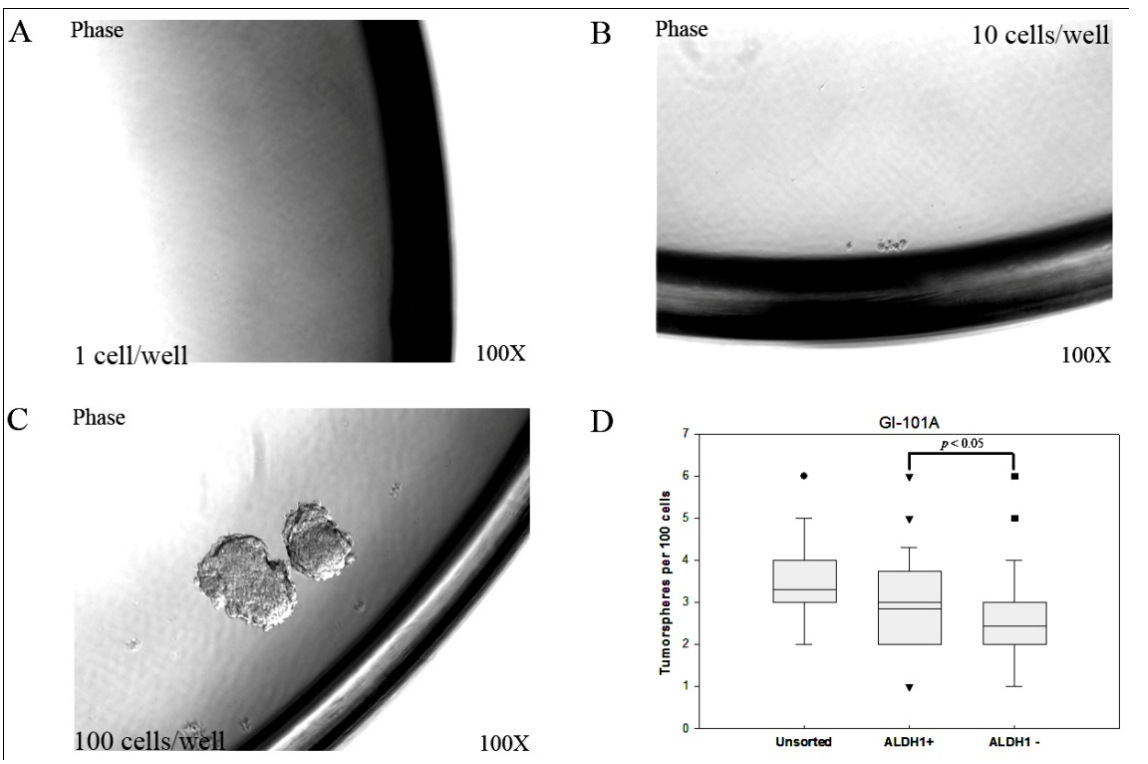

Fig. 4.6 Evaluation of the mammosphere formation efficiency of GI-101A ALDEFLEOR-positive and ALDEFLEOR-negative cells. (A-C): Sorted ALDH1+ cells were grown in anchorage independent condition with different cell density of (A) 1 cell/well, (B) 10 cells/well and (C) 100 cells/well for 12 days and checked under light microscope. (D) Statistical analysis of mammosphere number of three cells population. The mammosphere formation efficiency of ALDEFLEOR-positive cells was significantly higher than ALDEFLEOR-negative cells.

cells expand back into cultures nearly identical to the parental cell line after three passages (Fig. 4.8A, C, F, I, D, G, J) and unsorted cultures that were seeded in parallel (Fig. 4.8B, E, H). For ALDEFLUOR-positive population, this reconstitution and differentiation represents a change from nearly 64.2% ALDH1+ to 6.8% ALDH1+, whereas for ALDEFLUOR-negative population, reconstitution and differentiation represents a change from nearly 0% ALDH1+ to 7.74% ALDH1+.

4.3.4 GI-101A ALDEFLUOR-positive cells displayed chemo- and ionizing radiation-resistant properties

Given that breast cancer cell lines contain cells that exhibit properties of cancer stem-like cells, and cancer-initiating cells in primary human leukemia and glioblastoma are

A

Population	Tumors/Injection (by Week 5)		
	$5X10^2$	$5X10^3$	$5X10^4$
Unsorted	0/5	0/5	0/5
ALDH1+	0/5	0/5	3/3
ALDH1-	0/5	0/5	0/3

B

Population	Tumors/Injection (by Week 6)		
	$5X10^2$	$5X10^3$	$5X10^4$
Unsorted	0/5	0/5	2/5
ALDH1+	0/5	2/5	3/3
ALDH1-	0/5	1/5	3/3

C

Population	Tumors/Injection (by Week 8)		
	$5X10^2$	$5X10^3$	$5X10^4$
Unsorted	0/5	1/5	5/5
ALDH1+	0/5	4/5	3/3
ALDH1-	0/5	1/5	3/3

D

Population	Tumors/Injection (by Week 10)		
	$5X10^2$	$5X10^3$	$5X10^4$
Unsorted	0/5	3/5	5/5
ALDH1+	0/5	5/5	3/3
ALDH1-	0/5	5/5	3/3

E

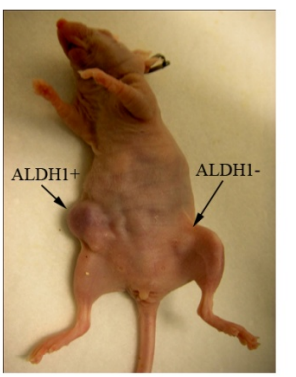

F

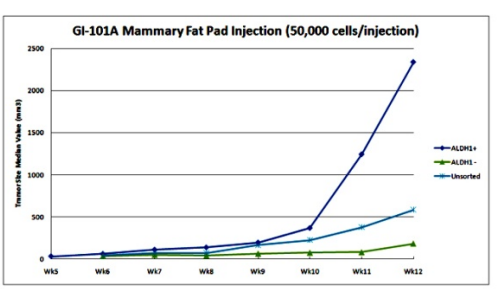

G

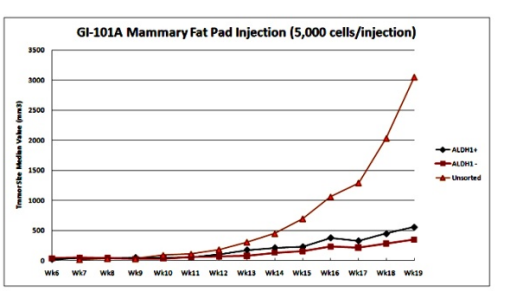

Fig. 4.7 The GI-101A ALDEFLUOR-positive cell population in athymic *nu*/*nu* nude mice has tumorigenic potential. (A-D) Representative tumor-forming frequency at different time points. (E) Representative tumor grown in *nu*/*nu* mouse at the ALDEFLUOR-positive cells' injection site (50,000 cells injected). Smaller tumor was detected at the ALDEFLUOR-negative cells' injection site (50,000 cells injected). (F-G) Tumor growth curves were plotted for the numbers of cells injected (50,000 cells and 5,000 cells) and for each population (ALDEFLUOR-positive, ALDEFLUOR-negative, unseparated). Tumor growth kinetics correlated with the latency and size of tumor formation and the number of ALDEFLUOR-positive cells.

resistant to chemotherapy (Costello, Mallet et al. 2000; Liu, Yuan et al. 2006), we sought to determine whether cell line-derived ALDH1+ cells would also preferentially survive treatment with chemotherapeutic agents. To this end, sorted ALDH1+, ALDH1- and unsorted GI-101A cells were treated for 4 days with different doses of breast cancer therapy chemical drug (5-FU: 10^{-7}, 10^{-6}, 10^{-5}, 10^{-4}, 10^{-3} mol/L;

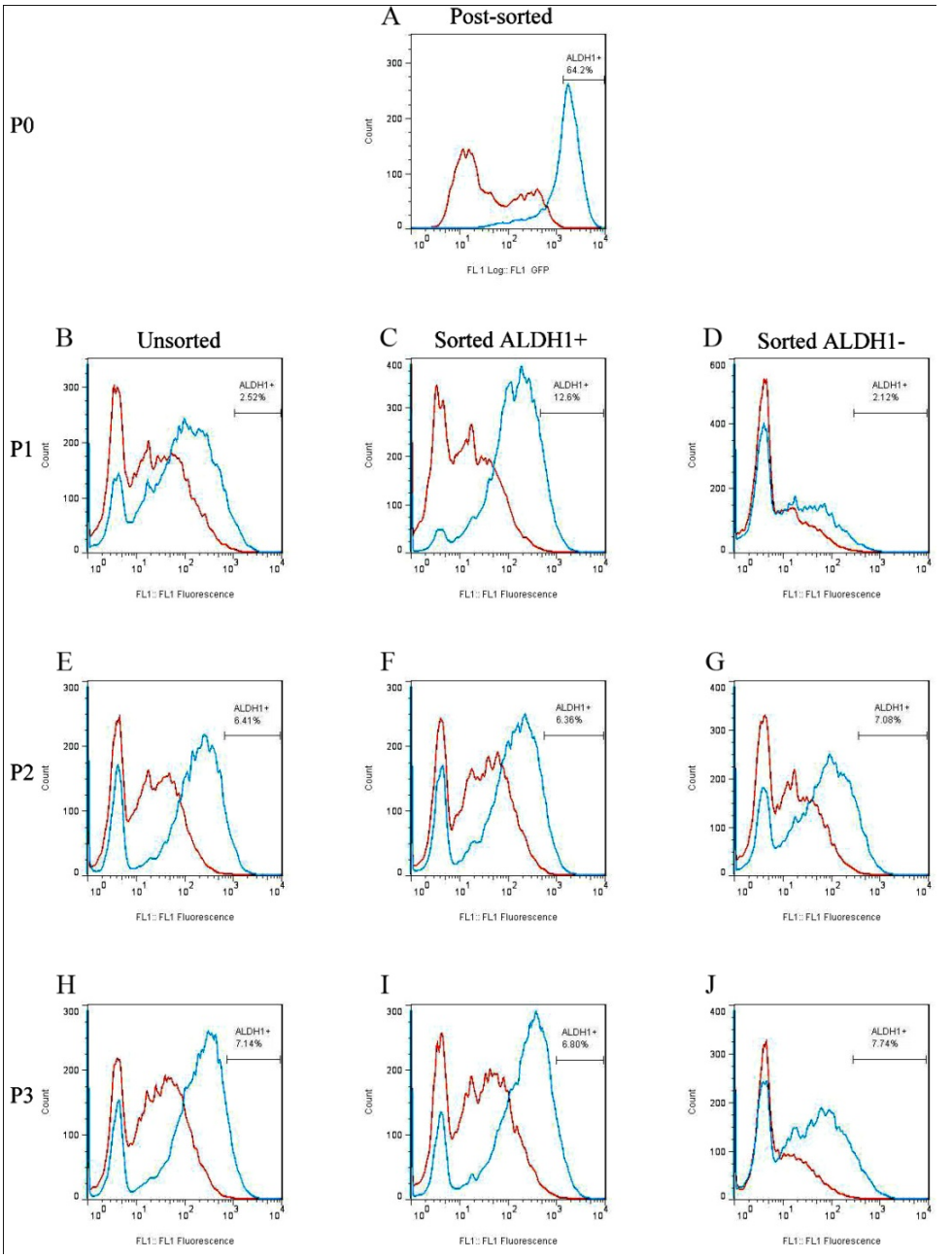

Fig. 4.8 Both GI-101A ALDEFLUOR-positive and ALDEFLUOR-negative cells were enriched for reconstitution of parent cell line. (A, C, E, F, I) The sorted ALDEFLUOR-positive cells were expanded and the cellular outgrowths were reanalyzed in each passage by flow cytometry to assess reconstitution of parent cell line. (D, G, J) The sorted ALDEFLUOR-negative cells were expanded and the cellular outgrowths were reanalyzed in each passage by flow cytometry to assess reconstitution of parental cell line. (B, E, H) The parental cell line was reanalyzed in parallel in each passage by flow cytometry.

Carboplatin: 10^{-7}, 10^{-6}, 10^{-5}, 10^{-4}, mol/L; Cisplatin: 10^{-7}, 10^{-6}, 10^{-5}, 10^{-4}, 10^{-3} mol/L; Mitomycin-C: 10^{-8}, 10^{-7}, 10^{-6}, 10^{-5}, 10^{-4} mol/L; Salinomycin: 10^{-7}, 10^{-6}, 10^{-5}, 10^{-4}, 10^{-3}

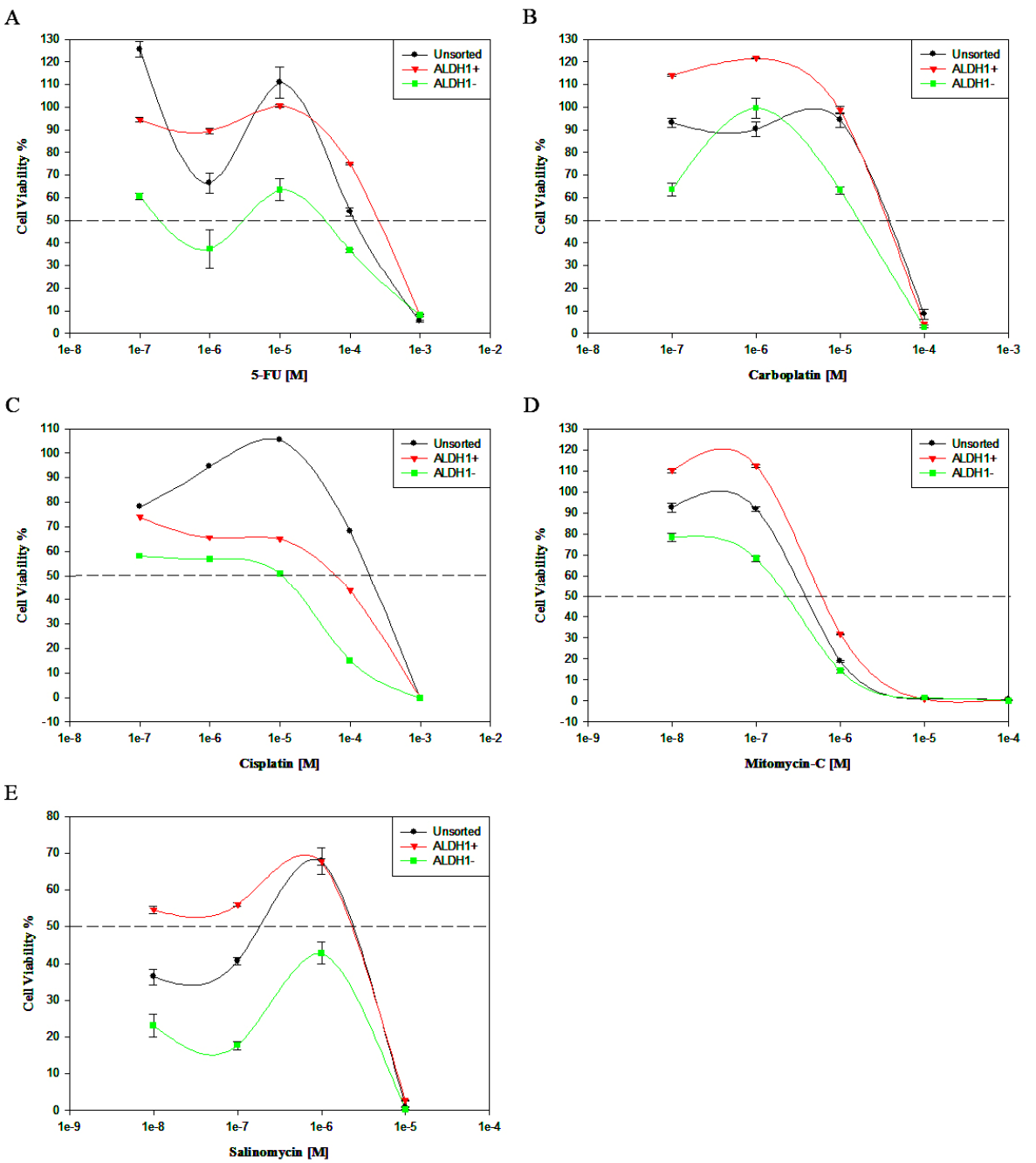

Fig. 4.9 Dose response curve of GI-101A ALDEFLUOR-positive, ALDEFLUOR-negative and unsorted cells treated with 5-FU (A), Carboplatin (B), Cisplatin (C), Mitomycin-C (D) and Salinomycin (E). Bars denote the standard error mean (n=4).

mol/L). As expected for chemo-resistance of cancer stem-like cells which derived from a cancer cell line, sorted ALDH1+ cells showed significant survival ability

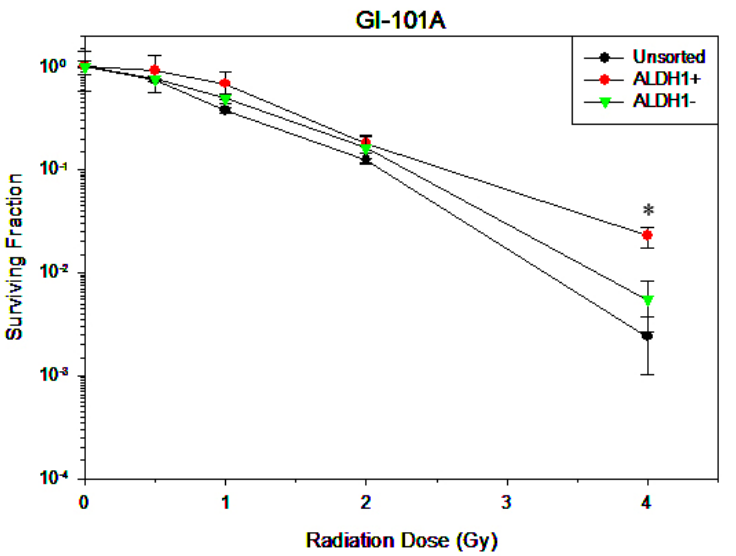

Fig. 4.10 Clonogenic radio-sensitivity of GI-101A ALDEFLUOR-positive, ALDEFLUOR-negative and unsorted cells. To determine surviving fractions, counts were normalized using the plating efficiency of the unirradiated corresponding control. Means and 95% confidence intervals from three independent experiments are shown (n=3).

compared to its counterpart ALDH1- cells (Fig. 4.9). To investigate the radio sensitivity of different fractions of GI-101A cells, we performed survival assays using increasing doses (0 Gy, 0.5 Gy, 1 Gy, 2 Gy, 4 Gy) of radiation. As shown in Fig. 4.10, the sorted ALDH1+ fraction had higher survival ability upon radiation treatment than the ALDH1- fraction.

4.3.5 Invasion and migration of GI-101A ALDEFLUOR-positive cells

The ALDEFLUOR-positive breast cancer cells have been reported to have cell invasion ability *in vitro* which is related to metastasis *in vivo* (Charafe-Jauffret, Ginestier et al. 2009; Croker, Goodale et al. 2009). We used a Basement Membrane Extract (BME) invasion assay, using 10% Fetal Bovine Serum as attractant, to examine the ability of ALDEFLUOR-positive and ALDEFLUOR-negative cell populations from GI-101A to invade. As shown in Fig. 4.11, ALDEFLUOR-positive

cells showed higher invasion through BME than the ALDEFLUOR-negative population. These results indicate that GI-0101A ALDEFLUOR-positive cells exhibited invasive behavior.

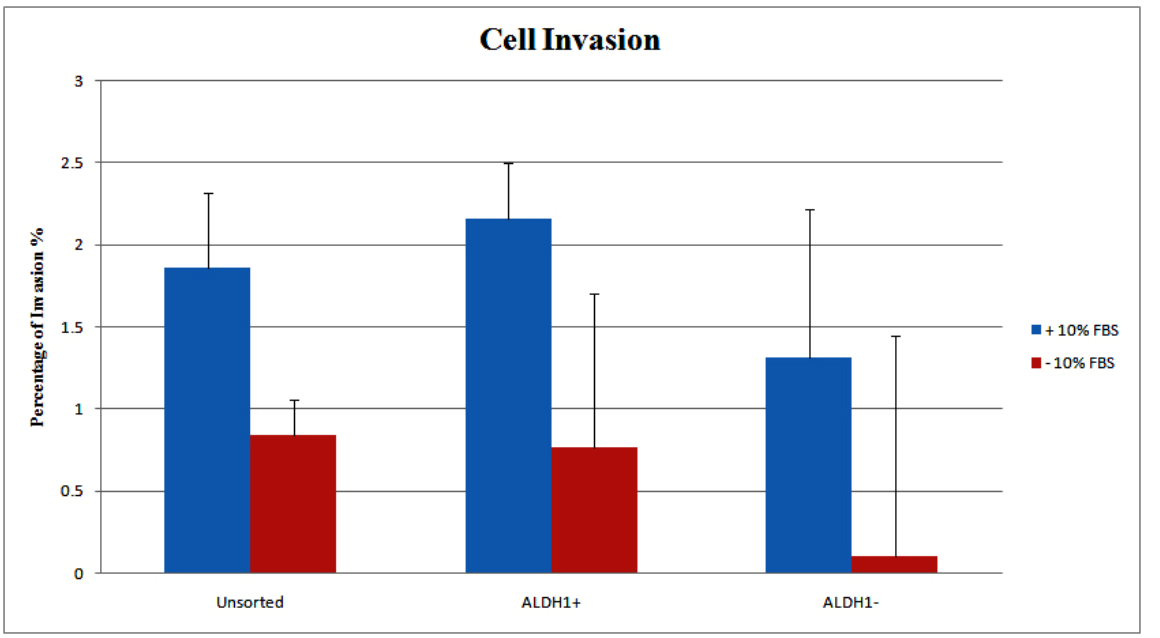

Fig. 4.11 Cell invasion ability of GI-101A ALDEFLUOR-positive cells. Bars denote the standard error mean (n=3).

4.3.6 CD44 and CD49f markers play a role in tumorigenicity of ALDEFLUOR-positive cells

In breast tumors, a $CD44^{+}/CD24^{-/low}/ESA^{+}/Lineage^{-}$ subpopulation was originally identified as the tumorigenic (tumor-initiating) fraction, based on the enhanced ability of these cells to form tumors in non-obese diabetic/severe combined immunodeficiency (NOD/SCID) mice when injected at a very low number (Al-Hajj, Wicha et al. 2003). Human breast cancer cell lines contain $CD44^{+}/CD24^{-/low}/ESA^{+}$ cells that have stem cell properties including anchorage-independent growth at clonal densities (self-renewal) and the ability to reconstruct the parental cell fractions, along with *in vivo* tumorigenicity (Ponti, Costa et al. 2005; Fillmore and Kuperwasser 2008). The $CD44^{+}/CD24^{-/low}$ phenotype is also correlated with the enhanced expression of pro-invasive genes and the ability to form distant metastasis (Abraham, Fritz et al. 2005; Balic, Lin et al. 2006; Sheridan, Kishimoto et al. 2006). In addition, tumorigenicity of prospective breast CSCs has been linked to the expression of α6

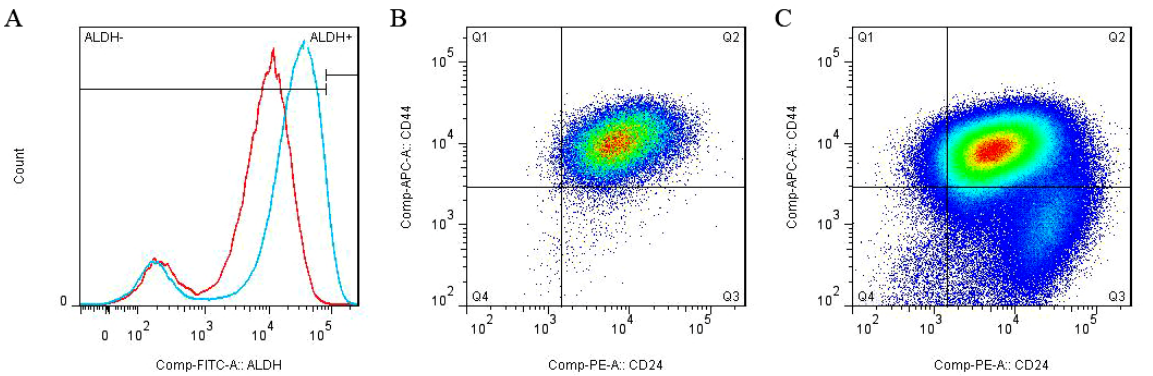

	ALDH+	ALDH -
+DEAB	0.09%	99.9%
- DEAB	7.59%	92.4%

	CD44+/CD24-	CD44+/CD24+	CD44-/CD24+	CD44-/CD24-
ALDH+	0.79%	97.1%	1.82%	0.25%
ALDH -	2.53%	82.7%	13.6%	1.24%

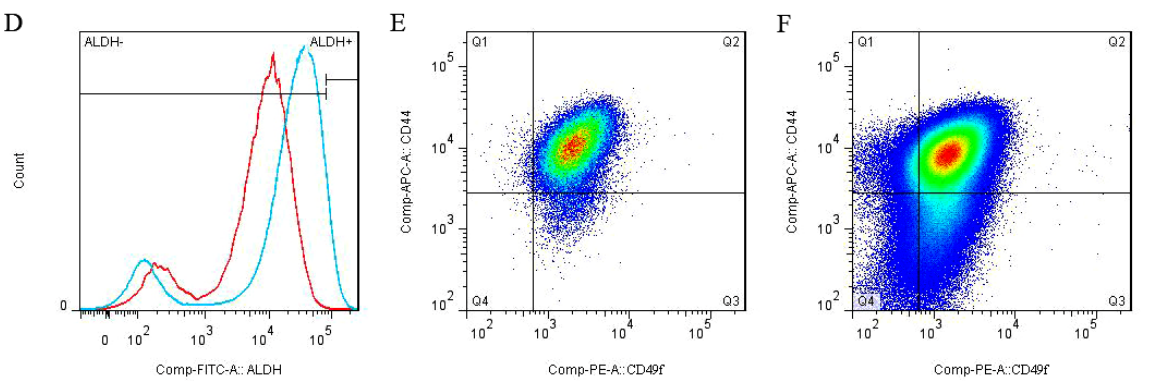

	ALDH+	ALDH -
+DEAB	0.09%	99.9%
- DEAB	8.37%	91.6%

	CD44+/CD49f-	CD44+/CD49f+	CD44-/CD49f+	CD44-/CD49f-
ALDH+	0.79%	94.2%	4.89%	0.12%
ALDH -	4.83%	77.0%	13.8%	4.35%

Fig. 4.12 Representatives of ALDEFLUOR assay followed by Flow Cytometry analysis of surface markers CD44/CD24 and CD44/CD49f. (A, D) The gated of ALDEFLUOR-positive and ALDEFLUOR-negative cells. (B) Analysis of CD44/CD24 expression in ALDEFLUOR-positive cells derived from (A). (C) Analysis of CD44/CD24 expression in ALDEFLUOR-negative cells derived from (A). (E) Analysis of CD44/CD49f expression in ALDEFLUOR-positive cells derived from (D). (F) Analysis of CD44/CD49f expression in ALDEFLUOR-negative cells derived from (D).

integrin (CD49f) (Cariati, Naderi et al. 2008) and β1 integrin (Crowe and Ohannessian 2004). To analyze the CD44/CD24/CD49f expression in ALDEFLUOR-positive and ALDEFLUOR-negative cells, we performed ALDEFLUOR assay followed

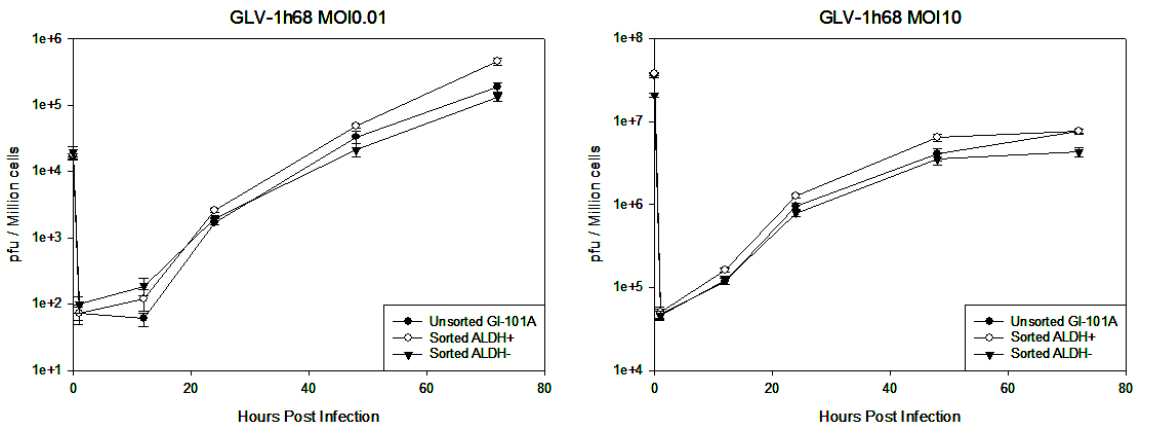

Fig. 4.13 GLV-1h68 growth curve in parent GI-101A cells and sorted ALDEFLUOR-positive and ALDEFLUOR-negative cells at MOI0.01 (left) or MOI10 (right). Bars denote the standard error mean (n=6).

by CD44, CD24 and CD49f staining of GI-101A cells. As indicated in Fig. 4.12, the percentage of $CD44^+$ in ALDEFLUOR-positive cells reached to 97.89% (Fig. 4.12B gate Q1+Q2) or 94.99% (Fig. 4.12E gate Q1+Q2). However, the percentage of $CD44^+$ in ALDEFLUOR-negative cells dropped to 85.23% (Fig. 4.12C gate Q1+Q2) or 81.83% (Fig. 4.12F gate Q1+Q2). Similarly, the percentage of $CD49f^+$ in ALDEFLUOR-positive cells reached 99.09% (Fig. 4.12E gate Q2+Q3) and the percentage of $CD49f^+$ in ALDEFLUOR-negative cells dropped to 90.8% (Fig. 4.12F gate Q1+Q2). Furthermore, there was no significant difference of the $CD24^+$ expression between ALDEFLUOR-positive cells (98.92%, Fig. 4.12B gate Q2+Q3) and ALDEFLUOR-negative cells (96.3%, Fig. 4.12C gate Q2+Q3). If we consider those surface marker expression in combination, unexpectedly, the percentage of $CD44^+/CD24^-$ in ALDEFLUOR-positive cells (0.79%, Fig. 4.12B gate Q1) was lower than that in ALDEFLUOR-negative cells (2.53%, Fig. 4.12C gate Q1). And the percentage of $CD44^+/CD49f^+$ in ALDEFLUOR-positive cells (94.2%, Fig. 4.12E gate Q2) was higher than it in ALDEFLUOR-negative cells (77.0%, Fig. 4.12F gate Q2).

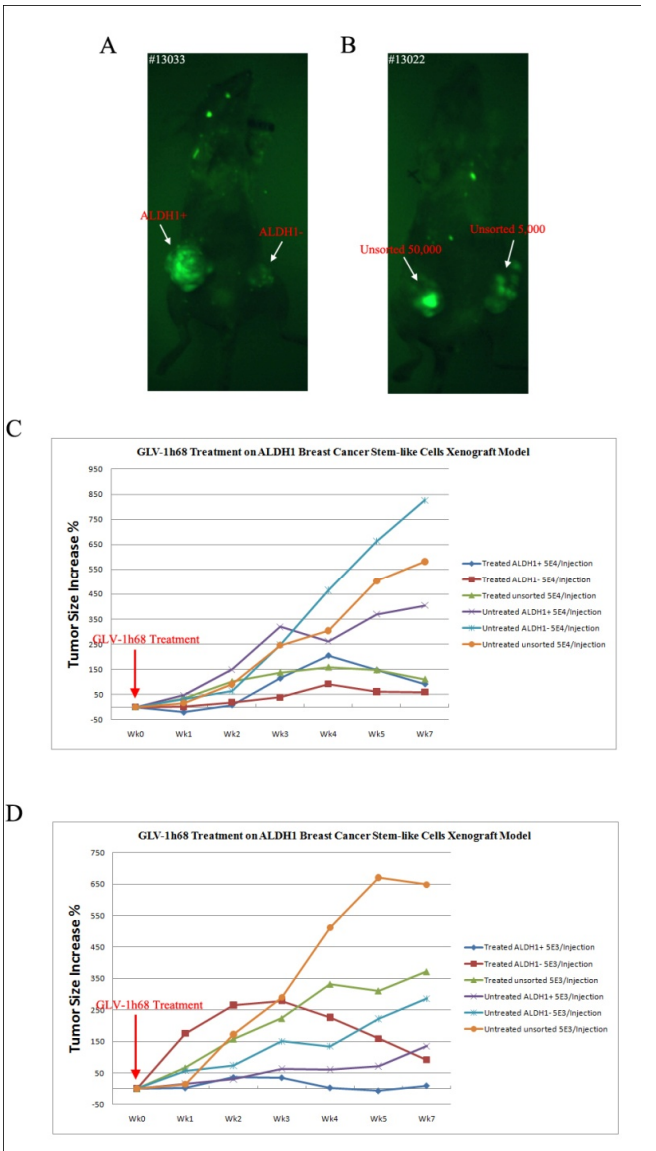

Fig. 4.14 Retro-orbital injection of vaccinia virus GLV-1h68 induces tumor regression of solid tumor xenografts from GI-101A Aldefluor cells. (A) An example of *in vivo* tumor GFP imaging of virus treated tumors derived from ALDEFLUOR-positive and ALDEFLUOR-negative cells. (B) Another example of *in vivo* tumor GFP imaging of virus treated 50,000 and 5,000 tumor derived from unsorted GI-101A cells. (C) 50,000 sorted and unsorted cells implanted in the mammary fat pads of athymic nude mice were injected with vaccinia virus GLV-1h68 (n=3 in each group) or PBS (n=1, 2 or 3) on day 0 (downward arrow). Tumor Percentage of increase in tumor size was determined based on the median value of tumor size before virus treatment (week 0) and after treatment. Each data point was calculated by using the following formula: 100 %×(week n-week 0)/week 0. (D) 5,000 sorted and unsorted cells implanted in the mammary fat pads of athymic nude mice were injected with vaccinia virus GLV-1h68 (n=2 or 3 in each group) or PBS (n=3, 4 or 2) on day 0 (downward arrow).

4.3.7 Viral replication in GI-101A ALDEFLUOR-positive and ALDEFLUOR-negative cells

To test the replication efficiency of vaccinia virus strain GLV-1h68 in sorted GI-101A ALDEFLUOR-positive and –negative cells, we performed a replication assay. The cells were infected with GLV-1h68 at an MOI of 0.01 or 10, followed by determination of viral titers at the time points 1, 12, 24, 48 and 72 hours post infection. Average data including standard deviation are shown (Fig. 4.13) for parental GI-101A and ALDEFLUOR-negative cells in comparison to ALDEFLUOR-positive cells. In 72 hours post infection, the virus titer of ALDEFLUOR-positive cells was about three times higher than ALDEFLUOR-negative cells upon MOI0.01 treatment and about two times higher upon MOI10 treatment.

4.3.8 Vaccinia virus GLV-1h68 induces tumor regression of GI-101A ALDEFLUOR-positive cell xenografts

Previously we have shown that GI-101A ALDEFLUOR-positive cells had more tumorigenic potential in nude mice and vaccinia virus GLV-1h68 could replicate more efficiently in the ALDEFLUOR-positive cells compared to the ALDEFLUOR-negative cells. To test the efficacy of oncolytic vaccinia virus to target and kill breast CSCs *in vivo*, we established palpable tumors in the mammary fat pads of athymic *nu*/*nu* nude mice using sorted GI-101A ALDEFLUOR-positive, ALDEFLUOR-negative and unsorted cells with the two doses of 50,000 or 5,000 cells/injection. For more comparable results, each mouse was implanted two counterparts' cell fractions in left and right mammary fat pads respectively (i.e. 50,000 ALDEFLUOR-positive cells in right fat pad and 50,000 ALDEFLUOR-negative cells in left fad pad). After 12 weeks of tumor implantation, each mouse was given 5×10^6 pfu GLV-1h68 virus through the retro-orbital path. Then the tumor size and tumor GFP expression was monitored weekly. As shown in Fig 4.14, the tumor growth was significantly inhibited after the virus treatment. Comparably, in the 5,000 cells/injection group, tumors derived from ALDEFLUOR-positive cells showed dramatic response upon virus treatment compared to tumors derived from ALDEFLUOR-negative or unsorted cells (Fig. 4.14D). The tumor fluorescence images also indicated that infected tumor derived from ALDEFLUOR-positive cells had more vaccinia virus replication (Fig. 4.14A), which proved the trends of tumor regression.

4.4 The Epithelia-Mesenchymal Transition (EMT) Generates Cells Enriched $CD44^{+}/CD24^{-/low}$ Population

4.4.1 Induction of an EMT in human mammary epithelia cells

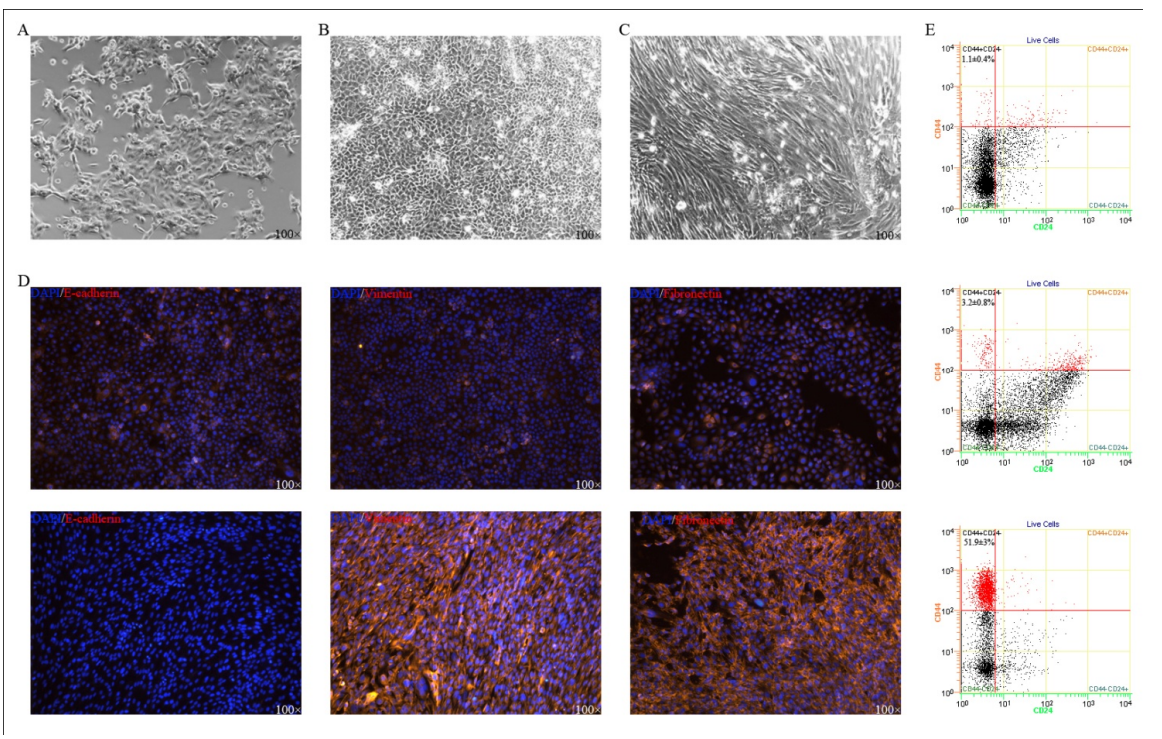

Fig. 4.15 Induction of an EMT in HMLE cells. Initial HMLE cells grown in DMEM/F-12 medium (A), the cells showed different morphology in the absence (B) or presence (C) of TGF-β1. (D) Immunostaining of EMT-induced (*bottom row*) or non-induced (*top row*) cells. The expression of E-cadherin (*left column*), vimentin (*middle column*) and fibronectin (*left column*) was determined. (E) Flow cytometry analysis of CD44/CD24 expression in initial (*top*), non-induced (*middle*) or EMT induced (*bottom*) cells.

The Epithelial-Mesenchymal Transition (EMT) is a key developmental program that is often activated during cancer invasion and metastasis. Human breast cancer stem cells could be generated from transformed human mammary epithelial cells by activating EMT progress (Mani, Guo et al. 2008; Morel, Lievre et al. 2008). Congruent with previously reported experiments using models of hematopoietic malignancies (Cozzio, Passegue et al. 2003; So, Karsunky et al. 2003; Huntly, Shigematsu et al.

2004; Krivtsov, Twomey et al. 2006), transformed breast cancer cells were obtained *in vitro* by introducing a series of oncogenes and cancer-associated genes into normal primary human mammary epithelial cells. This experimental system starts with primary human mammary epithelial cells (HMECs), which undergo sequential retroviral-mediated expression of the telomerase catalytic subunit (giving rise to HMEC/hTERT cells), SV40 large T and small t antigens (HMLE cells) and an oncogenic allele of H-Ras, H-Ras^{V12} (HMLER cells) (Elenbaas, Spirio et al. 2001). To determine whether adult cells that have undergone an EMT could generate more CD44^{+}/CD24$^{-/low}$ phenotype population, we induced HMLE cells (kindly provided by Dr. Robert A. Weinberg) by using TGF-β1 (2.5 ng/ml). After 12 days, there was significant change of HMLE cells' morphology in the absence (Fig. 4.15B) or presence (Fig. 4.15C) of TGF-β1. Historically, epithelial and mesenchymal cells have been identified on the basis of their unique visual appearance and the morphology of the multicellular structures they create (Shook and Keller 2003). The TGF-β1 induced HMLE cells showed typical mesenchymal characteristics which are in spindle and irregular shape with migratory protrusions compared to non-induced controls which displayed regularly spaced cell-cell junctions. To confirm the mesenchymal phenotype of TGF-β1 induced HMLE cells, we performed Immunostaining by using E-cadherin, vimentin and fibronectin these three widely used EMT markers. As shown in Fig. 4.15D, the E-cadherin expression was down-regulated in TGF-β1 induced HMLE cells (*bottom left*) compared to non-induced cells (*top left*); the vimentin expression was up-regulated in induced cells (*bottom middle*) compared to non-induced cells (*top middle*) and the Fibronectin expression was up-regulated in induced cells (*bottom right*) compared to non-induced cells (*top right*). Then we tested the expression of human breast cancer stem cells surface marker CD44/CD24 in HMLE cells which was undergoing EMT. As shown in Fig. 4.15E, CD44^{+}/CD24$^{-/low}$ population was enriched after 12 days EMT induction in the presence of TGF-β1 (*bottom*). However, the CD44^{+}/CD24$^{-/low}$ percentage of non-induced HMLE cells (*middle*) did not change much more compared to initial cells (*top*).

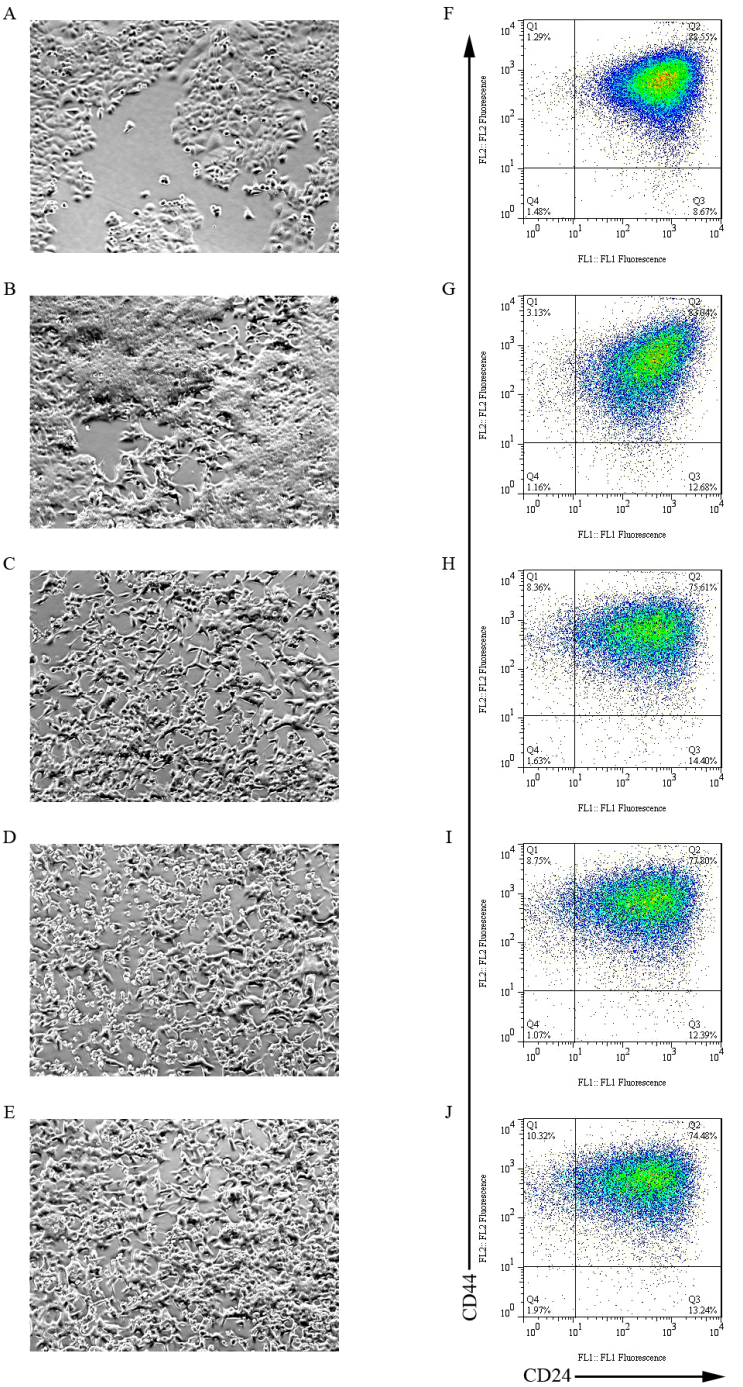

Fig. 4.16 Induction of an EMT in GI-101A cells with different combination of growth factors. (A-E) Morphology of cells without (A) or with treatment of TGF-β1 (B), EGF+TGF-β1 (C), EGF+bFGF (D) and EGF+bFGF +TGF-β1 (E). (F-J) Flow cytometry analysis of CD44/CD24 in cells without (F) or with treatment of TGF-β1 (G), EGF+TGF-β1 (H), EGF+bFGF (I) and EGF+bFGF +TGF-β1 (J).

4.4.2 Induction of an EMT in GI-101A cells

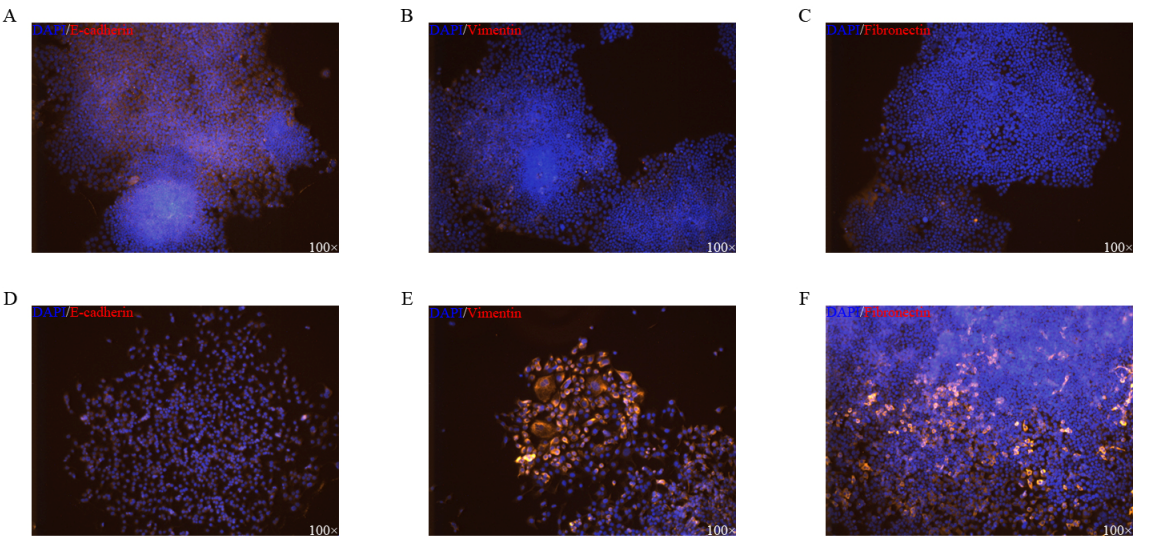

Fig. 4.17 Immunostaining of EMT induced (D-F) or non-induced (A-C) GI-101A cells. The expression of E-cadherin (A, D), vimentin (B, E) and fibronectin (C, F) was determined.

Similar to HMLE, we used some growth factors such as EGF, bFGF and TGF-β1to trigger EMT. Together with TGF-β1, EGF was an addition for EMT induction. Also there were some groups which used bFGF and TGF-β1 to induce EMT (Strutz, Zeisberg et al. 2002). To test the efficiency of these growth factors, we induced EMT in GI-101A cells with different combinations of growth factors, like TGF-β1 only (Fig. 4.16B), EGF+TGF-β1 (Fig. 4.14C), EGF+bFGF (Fig. 4.16D) and EGF+bFGF+TGF-β1 (Fig. 4.16E). As shown in Fig. 4.16 A-E, after 12 days of EMT induction, the morphology of cells in the presence of growth factors changed significantly compared to the control (Fig. 4.16A). According to the morphology, we found the growth factor combination of EGF+bFGF+TGF-β1 could induce EMT more efficiently than other combinations. To confirm this, we did flow cytometry analysis of CD44/CD24 in those cells. The results showed that GI-101A cell induced by triple growth factors contained the highest $CD44^{+}/CD24^{-/low}$ percentage (Fig. 4.16J). The percentage of $CD44^{+}/CD24^{-/low}$ in cells which have undergone treatment with other combinations of growth factors like TGF-β1 only (Fig. 4.16G), EGF+TGF-β1 (Fig. 4.16H), EGF+bFGF (Fig. 4.16I) were also higher than non-induced cells (Fig. 4.16F).

Furthermore, we checked the expression of E-cadherin, vimentin and fibronectin in triple growth factors treated and non-treated cells. As shown in Fig. 4.17, the E-cadherin expression was down-regulated in triple growth factors induced GI-101A cells (Fig. 4.17D) compared to non-induced cells (Fig. 4.17A); the vimentin expression was up-regulated in induced cells (Fig. 4.17E) compared to non-induced cells (Fig. 4.17B) and the fibronectin expression was up-regulated in induced cells (Fig. 4.17F) compared to non-induced cells (Fig. 4.17C).

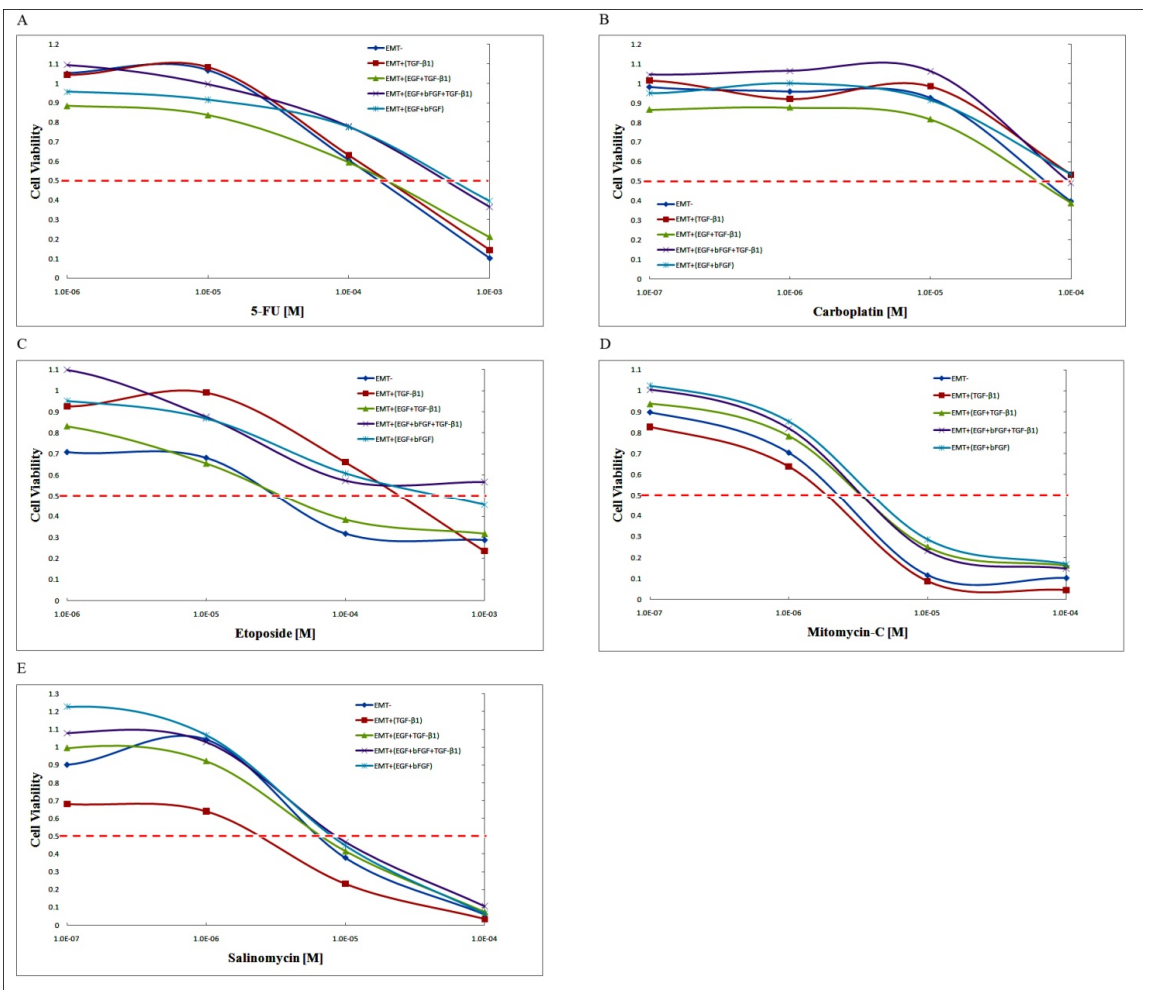

Fig. 4.18 Dose response curve of non-induced GI-101A cells and TGF-β1 only, EGF+TGF-β1, EGF+bFGF, EGF+bFGF+TGF-β1 induced EMT cells treated with 5-FU (A), Carboplatin (B), Etoposide (C), Mitomycin-C (D) and Salinomycin (E).

4.4.3 GI-101A EMT-induced cells displayed a chemo-resistant property

CSCs are resistant to many current cancer treatments, including chemo- and radiation therapy (Dean, Fojo et al. 2005; Bao, Wu et al. 2006; Diehn and Clarke 2006; Woodward, Chen et al. 2007; Eyler and Rich 2008; Li, Lewis et al. 2008; Diehn, Cho et al. 2009). This suggests that many cancer therapies, while killing the bulk of tumor cells, may ultimately fail because they do not eliminate CSCs, which survive to regenerate new tumors. The induction of an epithelial-mesenchymal transition (EMT) in normal or neoplastic mammary epithelial cell populations has been shown to result in the enrichment of cells with stem-like properties (Mani, Guo et al. 2008). Previously, GI-101A cells were induced to EMT by using growth factors. To determine whether those EMT induced breast cancer cells were enriched in cancer stem-like cells which displayed chemo-resistant ability, we treated those cells with different doses breast cancer therapy chemical drug (5-FU: 10^{-6}, 10^{-5}, 10^{-4}, 10^{-3} mol/L; Carboplatin: 10^{-7}, 10^{-6}, 10^{-5}, 10^{-4}, mol/L; Etoposide: 10^{-6}, 10^{-5}, 10^{-4}, 10^{-3} mol/L; Mitomycin-C: 10^{-7}, 10^{-6}, 10^{-5}, 10^{-4} mol/L; Salinomycin: 10^{-7}, 10^{-6}, 10^{-5}, 10^{-4} mol/L). As expected for chemo-resistance of cancer stem-like cells which enriched in EMT induce GI-101A cells, both the growth factor combinations of EGF+bFGF+TGF-β1 and EGF+bFGF induced GI-101A cells showed significant survival ability compared to other growth factors combination induced or non-induced cells (Fig. 4.18A-D). Unexpectedly, those EMT cells lost the chemo-resistant ability upon the treatment of Salinomycin, an inhibitor of cancer stem cells (Gupta, Onder et al. 2009) (Fig. 4.18E).

4.4.4 EMT induction promotes GI-101A cell invasion and migration

As described above, the morphology of EMT-induced GI-101A cells displayed increased cell motility and migratory capacity. We therefore examined the invasive and migrating ability of those EMT 6 days induced cells after plating on Basement Membrane Extract (BME) coated transwell and found those cells which were undergoing EMT migrated through BME more efficiently than the control cells (Fig. 4.19). As a chemoattracant, 10% Fetal Bovine Serum (FBS) showed less effect on invasion and migration of EMT cells.

4.4.5 Vaccinia virus preferentially replicates in EMT-induced cells

To test whether vaccinia virus could replicate more efficiently, we used two vaccinia virus strains. GLV-1h68, which carries the GFP gene and GLV-1h190, which carries the TuborRFP (a Far-Red Fluorescence) gene to infect HMLE or GI-101A cells which are undergoing EMT at MOI10. As shown in Fig. 4.20, both HMLE cells which were undergoing EMT upon TGF-β1 treatment (Fig. 4.20C-D) or not (Fig. 4.20A-B) were infected by GLV-1h190, a TuborRFP vaccinia virus, at MOI10. After 12 hours post

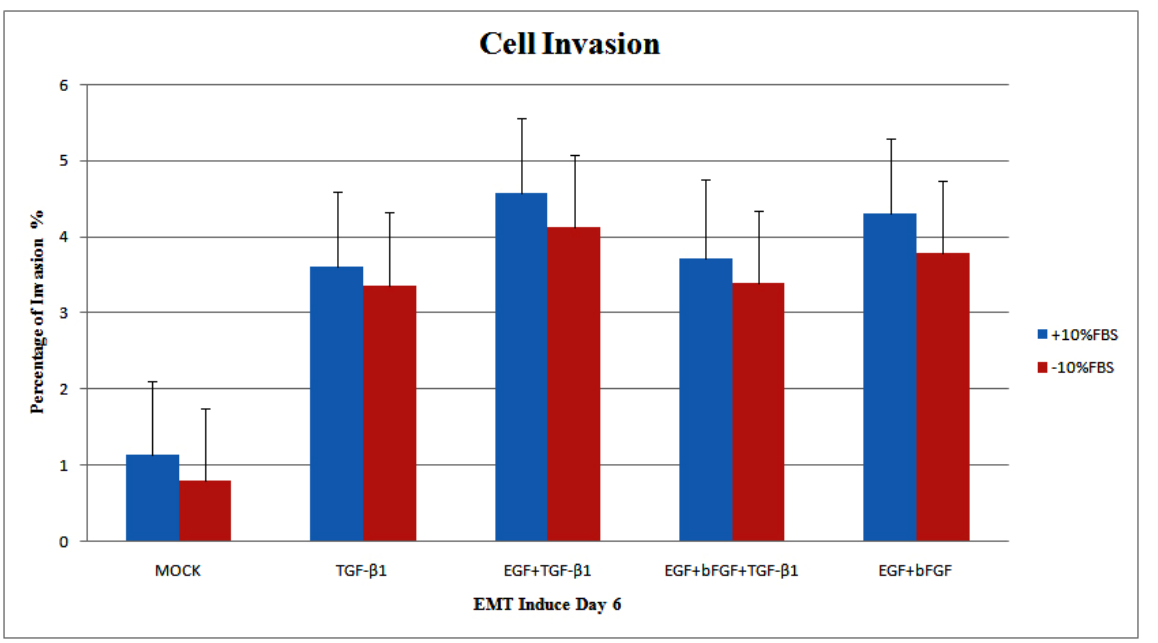

Fig. 4.19 EMT promotes GI-101A cells invasion and migration. Bars denote the standard error mean (n=3).

infection, there were only few non-TGF-β1 treatment HMLE cells that expressed TuborRFP protein (Fig. 4.20B); and for TGF-β1 treatment cells, all mesenchymal type cells expressed the TuborRFP protein and only few epithelial type cells were red (Fig. 4.20D). For breast cancer cell line GI-101A, after the cells were treated with TGF-β1 for 12 days, they were infected by GLV-1h68, a GFP vaccinia virus, at MOI10 for 12 hours. The images were taken at the same position of the plates every 2 hours. As shown in Fig. 4.21, during 6 hours to 12 hours post infection, the mesenchymal type GI-101A cell expressed GFP earlier and more efficiently compared to epithelia type cells. The cytopathogenic effect (CPE) in mesenchymal type cells was more

significant than in epithelia type cells. All the above indicates that the vaccinia virus is preferentially replicated in EMT cells from both normal tissue and tumors.

4.4.6 Isolation of a $CD44^+/CD24^-/ESA^+$ population from EMT-induced GI-101A cells

The intracellular marker $CD44^+/CD24^-/ESA^+$ was widely used in identification and isolation of human breast cancer stem cells since it was firstly utilized to process breast cancer stem cells patient sample (Al-Hajj, Wicha et al. 2003). Then more and

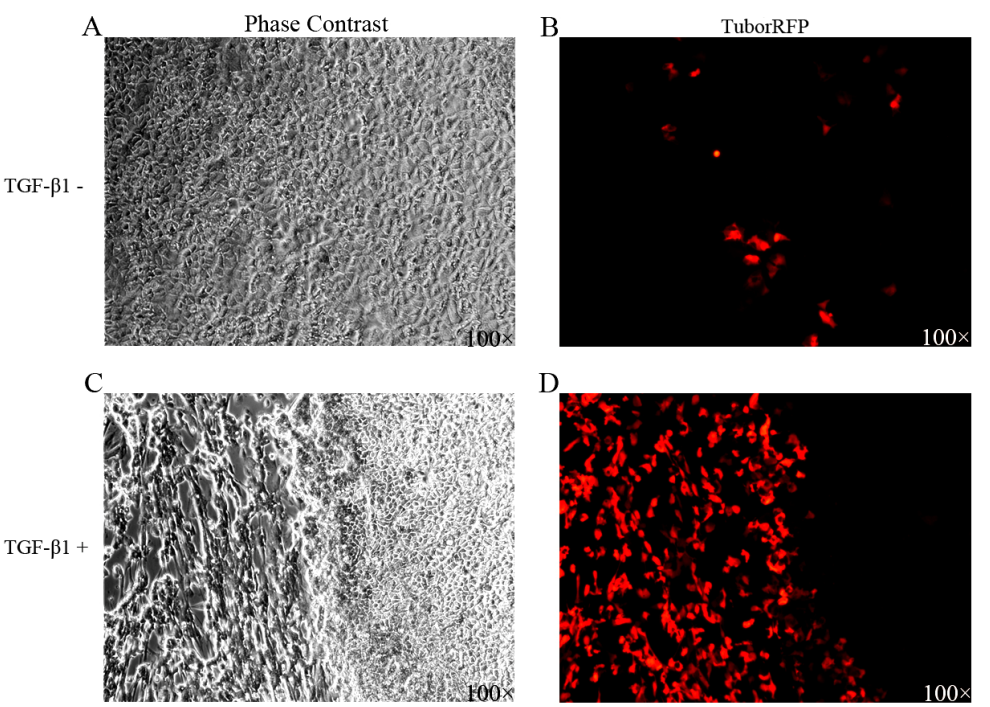

Fig. 4.20 TGF-β1-induced HMLE cells or normal HMLE cells infected by GLV-1h190 at MOI0. The images were captured at 12 hours post infection. (A-B) Phase contrast and fluorescence images of HMLE cells without TGF-β1 treatment. (C-D) Phase contrast and fluorescence images of HMLE cells with TGF-β1 treatment.

more investigators used it alone or combined with other methods and tools to discover human breast cancer stem cells from either cancer cell lines (Sheridan, Kishimoto et al. 2006; Fillmore and Kuperwasser 2008; Meyer, Fleming et al. 2009) or primary tumors (Ginestier, Hur et al. 2007; Wright, Calcagno et al. 2008; Mine, Matsueda et al. 2009). $CD44^+/CD24^-$ cells could be enriched by inducing Epithelial-

Mesenchymal Transition from normal mammary epithelia cells or cancer cell lines, according to our previous data or other laboratories (Mani, Guo et al. 2008; Morel, Lievre et al. 2008; Gupta, Onder et al. 2009). As described before, GI-101A cells were induced to EMT by treated with triple growth factors EGF (5 ng/ml), bFGF (10 ng/ml) and TGF-β1 (2.5 ng/ml) for 12 days. Then the cells were sorted by using BD FACS Aria III cells sorter. As shown in Fig. 4.22A-C, the cells were electronically gated to exclude dead cells, aggregates and doublets. Then the CD44/CD24 (Fig. 4.22D, F) and ESA (Fig. 4.22E, G) antigen were analyzed. The ESA expression in

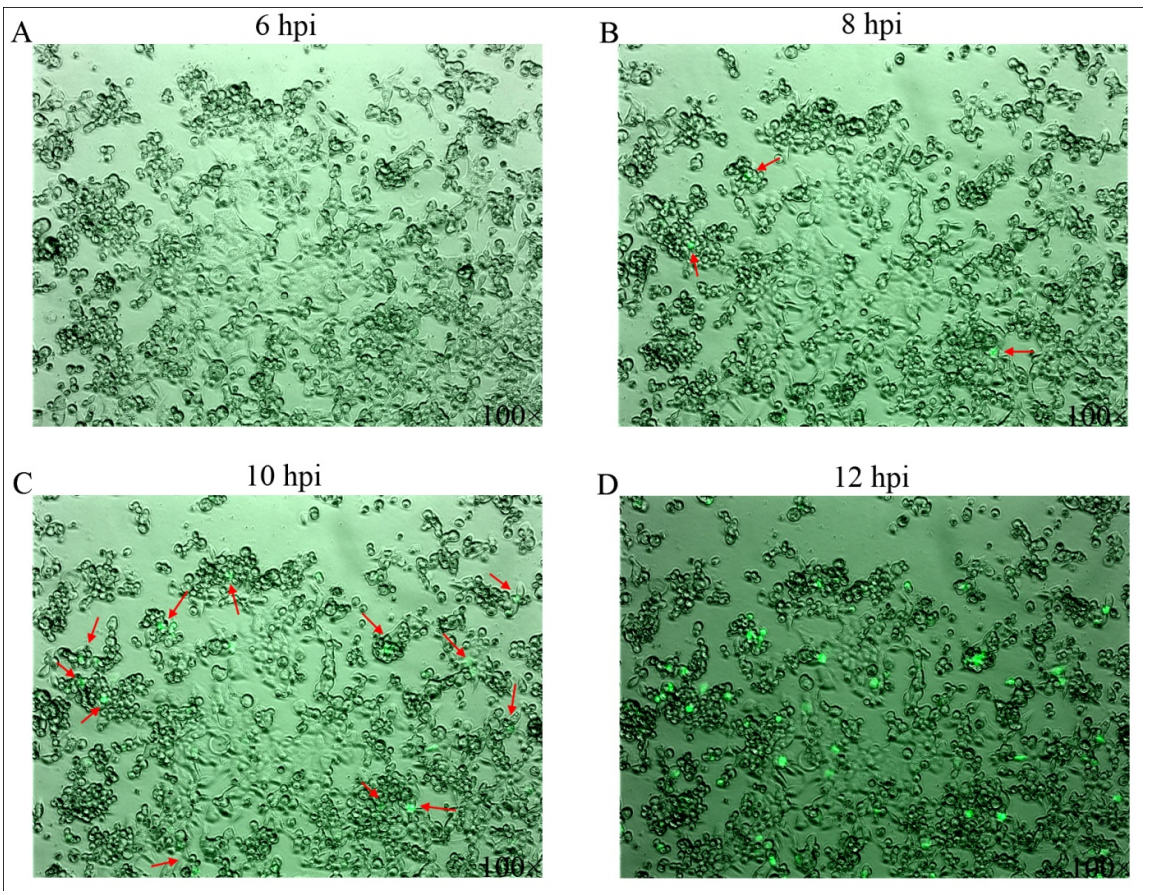

Fig. 4.21 TGF-β1-induced GI-101A cells infected by GLV-1h68 at MOI0. The images which merged from the phase contrast and the fluorescence were captured at 6 hpi (A), 8 hpi (B), 10 hpi (C) and 12 hpi (D). The red arrows indicate the GFP expression. All the images were taken at the same position of plates.

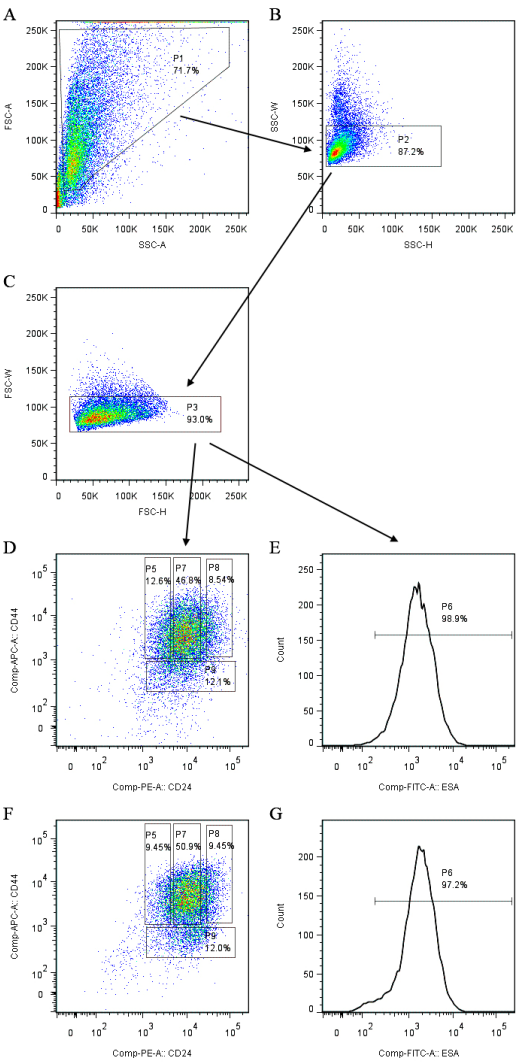

Fig. 4.22 Strategy for isolation of human breast cancer stem-like cells from the EMT-induced GI-101A cell line. Fluorescence-activated cell sorting (FACS) was used to isolate $CD44^{+}/CD24^{-}/ESA^{+}$, $CD44^{+}/CD24^{mid}/ESA^{+}$, $CD44^{+}/CD24^{+}/ESA^{+}$ and $CD44^{-}/CD24^{all}/ESA^{+}$ human breast cancer cells for functional assays. GI-101A cells were labeled with CD44-APC, CD24-PE and ESA-FITC antibody. Cell subsets were isolated using triple-color protocol on BD FACS Aria III cells sorter. (A-E): Representative scheme of a sequentially gated GI-101A cell line sort. (A) Cells were first selected for viability based on electronic gate P1. (B, C) Cells were then selected for singlet based on electronic gate P2 and P3. (D, E) Finally, cells were selected based on CD44, CD24 and ESA signal intensity and divided into $CD44^{+}/CD24^{-}/ESA^{+}$, $CD44^{+}/CD24^{mid}/ESA^{+}$, $CD44^{+}/CD24^{+}/ESA^{+}$ and $CD44^{-}/CD24^{all}/ESA^{+}$. (F, G) The same method was used to analyze non-induced cells.

EMT induced GI-101A cells (Fig. 4.22E) was similar to non-induced cells (Fig. 4.22G). The CD44 and CD24 expression in EMT induced GI-101A cells (Fig. 4.22D) was just slightly different compared to non-induced cells (Fig. 4.22F). To better study

A

Population	Tumors/Injections (10,000 cells/injection)									
	Wk 7	Wk 8	Wk 9	Wk 10	Wk 11	Wk 12	Wk 13	Wk 15	Wk 18	Wk 22
CD44+/CD24-/ESA+	0/5	1/5	2/5	2/5	2/5	3/5	3/5	3/5	2/4	2/4
CD44+/CD24+/ESA+	1/5	1/5	1/5	1/5	2/5	3/5	4/5	4/5	3/4	3/4
CD44+/CD24mid/ESA+	0/5	0/5	0/5	3/5	4/5	4/5	4/5	5/5	5/5	4/4
CD44-/CD24all/ESA+	0/5	0/5	0/5	0/5	0/5	0/5	0/5	0/5	1/5	1/5

B

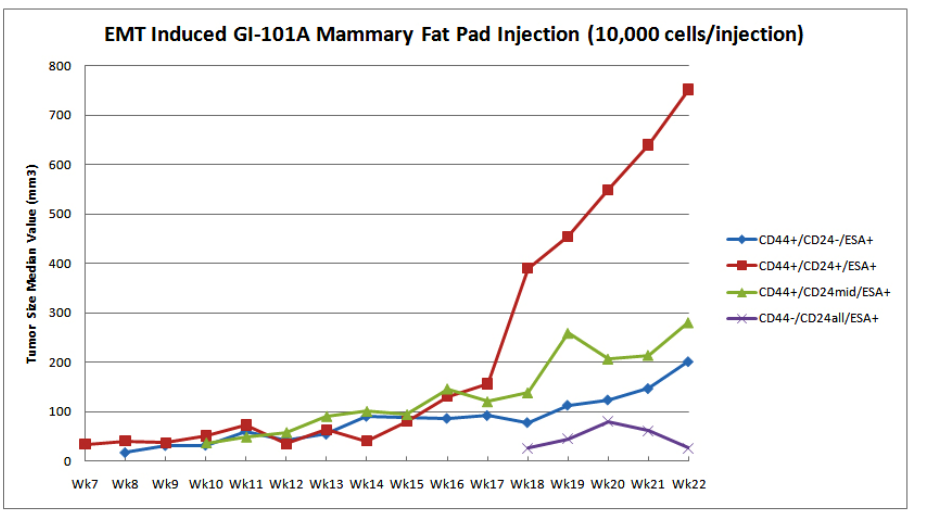

Fig. 4.23 The EMT-induced GI-101A CD44$^+$/CD24$^+$/ESA$^+$ cell population in athymic *nu*/*nu* nude mice has higher tumorigenic potential. (A) Representative tumor-forming frequency in different time point after xenograft. (B) Tumor growth curves were plotted for the 10,000 cells of each population (CD44$^+$/CD24$^-$/ESA$^+$, CD44$^+$/CD24^{mid}/ESA$^+$, CD44$^+$/CD24$^+$/ESA$^+$ and CD44$^-$ /CD24^{all}/ESA$^+$) injected.

the different fractions in EMT induced cells, we gated the four cells population which named CD44$^+$/CD24$^-$/ESA$^+$, CD44$^+$/CD24^{mid}/ESA$^+$, CD44$^+$/CD24$^+$/ESA$^+$ and CD44$^-$ /CD24^{all}/ESA$^+$ according to the expression of CD44/CD24 and ESA.

4.4.7 CD44$^+$/CD24$^+$/ESA$^+$ cells displayed and increased tumorigenic potential *in vivo*

Next, 10,000 purified CD44$^+$/CD24$^-$/ESA$^+$, CD44$^+$/CD24^{mid}/ESA$^+$, CD44$^+$/CD24$^+$/ESA$^+$ and CD44$^-$/CD24^{all}/ESA$^+$ cells were injected with Matrigel into the mammary fat-pad of six-week-old athymic *nu*/*nu* nude mice to assess the *in vivo* tumorigenicity of those cell fractions. As shown in Fig. 23, both tumor occurrence and tumor size were monitored after injection. The CD44$^+$/CD24$^+$/ESA$^+$ cells initiated tumors earlier than the other three fractions, however, the CD44$^+$/CD24^{mid}/ESA$^+$ had higher tumor occurrence than other three fractions (Fig. 23A). Regarding to the tumor growth potential, the CD44$^+$/CD24$^+$/ESA$^+$ cells showed the tumor growth advantage after 17 weeks xenograft compared to the other three fractions (Fig. 23B).

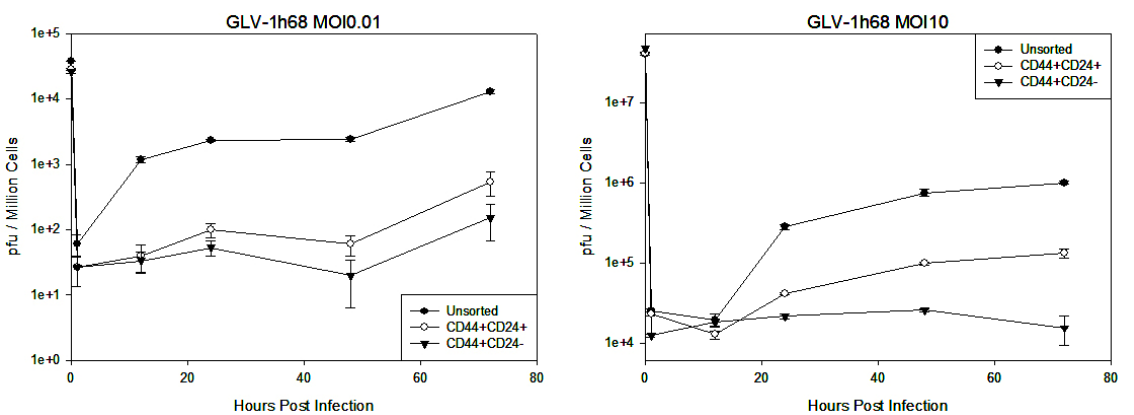

Fig. 4.24 GLV-1h68 growth curve in parental GI-101A cells and sorted CD44$^+$/CD24$^+$/ESA$^+$ and CD44$^+$/CD24$^-$/ESA$^+$ cells at MOI0.01 (left) or MOI10 (right). Bars denote the standard error mean (n=6).

4.4.8 Viral replication in CD44$^+$/CD24$^+$/ESA$^+$ and CD44$^+$/CD24$^-$/ESA$^+$ cells

To test the replication efficiency of vaccinia virus strain GLV-1h68 in sorted EMT-induced GI-101A CD44$^+$/CD24$^+$/ESA$^+$ and CD44$^+$/CD24$^-$/ESA$^+$ cells, we performed replication assays. The cells were infected with GLV-1h68 at an MOI of 0.01 or 10, followed by determination of viral titers at the time points 1, 12, 24, 48 and 72 hours post infection. Average data including standard deviation is shown (Fig. 4.24) for parental GI-101A and CD44$^+$/CD24$^-$/ESA$^+$ cells in comparison to CD44$^+$/CD24$^+$/ESA$^+$ cells. 72 hours post infection, the virus titer of CD44$^+$/CD24$^+$/ESA$^+$ cells was about

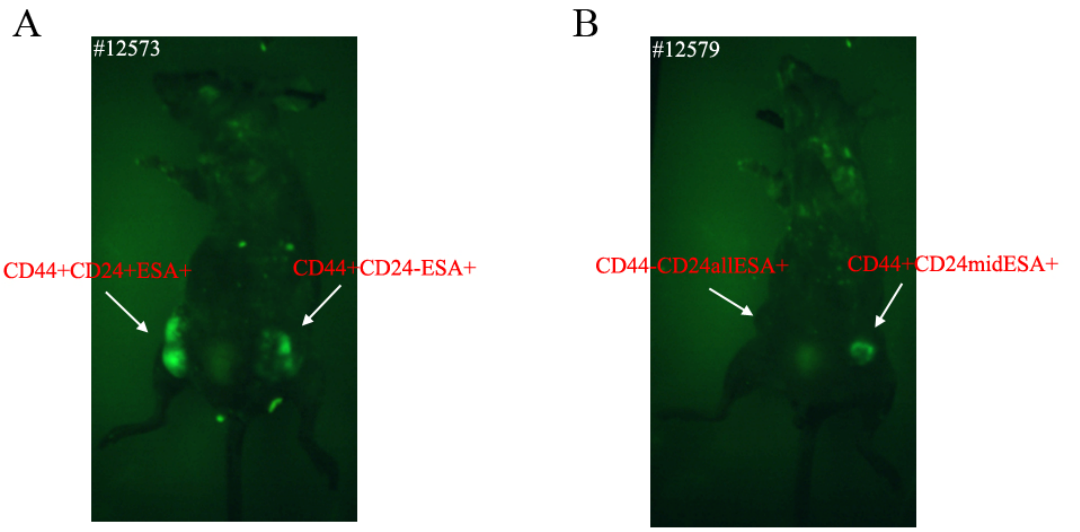

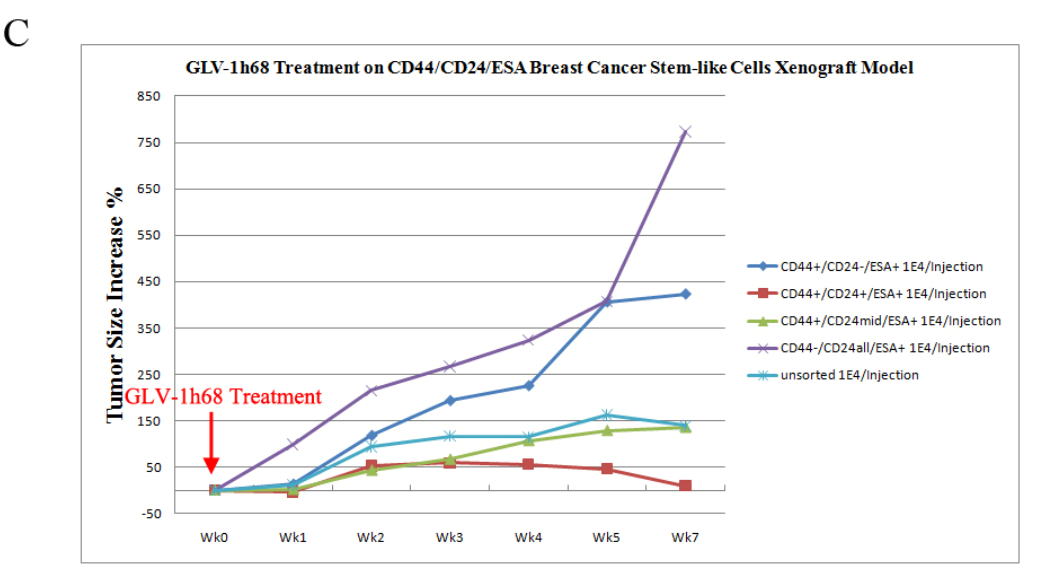

Fig. 4.25 Retro-orbital injection of vaccinia virus GLV-1h68 induces tumor regression of solid tumor xenografts from GI-101A CD44/CD24/ESA cells. (A) An example of *in vivo* tumor GFP imaging of virus treated $CD44^{+}/CD24^{+}/ESA^{+}$ and $CD44^{+}/CD24^{-}/ESA^{+}$ cells derived tumor. (B) Another example of *in vivo* tumor GFP imaging of virus treated $CD44^{-}/CD24^{all}/ESA^{+}$ and $CD44^{+}/CD24^{mid}/ESA^{+}$ GI-101A cells derived tumor. (C) 10,000 sorted and unsorted cells implanted in the mammary fat pads of athymic nude mice were injected with vaccinia virus GLV1h-68 (n=1, 2 or 4) on day 0 (downward arrow). Percentage of the increase in tumor size was determined based on the median value of tumor size before virus treatment (week 0) and after treatment. Each data point was calculated by using the following formula: 100 %×(week n-week 0)/week 0.

three times higher than $CD44^+/CD24^-/ESA^+$ cells upon MOI0.01 treatment and about eight times higher upon MOI10 treatment.

4.4.9 Vaccinia virus GLV-1h68 induces tumor regression of GI-101A $CD44^+/CD24^+/ESA^+$ cell-derived xenografts

Previously we have shown GI-101A $CD44^+/CD24^+/ESA^+$ cells had more tumorigenic potential in nude mice and vaccinia virus GLV-1h68 could replicate more efficiently in the $CD44^+/CD24^+/ESA^+$ cells compared to the $CD44^+/CD24^-/ESA^+$ cells. To test the efficacy of oncolytic vaccinia virus to target and kill breast CSCs *in vivo*, we established palpable tumors in the mammary fat pads of athymic *nu*/*nu* nude mice using sorted GI-101A $CD44^+/CD24^+/ESA^+$, $CD44^+/CD24^-/ESA^+$, $CD44^+/CD24^{mid}/ESA^+$, $CD44^-/CD24^{all}/ESA^+$ and unsorted cells with the dose of 10,000 cells/injection. For more comparable results, each mouse was implanted two counterparts' cell fractions in left and right mammary fat pads, respectively (i.e. 10,000 $CD44^+/CD24^+/ESA^+$ cells in right fat pad and 10,000 $CD44^+/CD24^-/ESA^+$ cells in left fad pad). After 22 weeks tumor implantation, each mouse was injected with 5×10^6 pfu GLV-1h68 virus via the retro-orbital path. Then the tumor size and tumor GFP expression was monitored weekly. As shown in Fig 4.25C, the $CD44^+/CD24^+/ESA^+$-derived tumor showed dramatic response upon virus treatment and tumor growth was significantly inhibited after the virus treatment. The tumor fluorescence images also indicated that infected tumors derived from $CD44^+/CD24^+/ESA^+$ cells showed a more efficient vaccine virus replication (Fig. 4.25A), which proved the trends of tumor regression. Unexpectedly, vaccinia virus treatment did not show any inhibitory effects on tumor growth of $CD44^-/CD24^{all}/ESA^+$ cells (Fig. 4.25C) and no GFP expression was detected *in vivo* (Fig. 4.25B).

5 Discussion

The cancer stem cell hypothesis has fundamental implications for cancer biology in addition to clinical implications for cancer risk assessment, early detection, prognostication, and prevention. The development of cancer therapeutics based on tumor regression may have produced agents which kill differentiated tumor cells while sparing the small cancer stem cell population (Wicha, Liu et al. 2006). The development of more effective cancer therapies may thus require targeting this important cancer stem cell population. The success of these new approaches hinges on the identification, isolation, and characterization of cancer stem cells.

Establishing an appropriate *in vitro* cancer stem cell model is critical for the study of cancer stem cell biology, because of limited supply of cancer stem cells from patient samples. In this study, Side Population (SP) assay, ALDEFLUOR assay, Epithelia-Mesenchymal Transition (EMT) assay and surface marker assay were tried to identify, isolate and characterize human breast cancer stem-like cells from cancer cell lines.

A small fraction of SP cells were identified by flow cytometry from the human breast cancer cell lines GI-101A and MCF7, as well as the human lung cancer cell line A549. One potential concern for claiming cancer stem cell-like properties of the SP cells is that the Hoechst 33342 dye may create bias by selectively injuring non-SP cells. Even for SP cells that have capability to pump out the toxic dye, the viability of cells was more or less reduced. Moreover, the SP assay, being performed on viable cell populations, enables subsequent functional characterization of the cells *in vitro* and *in vivo*, which is not possible with many other DNA-binding dyes. Furthermore, optimal SP resolution requires a flow cytometer equipped with an ultraviolet (UV) laser. If a UV laser is unavailable on the flow cytometer, Hoechst can also be excited by light with non-UV wavelengths. However, in our experience, neither Hoechst excitation by the near-UV or violet laser (Telford and Frolova 2004) nor the use of alternative non-UV excitable DNA dyes (Telford, Bradford et al. 2007) leads to a sharp SP resolution as observed with traditional UV sources. As of all, the drawback and restriction should be considered when the SP method is utilized.

As a novel approach, the ALDEFLUOR assay and ALDH1 immunostaining may prove to be useful for the detection and isolation of cancer stem cells in epithelial tumors, thus facilitating the application of cancer stem cell concepts to clinical practice (Ginestier, Hur et al. 2007). In the present study, we have successfully identified, isolated and characterized GI-101A ALDEFLUOR-positive cells as human breast cancer-stem like cells. Tumorigenicity or only few cells could initiate tumor formation in mouse model, which was considered the “gold standard” of cancer stem cells theory. We have proved that at least 5×10^3 ALDEFLUOR-positive cells can generate tumor in nude mice. Although ALDEFLUOR-negative cells also may form tumor finally, when regarding to tumor formation frequency, the earliest time when formed tumor and the tumor growth curve, the ALDEFLUOR-positive cells have more characteristics of cancer stem cells. This was also confirmed by *in vitro* mammosphere formation assay. Furthermore, the ALDEFLUOR-positive cells displayed both stronger chemo- and irradiation-resistance capability, which are important features of cancer stem cells. Self-renewal or asymmetrical division is also a unique feature associated with stem cells/cancer stem cells. We have shown these properties *in vitro*. When the sorted ALDEFLUOR-positive cells were cultured in plates, it would reproduce ALDEFLUOR-negative cells during the following passages and finally the ratio of ALDEFLUOR-positive and –negative cells would return to the same level of parental cells which are before sorting. To figure out the mechanism of the tumorigenicity of ALDEFLUOR-positive cells, we combined the ALDEFLUOR assay with surface markers analysis. It is very interesting that the ALDEFLUOR-positive cells exhibit more CD44, CD49f expression than ALDEFLUOR-negative cells. The results indicate that CD44 and CD49f are potential cancer stem cell markers in GI-101A cells.

Cancer stem cells may be responsible for mediating tumor metastasis. A link between cancer stem cells and metastasis was first suggested with the identification of stem cell genes in an 11-gene signature generated using comparative profiles of metastatic and primary tumors in a transgenic mouse model of prostate cancer and in cancer patients (Glinsky, Berezovska et al. 2005). This signature was also a powerful predictor of disease recurrence, survival after therapy, and distant metastasis in a variety of cancer types. We have demonstrated that ALDEFLUOR-positive cells

migrate more efficiently than ALDEFLUOR-negative cells in BME transwells, which indicated the metastatic potential of GI-101A ALDEFLUOR-positive cells. The ability to isolate metastatic cancer stem cells from cell lines should facilitate studies of the molecular mechanisms by which cancer stem cells mediate tumor metastasis.

EMT, which was first recognized as a crucial feature of embryogenesis, converts epithelial cells into mesenchymal cells through profound disruption of cell-cell junctions and extensive reorganization of the actin cytoskeleton (Hay, McElvaney et al. 1995). Although still controversial, this process is presumed to be required for tumor invasion and metastasis of carcinoma cells by promoting loss of contact inhibition, increased cell motility and enhanced invasiveness (Christiansen and Rajasekaran 2006). EMT is believed to be governed by complex networks largely influenced by signals from the neoplastic microenvironment. Indeed, *in vitro*, a variety of cytokines, including TGF-β1 and growth factors such as hepatocyte growth factor (HGF), epidermal growth factor (EGF) or fibroblast growth factor (FGF), can trigger EMT after activation of their cognate receptors in specific cell types. On this basis, we successfully induced EMT of the human mammary epithelia cell line HMLE and the cancer cell line GI-101A by using EGF, bFGF and TGF-β1. Further Immunostaining of E-cadherin, vimentin and fibronectin were used to confirm EMT. The results of a chemo-resistance and cell invasion assay in EMT-induced GI-01A cells and cell invasion assay indicated that EMT-induced cells were able to acquire the features of cancer stem cells. The connection between EMT and stem-like properties has also been strongly supported by the Weinberg laboratory (Mani, Guo et al. 2008). Using different EMT-inducers, they showed that the induction of EMT in immortalized human mammary epithelial cells is associated with the acquisition of stem-like characteristics. Additionally it was shown that normal, as well as neoplastic breast stem-like cells, express mesenchymal markers. According to Weinberg (Mani, Guo et al. 2008), EMT induction could enrich $CD44^+CD24^-$ cells. We confirmed the results in EMT-induced GI-101A cells, although there was only a slight increase. Then we isolated different fractions based on the expression of CD44, CD24 and ESA from EMT-induced GI-101A cells. Unexpectedly, the $CD44^+CD24^+ESA^+$ cells initiated tumors in nude mice more efficiently than $CD44^+CD24^-ESA^+$ cells. Al-Hajj et al. have shown that $CD44^+CD24^-$ tumor cells were highly tumorigenic in immune-deficient

mice and that cancer stem cells in this population appeared to be enriched (Al-Hajj, Wicha et al. 2003). So far, there are still lots of controversies about cancer stem cell markers. Our study definitely proved that the $CD44^+CD24^-$ are not universal markers in GI-101A or EMT-induced GI-101A cells. Moreover, whether $CD44^+CD24^+$ cells are cancer stem cells or not needs to be studied further.

According to our previous experimental results, oncolytic vaccinia virus GLV-1h68 seemed to be selective and effective in the killing of ALDEFLUOR-positive or $CD44^+CD24^+ESA^+$ cells *in vitro* and *in vivo*. When established ALDEFLUOR-positive or $CD44^+CD24^+ESA^+$–derived tumors were treated, tumor growth could be reduced, but complete tumor eradication was not seen in most mice. One possible reason could be that the tumor was overgrown when we monitored the tumorigenicity and the tumor size was too big to respond to vaccinia virus treatment. Another possibility could be that the virus treated mice carried two tumors in the mammary gland fat pad of both sides and the oncolytic capacity of the virus was not sufficient for the large tumor burden. To prove the data, new animal experiments will be designed and performed in near future. Even though the obtained results indicated so far that oncolytic vaccinia virus is a promising therapy agent which can target and eradicate cancer stem cells.

References

Abraham, B. K., P. Fritz, et al. (2005). "Prevalence of CD44+/CD24-/low cells in breast cancer may not be associated with clinical outcome but may favor distant metastasis." Clin Cancer Res 11(3): 1154-9.

Akiyoshi, T., M. Nakamura, et al. (2006). "Gli1, downregulated in colorectal cancers, inhibits proliferation of colon cancer cells involving Wnt signalling activation." Gut 55(7): 991-9.

Al-Assar, O., R. J. Muschel, et al. (2009). "Radiation response of cancer stem-like cells from established human cell lines after sorting for surface markers." Int J Radiat Oncol Biol Phys 75(4): 1216-25.

Albright, N. (1987). "Computer programs for the analysis of cellular survival data." Radiat Res 112(2): 331-40.

Al-Hajj, M., M. W. Becker, et al. (2004). "Therapeutic implications of cancer stem cells." Curr Opin Genet Dev 14(1): 43-7.

Al-Hajj, M., M. S. Wicha, et al. (2003). "Prospective identification of tumorigenic breast cancer cells." Proc Natl Acad Sci U S A 100(7): 3983-8.

Anand, P., A. B. Kunnumakkara, et al. (2008). "Cancer is a preventable disease that requires major lifestyle changes." Pharm Res 25(9): 2097-116.

Angstreich, G. R., W. Matsui, et al. (2005). "Effects of imatinib and interferon on primitive chronic myeloid leukaemia progenitors." Br J Haematol 130(3): 373-81.

Armstrong, L., M. Stojkovic, et al. (2004). "Phenotypic characterization of murine primitive hematopoietic progenitor cells isolated on basis of aldehyde dehydrogenase activity." Stem Cells 22(7): 1142-51.

Asselin-Labat, M. L., K. D. Sutherland, et al. (2007). "Gata-3 is an essential regulator of mammary-gland morphogenesis and luminal-cell differentiation." Nat Cell Biol 9(2): 201-9.

Auzenne, E., S. C. Ghosh, et al. (2007). "Hyaluronic acid-paclitaxel: antitumor efficacy against CD44(+) human ovarian carcinoma xenografts." Neoplasia 9(6): 479-86.

Balic, M., H. Lin, et al. (2006). "Most early disseminated cancer cells detected in bone marrow of breast cancer patients have a putative breast cancer stem cell phenotype." Clin Cancer Res 12(19): 5615-21.

Bao, S., Q. Wu, et al. (2006). "Glioma stem cells promote radioresistance by preferential activation of the DNA damage response." Nature 444(7120): 756-60.

Bartkowiak, K., M. Wieczorek, et al. (2009). "Two-Dimensional Differential Gel Electrophoresis of a Cell Line Derived from a Breast Cancer Micrometastasis Revealed a Stem/Progenitor Cell Protein Profile." J Proteome Res.

Beachy, P. A., S. S. Karhadkar, et al. (2004). "Tissue repair and stem cell renewal in carcinogenesis." Nature 432(7015): 324-31.

Behbod, F. and J. M. Rosen (2005). "Will cancer stem cells provide new therapeutic targets?" Carcinogenesis 26(4): 703-11.

Ben-Porath, I., M. W. Thomson, et al. (2008). "An embryonic stem cell-like gene expression signature in poorly differentiated aggressive human tumors." Nat Genet 40(5): 499-507.

Berezovska, O. P., A. B. Glinskii, et al. (2006). "Essential role for activation of the Polycomb group (PcG) protein chromatin silencing pathway in metastatic prostate cancer." Cell Cycle 5(16): 1886-901.

Bersenev, A. (2009). "Complexity of cancer stem cells." Hematopoiesis Blog, from http://hematopoiesis.info/2009/05/06/complexity-of-cancer-stem-cells/.

Berx, G., E. Raspe, et al. (2007). "Pre-EMTing metastasis? Recapitulation of morphogenetic processes in cancer." Clin Exp Metastasis 24(8): 587-97.

Blasco, R. and B. Moss (1992). "Role of cell-associated enveloped vaccinia virus in cell-to-cell spread." J Virol 66(7): 4170-9.

Boiko, A. D., O. V. Razorenova, et al. (2010). "Human melanoma-initiating cells express neural crest nerve growth factor receptor CD271." Nature 466(7302): 133-7.

Bollmann, F. M. (2008). "The many faces of telomerase: emerging extratelomeric effects." Bioessays 30(8): 728-32.

Bolos, V., M. Blanco, et al. (2009). "Notch signalling in cancer stem cells." Clin Transl Oncol 11(1): 11-9.

Bonnet, D. and J. E. Dick (1997). "Human acute myeloid leukemia is organized as a hierarchy that originates from a primitive hematopoietic cell." Nat Med 3(7): 730-7.

Brabletz, T., F. Hlubek, et al. (2005). "Invasion and metastasis in colorectal cancer: epithelial-mesenchymal transition, mesenchymal-epithelial transition, stem cells and beta-catenin." Cells Tissues Organs 179(1-2): 56-65.

Brabletz, T., A. Jung, et al. (2001). "Variable beta-catenin expression in colorectal cancers indicates tumor progression driven by the tumor environment." Proc Natl Acad Sci U S A 98(18): 10356-61.

Broyles, S. S. (2003). "Vaccinia virus transcription." J Gen Virol 84(Pt 9): 2293-303.

Cancer-Research-UK. (2007). "UK cancer incidence statistics by age."

Cariati, M., A. Naderi, et al. (2008). "Alpha-6 integrin is necessary for the tumourigenicity of a stem cell-like subpopulation within the MCF7 breast cancer cell line." Int J Cancer 122(2): 298-304.

Charafe-Jauffret, E., C. Ginestier, et al. (2009). "Breast cancer stem cells: tools and models to rely on." BMC Cancer 9: 202.

Charafe-Jauffret, E., C. Ginestier, et al. (2009). "Aldehyde dehydrogenase 1-positive cancer stem cells mediate metastasis and poor clinical outcome in inflammatory breast cancer." Clin Cancer Res 16(1): 45-55.

Charafe-Jauffret, E., C. Ginestier, et al. (2009). "Breast cancer cell lines contain functional cancer stem cells with metastatic capacity and a distinct molecular signature." Cancer Res 69(4): 1302-13.

Christgen, M., M. Ballmaier, et al. (2007). "Identification of a distinct side population of cancer cells in the Cal-51 human breast carcinoma cell line." Mol Cell Biochem 306(1-2): 201-12.

Christgen, M., R. Geffers, et al. (2009). "Down-regulation of the fetal stem cell factor SOX17 by H33342: a mechanism responsible for differential gene expression in breast cancer side population cells." J Biol Chem 285(9): 6412-8.

Christiansen, J. J. and A. K. Rajasekaran (2006). "Reassessing epithelial to mesenchymal transition as a prerequisite for carcinoma invasion and metastasis." Cancer Res 66(17): 8319-26.

Clarke, M. F., J. E. Dick, et al. (2006). "Cancer stem cells--perspectives on current status and future directions: AACR Workshop on cancer stem cells." Cancer Res 66(19): 9339-44.

Corti, S., F. Locatelli, et al. (2006). "Identification of a primitive brain-derived neural stem cell population based on aldehyde dehydrogenase activity." Stem Cells 24(4): 975-85.

Costello, R. T., F. Mallet, et al. (2000). "Human acute myeloid leukemia CD34+/CD38- progenitor cells have decreased sensitivity to chemotherapy and Fas-induced apoptosis, reduced immunogenicity, and impaired dendritic cell transformation capacities." Cancer Res 60(16): 4403-11.

Coukos, G., A. Makrigiannakis, et al. (2000). "Oncolytic herpes simplex virus-1 lacking ICP34.5 induces p53-independent death and is efficacious against chemotherapy-resistant ovarian cancer." Clin Cancer Res 6(8): 3342-53.

Cozzio, A., E. Passegue, et al. (2003). "Similar MLL-associated leukemias arising from self-renewing stem cells and short-lived myeloid progenitors." Genes Dev 17(24): 3029-35.

Cripe, T. P., P. Y. Wang, et al. (2009). "Targeting cancer-initiating cells with oncolytic viruses." Mol Ther 17(10): 1677-82.

Croker, A. K., D. Goodale, et al. (2009). "High aldehyde dehydrogenase and expression of cancer stem cell markers selects for breast cancer cells with enhanced malignant and metastatic ability." J Cell Mol Med 13(8B): 2236-52.

Crowe, D. L. and A. Ohannessian (2004). "Recruitment of focal adhesion kinase and paxillin to beta1 integrin promotes cancer cell migration via mitogen activated protein kinase activation." BMC Cancer 4: 18.

Dalerba, P., S. J. Dylla, et al. (2007). "Phenotypic characterization of human colorectal cancer stem cells." Proc Natl Acad Sci U S A 104(24): 10158-63.

Dean, M., T. Fojo, et al. (2005). "Tumour stem cells and drug resistance." Nat Rev Cancer 5(4): 275-84.

Deng, S., X. Yang, et al. (2010). "Distinct expression levels and patterns of stem cell marker, aldehyde dehydrogenase isoform 1 (ALDH1), in human epithelial cancers." PLoS One 5(4): e10277.

Dey, D., M. Saxena, et al. (2009). "Phenotypic and functional characterization of human mammary stem/progenitor cells in long term culture." PLoS One 4(4): e5329.

Diehn, M., R. W. Cho, et al. (2009). "Association of reactive oxygen species levels and radioresistance in cancer stem cells." Nature 458(7239): 780-3.

Diehn, M. and M. F. Clarke (2006). "Cancer stem cells and radiotherapy: new insights into tumor radioresistance." J Natl Cancer Inst 98(24): 1755-7.

Dievart, A., N. Beaulieu, et al. (1999). "Involvement of Notch1 in the development of mouse mammary tumors." Oncogene 18(44): 5973-81.

Dirks, P. (2010). "Cancer stem cells: Invitation to a second round." Nature 466(7302): 40-1.

Dodge, M. E. and L. Lum (2010). "Drugging the Cancer Stem Cell Compartment: Lessons Learned from the Hedgehog and Wnt Signal Transduction Pathways." Annu Rev Pharmacol Toxicol.

Donnenberg, V. S. and A. D. Donnenberg (2005). "Multiple drug resistance in cancer revisited: the cancer stem cell hypothesis." J Clin Pharmacol 45(8): 872-7.

Dontu, G. (2008). "Breast cancer stem cell markers - the rocky road to clinical applications." Breast Cancer Res 10(5): 110.

Dontu, G., W. M. Abdallah, et al. (2003). "In vitro propagation and transcriptional profiling of human mammary stem/progenitor cells." Genes Dev 17(10): 1253-70.

Dontu, G., K. W. Jackson, et al. (2004). "Role of Notch signaling in cell-fate determination of human mammary stem/progenitor cells." Breast Cancer Res 6(6): R605-15.

Duester, G. (2000). "Families of retinoid dehydrogenases regulating vitamin A function: production of visual pigment and retinoic acid." Eur J Biochem 267(14): 4315-24.

Dunham, W. (2007). "Report sees 7.6 million global 2007 cancer deaths."

EBCT (1998). "Polychemotherapy for early breast cancer: an overview of the randomised trials. Early Breast Cancer Trialists' Collaborative Group." Lancet 352(9132): 930-42.

EBCT (1998). "Tamoxifen for early breast cancer: an overview of the randomised trials. Early Breast Cancer Trialists' Collaborative Group." Lancet 351(9114): 1451-67.

Elenbaas, B., L. Spirio, et al. (2001). "Human breast cancer cells generated by oncogenic transformation of primary mammary epithelial cells." Genes Dev 15(1): 50-65.

Engelmann, K., H. Shen, et al. (2008). "MCF7 side population cells with characteristics of cancer stem/progenitor cells express the tumor antigen MUC1." Cancer Res 68(7): 2419-26.

Eriksson, M., K. Guse, et al. (2007). "Oncolytic adenoviruses kill breast cancer initiating CD44+CD24-/low cells." Mol Ther 15(12): 2088-93.

Eyler, C. E. and J. N. Rich (2008). "Survival of the fittest: cancer stem cells in therapeutic resistance and angiogenesis." J Clin Oncol 26(17): 2839-45.

Fillmore, C. M. and C. Kuperwasser (2008). "Human breast cancer cell lines contain stem-like cells that self-renew, give rise to phenotypically diverse progeny and survive chemotherapy." Breast Cancer Res 10(2): R25.

Gasparini, P., G. Bertolini, et al. (2010). "Molecular cytogenetic characterization of stem-like cancer cells isolated from established cell lines." Cancer Lett.

Gavert, N. and A. Ben-Ze'ev (2008). "Epithelial-mesenchymal transition and the invasive potential of tumors." Trends Mol Med 14(5): 199-209.

Ginestier, C., M. H. Hur, et al. (2007). "ALDH1 is a marker of normal and malignant human mammary stem cells and a predictor of poor clinical outcome." Cell Stem Cell 1(5): 555-67.

Glinsky, G. V., O. Berezovska, et al. (2005). "Microarray analysis identifies a death-from-cancer signature predicting therapy failure in patients with multiple types of cancer." J Clin Invest 115(6): 1503-21.

Goodell, M. A., K. Brose, et al. (1996). "Isolation and functional properties of murine hematopoietic stem cells that are replicating in vivo." J Exp Med 183(4): 1797-806.

Graham, S. M., H. G. Jorgensen, et al. (2002). "Primitive, quiescent, Philadelphia-positive stem cells from patients with chronic myeloid leukemia are insensitive to STI571 in vitro." Blood 99(1): 319-25.

Guarino, M., B. Rubino, et al. (2007). "The role of epithelial-mesenchymal transition in cancer pathology." Pathology 39(3): 305-18.

Guo, J., J. Zhou, et al. (2010). "Effects of stealth liposomal daunorubicin plus tamoxifen on the breast cancer and cancer stem cells." J Pharm Pharm Sci 13(2): 136-51.

Gupta, P. B., C. L. Chaffer, et al. (2009). "Cancer stem cells: mirage or reality?" Nat Med 15(9): 1010-2.

Gupta, P. B., T. T. Onder, et al. (2009). "Identification of selective inhibitors of cancer stem cells by high-throughput screening." Cell 138(4): 645-59.

Gurney, J., M. Smith, et al. (1999). Cancer among infants. Cancer Incidence and Survival among Children and Adolescents, United States SEER program 1975–1995. R. LAG, S. MA, G. JGet al. Bethesda, MD, National Cancer Institute, SEER Program.

Guzman, M. L. and C. T. Jordan (2004). "Considerations for targeting malignant stem cells in leukemia." Cancer Control 11(2): 97-104.

Han, J. S. and D. L. Crowe (2009). "Tumor initiating cancer stem cells from human breast cancer cell lines." Int J Oncol 34(5): 1449-53.

Harrison, S. C., B. Alberts, et al. (2004). "Discovery of antivirals against smallpox." Proc Natl Acad Sci U S A 101(31): 11178-92.

Haupt, Y., M. L. Bath, et al. (1993). "bmi-1 transgene induces lymphomas and collaborates with myc in tumorigenesis." Oncogene 8(11): 3161-4.

Hay, J. G., N. G. McElvaney, et al. (1995). "Modification of nasal epithelial potential differences of individuals with cystic fibrosis consequent to local administration of a normal CFTR cDNA adenovirus gene transfer vector." Hum Gene Ther 6(11): 1487-96.

Hemmati, H. D., I. Nakano, et al. (2003). "Cancerous stem cells can arise from pediatric brain tumors." Proc Natl Acad Sci U S A 100(25): 15178-83.

Henderson, D. and B. Moss (1988). Smallpox and Vaccinia. Vaccines (3rd ed.). P. SA and O. WA. Philadelphia, Pennsylvania, WB Saunders.

Hendrix, M. J., E. A. Seftor, et al. (2007). "Reprogramming metastatic tumour cells with embryonic microenvironments." Nat Rev Cancer 7(4): 246-55.

Hermann, P. C., S. L. Huber, et al. (2007). "Distinct populations of cancer stem cells determine tumor growth and metastatic activity in human pancreatic cancer." Cell Stem Cell 1(3): 313-23.

Hess, D. A., T. E. Meyerrose, et al. (2004). "Functional characterization of highly purified human hematopoietic repopulating cells isolated according to aldehyde dehydrogenase activity." Blood 104(6): 1648-55.

Hess, D. A., L. Wirthlin, et al. (2006). "Selection based on CD133 and high aldehyde dehydrogenase activity isolates long-term reconstituting human hematopoietic stem cells." Blood 107(5): 2162-9.

Hiraga, T., S. Ito, et al. (2010). "Side population in MDA-MB-231 human breast cancer cells exhibits cancer stem cell-like properties without higher bone-metastatic potential." Oncol Rep 25(1): 289-96.

Hirschmann-Jax, C., A. E. Foster, et al. (2004). "A distinct "side population" of cells with high drug efflux capacity in human tumor cells." Proc Natl Acad Sci U S A 101(39): 14228-33.

Ho, M. M., A. V. Ng, et al. (2007). "Side population in human lung cancer cell lines and tumors is enriched with stem-like cancer cells." Cancer Res 67(10): 4827-33.

Howe, H. L., P. A. Wingo, et al. (2001). "Annual report to the nation on the status of cancer (1973 through 1998), featuring cancers with recent increasing trends." J Natl Cancer Inst 93(11): 824-42.

Huang, M., Y. Li, et al. (2010). "Whole Genome Expression Profiling Reveals a Significant Role for the Cell Junction and Apoptosis Pathways in Breast Cancer Stem Cells." Mol Biotechnol.

Hughes, L., C. Malone, et al. (2008). "Characterisation of breast cancer cell lines and establishment of a novel isogenic subclone to study migration, invasion and tumourigenicity." Clin Exp Metastasis 25(5): 549-57.

Huntly, B. J., H. Shigematsu, et al. (2004). "MOZ-TIF2, but not BCR-ABL, confers properties of leukemic stem cells to committed murine hematopoietic progenitors." Cancer Cell 6(6): 587-96.

Hurst, J., N. Maniar, et al. (1993). "A novel model of a metastatic human breast tumour xenograft line." Br J Cancer 68(2): 274-6.

Itoh, Y., T. Joh, et al. (2005). "IL-8 promotes cell proliferation and migration through metalloproteinase-cleavage proHB-EGF in human colon carcinoma cells." Cytokine 29(6): 275-82.

Jemal, A., R. Siegel, et al. (2008). "Cancer statistics, 2008." CA Cancer J Clin 58(2): 71-96.

Jemal, A., R. Siegel, et al. (2010). "Cancer statistics, 2010." CA Cancer J Clin 60(5): 277-300.

Jiang, H., C. Gomez-Manzano, et al. (2007). "Examination of the therapeutic potential of Delta-24-RGD in brain tumor stem cells: role of autophagic cell death." J Natl Cancer Inst 99(18): 1410-4.

Jiang, L., J. Li, et al. (2009). "Bmi-1, stem cells and cancer." Acta Biochim Biophys Sin (Shanghai) 41(7): 527-34.

Johnson, L., A. K. Gupta, et al. (2006). "Characterization of vaccinia virus particles using microscale silicon cantilever resonators and atomic force microscopy." Sensors and Actuators B Chemical 115: 189-197.

Jones, R. J., W. H. Matsui, et al. (2004). "Cancer stem cells: are we missing the target?" J Natl Cancer Inst 96(8): 583-5.

Jordan, C. T., M. L. Guzman, et al. (2006). "Cancer stem cells." N Engl J Med 355(12): 1253-61.

Kim, J. H., S. Y. Yoon, et al. (2004). "Overexpression of Bmi-1 oncoprotein correlates with axillary lymph node metastases in invasive ductal breast cancer." Breast 13(5): 383-8.

Kinzler, K. W. and B. Vogelstein (2002). Introduction. The genetic basis of human cancer (2nd, illustrated, revised ed). New York, McGraw-Hill, Medical Pub. Division.

Kleer, C. G., Q. Cao, et al. (2003). "EZH2 is a marker of aggressive breast cancer and promotes neoplastic transformation of breast epithelial cells." Proc Natl Acad Sci U S A 100(20): 11606-11.

Knipe, D. M., P. M. Howley, et al. (2007). Field's Virology (5th ed.).

Krivtsov, A. V., D. Twomey, et al. (2006). "Transformation from committed progenitor to leukaemia stem cell initiated by MLL-AF9." Nature 442(7104): 818-22.

Kruger, J. A., C. D. Kaplan, et al. (2006). "Characterization of stem cell-like cancer cells in immune-competent mice." Blood 108(12): 3906-12.

Lang, S. H., F. M. Frame, et al. (2009). "Prostate cancer stem cells." J Pathol 217(2): 299-306.

Lev, D. C., G. Kiriakova, et al. (2003). "Selection of more aggressive variants of the gI101A human breast cancer cell line: a model for analyzing the metastatic phenotype of breast cancer." Clin Exp Metastasis 20(6): 515-23.

Levi, B. P., O. H. Yilmaz, et al. (2009). "Aldehyde dehydrogenase 1a1 is dispensable for stem cell function in the mouse hematopoietic and nervous systems." Blood 113(8): 1670-80.

Li, C., D. G. Heidt, et al. (2007). "Identification of pancreatic cancer stem cells." Cancer Res 67(3): 1030-7.

Li, F. (2009). "Every single cell clones from cancer cell lines growing tumors in vivo may not invalidate the cancer stem cell concept." Mol Cells 27(4): 491-2.

Li, X., M. T. Lewis, et al. (2008). "Intrinsic resistance of tumorigenic breast cancer cells to chemotherapy." J Natl Cancer Inst 100(9): 672-9.

Li, Y., L. Kong, et al. (2007). "Mutant TNFalpha negatively regulates human breast cancer stem cells from MCF7 in vitro." Cancer Biol Ther 6(9): 1480-9.

Liu, G., X. Yuan, et al. (2006). "Analysis of gene expression and chemoresistance of CD133+ cancer stem cells in glioblastoma." Mol Cancer 5: 67.

Liu, T. C., E. Galanis, et al. (2007). "Clinical trial results with oncolytic virotherapy: a century of promise, a decade of progress." Nat Clin Pract Oncol 4(2): 101-17.

Liu, T. C. and D. Kirn (2008). "Gene therapy progress and prospects cancer: oncolytic viruses." Gene Ther 15(12): 877-84.

Liu, Y., W. L. Lu, et al. (2008). "A potential target associated with both cancer and cancer stem cells: a combination therapy for eradication of breast cancer using vinorelbine stealthy liposomes plus parthenolide stealthy liposomes." J Control Release 129(1): 18-25.

Louie, E., S. Nik, et al. (2010). "Identification of a stem-like cell population by exposing metastatic breast cancer cell lines to repetitive cycles of hypoxia and reoxygenation." Breast Cancer Res 12(6): R94.

Magnifico, A., L. Albano, et al. (2009). "Tumor-initiating cells of HER2-positive carcinoma cell lines express the highest oncoprotein levels and are sensitive to trastuzumab." Clin Cancer Res 15(6): 2010-21.

Mahller, Y. Y., J. P. Williams, et al. (2009). "Neuroblastoma cell lines contain pluripotent tumor initiating cells that are susceptible to a targeted oncolytic virus." PLoS One 4(1): e4235.

Maitland, N. J. and A. T. Collins (2008). "Prostate cancer stem cells: a new target for therapy." J Clin Oncol 26(17): 2862-70.

Mani, S. A., W. Guo, et al. (2008). "The epithelial-mesenchymal transition generates cells with properties of stem cells." Cell 133(4): 704-15.

Marcato, P., C. A. Dean, et al. (2009). "Oncolytic reovirus effectively targets breast cancer stem cells." Mol Ther 17(6): 972-9.

Matsui, W., C. A. Huff, et al. (2004). "Characterization of clonogenic multiple myeloma cells." Blood 103(6): 2332-6.

Matsui, W., Q. Wang, et al. (2008). "Clonogenic multiple myeloma progenitors, stem cell properties, and drug resistance." Cancer Res 68(1): 190-7.

Mccarthy, K. and M. Mcentegart (1989). "OBITUARY NOTICE: Allan Watt Downie." J . Med. Microbiol 28: 291-295.

Meyer, M. J., J. M. Fleming, et al. (2009). "Dynamic regulation of CD24 and the invasive, CD44posCD24neg phenotype in breast cancer cell lines." Breast Cancer Res 11(6): R82.

Meyer, M. J., J. M. Fleming, et al. (2010). "CD44posCD49fhiCD133/2hi defines xenograft-initiating cells in estrogen receptor-negative breast cancer." Cancer Res 70(11): 4624-33.

Minn, A. J., G. P. Gupta, et al. (2007). "Lung metastasis genes couple breast tumor size and metastatic spread." Proc Natl Acad Sci U S A 104(16): 6740-5.

Molofsky, A. V., R. Pardal, et al. (2003). "Bmi-1 dependence distinguishes neural stem cell self-renewal from progenitor proliferation." Nature 425(6961): 962-7.

Montanaro, F., K. Liadaki, et al. (2004). "Demystifying SP cell purification: viability, yield, and phenotype are defined by isolation parameters." Exp Cell Res 298(1): 144-54.

Morel, A. P., M. Lievre, et al. (2008). "Generation of breast cancer stem cells through epithelial-mesenchymal transition." PLoS One 3(8): e2888.

Morrissey, J. J. and S. Raney (1998). "A metastatic breast tumor cell line, GI-101A, is estrogen receptor positive and responsive to estrogen but resistant to tamoxifen." Cell Biol Int 22(6): 413-9.

Mylona, E., I. Giannopoulou, et al. (2008). "The clinicopathologic and prognostic significance of CD44+/CD24(-/low) and CD44-/CD24+ tumor cells in invasive breast carcinomas." Hum Pathol 39(7): 1096-102.

Nakanishi, T., S. Chumsri, et al. (2010). "Side-population cells in luminal-type breast cancer have tumour-initiating cell properties, and are regulated by HER2 expression and signalling." Br J Cancer 102(5): 815-26.

Neth, P., M. Ciccarella, et al. (2006). "Wnt signaling regulates the invasion capacity of human mesenchymal stem cells." Stem Cells 24(8): 1892-903.

Neumeister, V. and D. Rimm (2009). "Is ALDH1 a good method for definition of breast cancer stem cells?" Breast Cancer Res Treat 123(1): 109-11.

Neve, R. M., K. Chin, et al. (2006). "A collection of breast cancer cell lines for the study of functionally distinct cancer subtypes." Cancer Cell 10(6): 515-27.

O'Brien, C. A., A. Pollett, et al. (2007). "A human colon cancer cell capable of initiating tumour growth in immunodeficient mice." Nature 445(7123): 106-10.

Oda, K. I. and W. K. Joklik (1967). "Hybridization and sedimentation studies on "early" and "late" vaccinia messenger RNA." J Mol Biol 27(3): 395-419.

Otsuki, A., A. Patel, et al. (2008). "Histone deacetylase inhibitors augment antitumor efficacy of herpes-based oncolytic viruses." Mol Ther 16(9): 1546-55.

Parato, K. A., D. Senger, et al. (2005). "Recent progress in the battle between oncolytic viruses and tumours." Nat Rev Cancer 5(12): 965-76.

Pardal, R., M. F. Clarke, et al. (2003). "Applying the principles of stem-cell biology to cancer." Nat Rev Cancer 3(12): 895-902.

Park, I. K., D. Qian, et al. (2003). "Bmi-1 is required for maintenance of adult self-renewing haematopoietic stem cells." Nature 423(6937): 302-5.

Patrawala, L., T. Calhoun, et al. (2005). "Side population is enriched in tumorigenic, stem-like cancer cells, whereas ABCG2+ and ABCG2- cancer cells are similarly tumorigenic." Cancer Res 65(14): 6207-19.

Pearce, D. J. and D. Bonnet (2007). "The combined use of Hoechst efflux ability and aldehyde dehydrogenase activity to identify murine and human hematopoietic stem cells." Exp Hematol 35(9): 1437-46.

Pearce, D. J., D. Taussig, et al. (2005). "Characterization of cells with a high aldehyde dehydrogenase activity from cord blood and acute myeloid leukemia samples." Stem Cells 23(6): 752-60.

Perou, C. M., T. Sorlie, et al. (2000). "Molecular portraits of human breast tumours." Nature 406(6797): 747-52.

Peto, R., J. Boreham, et al. (2000). "UK and USA breast cancer deaths down 25% in year 2000 at ages 20-69 years." Lancet 355(9217): 1822.

Ponti, D., A. Costa, et al. (2005). "Isolation and in vitro propagation of tumorigenic breast cancer cells with stem/progenitor cell properties." Cancer Res 65(13): 5506-11.

Power, A. T. and J. C. Bell (2007). "Cell-based delivery of oncolytic viruses: a new strategic alliance for a biological strike against cancer." Mol Ther 15(4): 660-5.

Rappa, G. and A. Lorico (2010). "Phenotypic characterization of mammosphere-forming cells from the human MA-11 breast carcinoma cell line." Exp Cell Res.

Rathinavelu, P., A. Malave, et al. (1999). "Expression of mdm-2 oncoprotein in the primary and metastatic sites of mammary tumor (GI-101) implanted athymic nude mice." Cancer Biochem Biophys 17(1-2): 133-46.

Redding, N., H.-Y. Zhou, et al. (2009). The utility of oncolytic viruses against neuroblastoma. The 5th International Meeting on Replicating Oncolytic Virus Therapeutics. Banff, Canada.

Reya, T., S. J. Morrison, et al. (2001). "Stem cells, cancer, and cancer stem cells." Nature 414(6859): 105-11.

Rheingold, S., A. Neugut, et al. (2003). Secondary Cancers: Incidence, Risk Factors, and Management. Cancer medicine 6. E. K. Frei, Donald W.; Holland, James F. Hamilton, Ont.

Rosel, J. and B. Moss (1985). "Transcriptional and translational mapping and nucleotide sequence analysis of a vaccinia virus gene encoding the precursor of the major core polypeptide 4b." J Virol 56(3): 830-8.

Ryan, K. and C. Ray (2004). Sherris Medical Microbiology (4th ed.), McGraw Hill.

Sajithlal, G. B., K. Rothermund, et al. (2010). "Permanently Blocked Stem Cells Derived From Breast Cancer Cell Lines." Stem Cells.

Schatton, T., G. F. Murphy, et al. (2008). "Identification of cells initiating human melanomas." Nature 451(7176): 345-9.

Seo, D. C., J. M. Sung, et al. (2007). "Gene expression profiling of cancer stem cell in human lung adenocarcinoma A549 cells." Mol Cancer 6: 75.

Setoguchi, T., T. Taga, et al. (2004). "Cancer stem cells persist in many cancer cell lines." Cell Cycle 3(4): 414-5.

Shackleton, M., F. Vaillant, et al. (2006). "Generation of a functional mammary gland from a single stem cell." Nature 439(7072): 84-8.

She, M. and X. Chen (2009). "Targeting Signal Pathways active in Cancer Stem Cells to Overcome Drug Resistance." Zhongguo Fei Ai Za Zhi 12(1): 3-7.

Shen, Y. and J. Nemunaitis (2005). "Fighting cancer with vaccinia virus: teaching new tricks to an old dog." Mol Ther 11(2): 180-95.

Sheridan, C., H. Kishimoto, et al. (2006). "CD44+/CD24- breast cancer cells exhibit enhanced invasive properties: an early step necessary for metastasis." Breast Cancer Res 8(5): R59.

Shook, D. and R. Keller (2003). "Mechanisms, mechanics and function of epithelial-mesenchymal transitions in early development." Mech Dev 120(11): 1351-83.

Sieczkarski, S. B. and G. R. Whittaker (2005). "Viral entry." Curr Top Microbiol Immunol 285: 1-23.

Singh, B., K. R. Cook, et al. (2010). "Role of COX-2 in Tumorospheres Derived from a Breast Cancer Cell Line." J Surg Res.

Singh, S. K., I. D. Clarke, et al. (2003). "Identification of a cancer stem cell in human brain tumors." Cancer Res 63(18): 5821-8.

Skog, J., K. Edlund, et al. (2007). "Adenoviruses 16 and CV23 efficiently transduce human low-passage brain tumor and cancer stem cells." Mol Ther 15(12): 2140-5.

Smith and G. L (2004). Poxvirus strategies to evade the host response to infection. London.

Smith, G. L. and B. Moss (1983). "Infectious poxvirus vectors have capacity for at least 25 000 base pairs of foreign DNA." Gene 25(1): 21-8.

So, C. W., H. Karsunky, et al. (2003). "MLL-GAS7 transforms multipotent hematopoietic progenitors and induces mixed lineage leukemias in mice." Cancer Cell 3(2): 161-71.

Sodeik, B., R. W. Doms, et al. (1993). "Assembly of vaccinia virus: role of the intermediate compartment between the endoplasmic reticulum and the Golgi stacks." J Cell Biol 121(3): 521-41.

Sophos, N. A. and V. Vasiliou (2003). "Aldehyde dehydrogenase gene superfamily: the 2002 update." Chem Biol Interact 143-144: 5-22.

Sorlie, T., C. M. Perou, et al. (2001). "Gene expression patterns of breast carcinomas distinguish tumor subclasses with clinical implications." Proc Natl Acad Sci U S A 98(19): 10869-74.

Sorlie, T., R. Tibshirani, et al. (2003). "Repeated observation of breast tumor subtypes in independent gene expression data sets." Proc Natl Acad Sci U S A 100(14): 8418-23.

Steinhardt, E., C. Israeli, et al. (1913). "Studies on the cultivation of the virus of vaccinia." J. Inf Dis 13: 294-300.

Steiniger, S. C., J. A. Coppinger, et al. (2008). "Quantitative mass spectrometry identifies drug targets in cancer stem cell-containing side population." Stem Cells 26(12): 3037-46.

Stern, W. and S. Dales (1974). "Biogenesis of vaccinia: concerning the origin of the envelope phospholipids." Virology 62(2): 293-306.

Stingl, J., P. Eirew, et al. (2006). "Purification and unique properties of mammary epithelial stem cells." Nature 439(7079): 993-7.

Strutz, F., M. Zeisberg, et al. (2002). "Role of basic fibroblast growth factor-2 in epithelial-mesenchymal transformation." Kidney Int 61(5): 1714-28.

Stuelten, C. H., S. D. Mertins, et al. (2010). "Complex display of putative tumor stem cell markers in the NCI60 tumor cell line panel." Stem Cells 28(4): 649-60.

Sung, J. M., H. J. Cho, et al. (2008). "Characterization of a stem cell population in lung cancer A549 cells." Biochem Biophys Res Commun 371(1): 163-7.

Tanaka, H., M. Nakamura, et al. (2009). "The Hedgehog signaling pathway plays an essential role in maintaining the CD44+CD24-/low subpopulation and the side population of breast cancer cells." Anticancer Res 29(6): 2147-57.

Telford, W. G., J. Bradford, et al. (2007). "Side population analysis using a violet-excited cell-permeable DNA binding dye." Stem Cells 25(4): 1029-36.

Telford, W. G. and E. G. Frolova (2004). "Discrimination of the Hoechst side population in mouse bone marrow with violet and near-ultraviolet laser diodes." Cytometry A 57(1): 45-52.

Thompson, E. W. and E. D. Williams (2008). "EMT and MET in carcinoma--clinical observations, regulatory pathways and new models." Clin Exp Metastasis 25(6): 591-2.

Todo, T., R. L. Martuza, et al. (2001). "Oncolytic herpes simplex virus vector with enhanced MHC class I presentation and tumor cell killing." Proc Natl Acad Sci U S A 98(11): 6396-401.

Tolonen, N., L. Doglio, et al. (2001). "Vaccinia virus DNA replication occurs in endoplasmic reticulum-enclosed cytoplasmic mini-nuclei." Mol Biol Cell 12(7): 2031-46.

Topczewska, J. M., L. M. Postovit, et al. (2006). "Embryonic and tumorigenic pathways converge via Nodal signaling: role in melanoma aggressiveness." Nat Med 12(8): 925-32.

Tse, J. C. and R. Kalluri (2007). "Mechanisms of metastasis: epithelial-to-mesenchymal transition and contribution of tumor microenvironment." J Cell Biochem 101(4): 816-29.

Tucker and B. Jonathan (2001). Scourge : The Once and Future Threat of Smallpox. New York, Grove/Atlantic Inc.

Turley, E. A., M. Veiseh, et al. (2008). "Mechanisms of disease: epithelial-mesenchymal transition--does cellular plasticity fuel neoplastic progression?" Nat Clin Pract Oncol 5(5): 280-90.

Ucar, D., C. R. Cogle, et al. (2009). "Aldehyde dehydrogenase activity as a functional marker for lung cancer." Chem Biol Interact 178(1-3): 48-55.

Vaillant, F., M. L. Asselin-Labat, et al. (2008). "The mammary progenitor marker CD61/beta3 integrin identifies cancer stem cells in mouse models of mammary tumorigenesis." Cancer Res 68(19): 7711-7.

Valk-Lingbeek, M. E., S. W. Bruggeman, et al. (2004). "Stem cells and cancer; the polycomb connection." Cell 118(4): 409-18.

van Golen, K. L., S. Davies, et al. (1999). "A novel putative low-affinity insulin-like growth factor-binding protein, LIBC (lost in inflammatory breast cancer), and RhoC GTPase correlate with the inflammatory breast cancer phenotype." Clin Cancer Res 5(9): 2511-9.

van 't Veer, L. J., H. Dai, et al. (2002). "Gene expression profiling predicts clinical outcome of breast cancer." Nature 415(6871): 530-6.

Varambally, S., S. M. Dhanasekaran, et al. (2002). "The polycomb group protein EZH2 is involved in progression of prostate cancer." Nature 419(6907): 624-9.

Wakimoto, H., S. Kesari, et al. (2009). "Human glioblastoma-derived cancer stem cells: establishment of invasive glioma models and treatment with oncolytic herpes simplex virus vectors." Cancer Res 69(8): 3472-81.

Wang, K. H., A. P. Kao, et al. (2009). "Modulation of tumorigenesis and oestrogen receptor-alpha expression by cell culture conditions in a stem cell-derived breast epithelial cell line." Biol Cell 102(3): 159-72.

Wang, T., K. Lee, et al. (2007). "PRIMA-1 induces apoptosis by inhibiting JNK signaling but promoting the activation of Bax." Biochem Biophys Res Commun 352(1): 203-12.

Wang, Y., J. Yang, et al. (2009). "Expression of mutant p53 proteins implicates a lineage relationship between neural stem cells and malignant astrocytic glioma in a murine model." Cancer Cell 15(6): 514-26.

Weinberg, R. A. (2007). The Biology of Cancer, Garland Science.

Weinberg, R. A. (2008). "Twisted epithelial-mesenchymal transition blocks senescence." Nat Cell Biol 10(9): 1021-3.

WHO. (2006). "Cancer." from http://www.who.int/mediacentre/factsheets/fs297/en/.

WHO. (2009). "Cancer." from http://www.who.int/nmh/publications/fact_sheet_cancers_en.pdf.

Wicha, M. S., S. Liu, et al. (2006). "Cancer stem cells: an old idea--a paradigm shift." Cancer Res 66(4): 1883-90; discussion 1895-6.

Wong, D. J., H. Liu, et al. (2008). "Module map of stem cell genes guides creation of epithelial cancer stem cells." Cell Stem Cell 2(4): 333-44.

Woodward, W. A., M. S. Chen, et al. (2007). "WNT/beta-catenin mediates radiation resistance of mouse mammary progenitor cells." Proc Natl Acad Sci U S A 104(2): 618-23.

Wright, M. H., A. M. Calcagno, et al. (2008). "Brca1 breast tumors contain distinct CD44+/CD24- and CD133+ cells with cancer stem cell characteristics." Breast Cancer Res 10(1): R10.

Yang, M. H., M. Z. Wu, et al. (2008). "Direct regulation of TWIST by HIF-1alpha promotes metastasis." Nat Cell Biol 10(3): 295-305.

Yin, L., P. Castagnino, et al. (2008). "ABCG2 expression and side population abundance regulated by a transforming growth factor beta-directed epithelial-mesenchymal transition." Cancer Res 68(3): 800-7.

Yu, J., D. R. Rhodes, et al. (2007). "A polycomb repression signature in metastatic prostate cancer predicts cancer outcome." Cancer Res 67(22): 10657-63.

Yu, Y. A., S. Shabahang, et al. (2004). "Visualization of tumors and metastases in live animals with bacteria and vaccinia virus encoding light-emitting proteins." Nat Biotechnol 22(3): 313-20.

Zhang, Q., Y. A. Yu, et al. (2007). "Eradication of solid human breast tumors in nude mice with an intravenously injected light-emitting oncolytic vaccinia virus." Cancer Res 67(20): 10038-46.

Zhang, S., C. Balch, et al. (2008). "Identification and characterization of ovarian cancer-initiating cells from primary human tumors." Cancer Res 68(11): 4311-20.

Zhou, B. P. and M. C. Hung (2005). "Wnt, hedgehog and snail: sister pathways that control by GSK-3beta and beta-Trcp in the regulation of metastasis." Cell Cycle 4(6): 772-6.

Zhou, J., J. Wulfkuhle, et al. (2007). "Activation of the PTEN/mTOR/STAT3 pathway in breast cancer stem-like cells is required for viability and maintenance." Proc Natl Acad Sci U S A 104(41): 16158-63.

Zhou, J., H. Zhang, et al. (2008). "NF-kappaB pathway inhibitors preferentially inhibit breast cancer stem-like cells." Breast Cancer Res Treat 111(3): 419-27.

Zhou, J., H. Zhang, et al. (2009). "Cancer stem/progenitor cell active compound 8-quinolinol in combination with paclitaxel achieves an improved cure of breast cancer in the mouse model." Breast Cancer Res Treat 115(2): 269-77.

Zhou, S., J. D. Schuetz, et al. (2001). "The ABC transporter Bcrp1/ABCG2 is expressed in a wide variety of stem cells and is a molecular determinant of the side-population phenotype." Nat Med 7(9): 1028-34.

Acknowledgements

First of all I would like to thank Prof. Dr. Aladar A. Szalay for giving me the opportunity to work on such an interesting and exciting project and for his supervision and continuous encouragement. As a foreign student who arrived in a country in which he had never been, Dr. Szalay gave me a very warm welcome and treated me like his own child. He was always available for every little question and constantly cared about my well being not only in the lab but also outside of the lab.

Next I would like to thank all the members in the Würzburg lab. Although I only stayed in Würzburg for half a year, everybody provided me kind help. I want to thank especially Prof. Dr. Friedrich Grummt for his proof-reading of this thesis. I also want to thank Dr. Elisabeth Hofmann, PD Dr. Ivaylo Gentschev, Dr. Jochen Strizker, and Ms. Johanna Langbein.

I have spent over two years working at Genelux Corporation, so I would like to thank all the members for their help and support and for a great work atmosphere. Especially I want to thank Dr. Nanhai Chen, Dr. Qian Zhang and Dr. Tony Yu for their guidance and very helpful discussions. I also would like to thank Mr. Terry Trevino, Mr. Jason Aguilar, and Mrs. Melody Fells for their technical support. Dr. Rohit Duggal, although he joined Genelux Corporation in last year, gave me lots of advice on the project of cancer stem cells. I especially appreciate Dr. Ulrike Geissinger for her translation work and proof-reading of this thesis. I also want to thank Mrs. Camha Hoang for helping with all organizational things and for her friendship throughout last two years.

I am very grateful for the fellowship provided by University of Würzburg and stipend provided by Genelux Corporation and the opportunity to work and live in San Diego for the time of the thesis.

Finally, I would like to thank my wife, Ting Huang. During my three years of thesis work, she always loved, understood, helped and supported me. No matter where she was. I also would like to thank my families; they are always my precious treasure in the past, the present and the future.

Publication & Patent

Journal Papers:

1. **Wang H**, Li P, Zhai Q*. Cloning, Expression and Purification of a Novel Human GCN5-related Acetyltransferase, MAK3. CHINESE JOURNAL OF CELL BIOLOGY. 2005 Dec. 27(6):667-672.

2. Liu Z, Liu Y, **Wang H**, Ge X, Jin Q, Ding G, Hu Y, Zhou B, Chen Z, Ge X, Zhang B, Man X, Zhai Q*. Patt1, a novel protein acetyltransferase that is highly expressed in liver and downregulated in hepatocellular carcinoma, enhances apoptosis of hepatoma cells. Int J Biochem Cell Biol. 2009 Dec; 41(12):2528-37. Epub 2009 Aug 18.

3. Wen, M., Arora, R., **Wang, H**., Liu, L., Kimata, J.T., and Zhou, P*. GPI-anchored single chain Fv - an effective way to capture transiently-exposed neutralization epitopes on HIV-1 envelope spike. Retrovirology 7:79-90, 2010

4. Enhanced Replication of Oncolytic Vaccinia Virus GLV-1h68 in Human Breast Cancer Stem-like Cells. *Submitted.*

Patent:

1. Zhou Paul, **Wang Huiqiang**, Li Ping. Antiviral peptides comprising lipid attachment signals and methods of use. European Patent Office, EP2096121 (A1). 2009-09-02